REMARKS

Claims 1-37 were pending in this case. In the Office Action, several items were discussed. The following Remarks I through V are in response to the discussed items:

I. The Examiner suggested that the title be changed to "N-Sulfamido and N-Ureido Pyrazolopyrimidines as Cyclin Dependent Kinase Inhibitors". Applicants believe that since the invention covers N-Sulfamido, N-Ureido and N-Carbamoyl pyrazolopyrimidines, changing the title to "N-Sulfamido, N-Carbamoyl and N-Ureido Pyrazolopyrimidines as Cyclin Dependent Kinase Inhibitors" would be more appropriate. The Examiner's comments on this would be highly appreciated.

II. Claims 1 and 28-37 were rejected under 35 U.S.C. § 112, second paragraph, for use of the terms "heteroarylalkyl", "heterocycloalkyl" and "heterocyclylalkyl". It is stated that the terms are not defined in the specification while the components of each word are defined. Applicants would like to respectfully point out that "heteroarylalkyl" is defined on page 14, line 7. Terms such as "hydroxyalkyl" "alkynylalkyl", "arylalkyl, "alkylaryl" etc are also defined in the specification, at the same pointing out in each case which end of the moiety is attached to the parent molecule. Applicants believe that a similar reading should be applied to the other terms too, especially since the components of each term are defined. Withdrawal of the under 35 U.S.C. § 112, second paragraph rejection is, therefore, respectfully requested.

III. Claims 28-30 and 32-34 were rejected under § 112, second paragraph, as being indefinite. The use of the phrases "a patient in need of" and "inhibiting one or more cyclin dependent kinases" was objected to. The term "a patient in need of" is deleted in this amendment. As far as "inhibiting one or more cyclin dependent kinases" ("CDKs") is concerned, the specification provides not only an enormous number of compounds inhibiting the CDKs, but page 59 onwards provides assays of how to measure the inhibitive effect of the compounds on CDKs. As the Examiner points out, the specification does provide a representative list of diseases associated with CDKs.

Furthermore, the cyclin dependent kinases (CDKS) are key regulators of the cell cycle. In mammalian cells, entry into S-phase, control of DNA synthesis and ultimately cell division at mitosis are under the control of these enzymes. Activity of the CDKs is rate limiting for entry into S-phase. Commencement of S-phase is negatively regulated by the retinoblastoma tumor suppressor gene product, Rb. Rb itself regulates the activity of the E2F family of transcription factors. E2F target gene expression is essential for onset of DNA synthesis and entry into the cell cycle. Phosphorylation of Rb by the CDKs releases the repression of E2Fs and allows DNA synthesis to commence. This particular pathway contributes to the so-called "Restriction Point" hypothesis. Hence, CDK activity is required to phosphorylate Rb and drives entry into the cells cycle. These data predict that a key phenotype observable following CDK inhibition will be cell cycle arrest. This is readily observable in a variety of assays.

The CDKs also play key roles during late S-phase wherein the activities of CDK2 and CDK1 in association with cyclin A are required to suppress the transcriptional activity of E2F, thus signaling the end of DNA synthesis. Prolonged and inappropriate activation of the E2Fs during this stage of the cell cycle is correlated with the onset of apoptosis. Hence, in asynchronously growing populations of tumor cells, failure to down-regulate E2F activity during late S-phase is expected to induce apoptosis. Therefore, another key phenotype anticipated following CDK inhibition is apoptosis. Both cell cycle arrest and onset of apoptosis should be correlated with the complete inhibition of CDKs, and subsequent dephosphorylation of the Rb tumor suppressor protein. Thus, potent and selective inhibitors of CDK2 and CDK1 are expected to suppress phosphorylation of Rb.

The connection between the inhibition of CDKs and various diseases has been supported by several authors. In fact, Fischer, *Expert Opinion on Investigational Drugs* (June 2003) that the Examiner has pointed out in another section of the Office Action, states (on page 965 right hand column, line 3 onwards):

> "Clearly, CDK inhibitors continue to hold much promise as a new modality in the treatment of cancer, despite the recent realisation that CDKs regulate important physiological functions that are not directly related to cell-cycle progression. Furthermore, it is becoming increasingly clear that CDK inhibitors may find clinical

application in proliferative diseases other than cancer, particularly inflammatory disorders. For example, ROS was shown to suppress the proliferation of mesangial cells and nephron tubule podocytes, ... New understanding of CDK biology, particularly as far as the functions of certain CDKs in the regulation of transcription and neuronal functions are concerned, have provided novel biomedical rationales for yet additional indications. Particularly exciting is the prospect that CDK inhibitors may provide novel antiviral agents".

Thus, the authors point out that CDK inhibitors are not only a "treatment of cancer" but also "may find clinical application in proliferative diseases other than cancer etc. Applicants would like to point out that this is an exciting, evolving area of research. Applicants have provided several compounds that could be useful not only in the various diseases that are listed in the specification but are also currently under investigation by various researchers. Withdrawal of the §112, second paragraph rejection is, therefore, respectfully requested.

IV. Claims 1-37 were rejected under 35 U.S.C. §112, second paragraph, for use of the term "solvates". Applicants would like to point out that while the specification may not necessarily provide working examples of solvates, it provides sufficient description of solvates. Applicants thus believe that there is sufficient support for "solvates" in the specification. However, in the interest of advancing the prosecution, the term "solvate" is now removed from the claims, as suggested by the Examiner, wherever it occurred. Claim 1 did not contain the word "solvate". Instead Applicants have added "pharmaceutically acceptable salt thereof" to claim 1, which is not new matter.

V. Claims 28-36 were rejected under 35 U.S.C. § 112, first paragraph. It is stated that the specification "does not reasonably provide enablement for treating any human disease." As stated previously, the invention discloses a large number of compounds, and an assay to measure the CDK inhibitory activity. The Examiner cites the *Fischer* article (*Expert Opinion on Investigational Drugs*) referred to above, and states that the CDK inhibitor flavopiridol failed to show anti-tumor efficacy, 7-hydroxystaurosporine failed to show adequate PK properties, roscovitine had not been tested in efficacy trials, BMS-387032 had only been studied in Phase I, and states "recent

reports have questioned the validity of CDK2 as a good target for ... cancer." Applicants respectfully traverse the rejection for reasons stated below:

As discussed above under Section IV, and without repeating everything stated therein, Applicants believe that CDKs do indeed play a role in the regulation of tumor cell progression and cancer. This fact, again as stated above, is acknowledged in the *Fischer* article cited by the Examiner, as well as by several other authors. Thus, for example, B. Hu et al, *Molecular and Cellular Biology*, Vol. 21 (8), 2755-2766 (2001) (**EXHIBIT I**) state (page 2755, left hand column): "Addition of Cdk2 inhibitors... can block initiation of DNA synthesis. .... Evidence of amore limited scope suggests additional potential roles for Cdk2 in later cell cycle events."

S. van den Heuvel, *Science*, Vol. 262 (December 24, 1993) page 2050 (**EXHIBIT II**) states (see Abstract on page 2050): "...Cdk3, in addition to Cdc2 and Cdk2, executes a distinct and essential function in the mammalian cell cycle."

Furthermore, as far as flavopiridol (alvocidib) and other compounds are concerned, there are several reports that such compounds are indeed under further study in trials. For example, J. Byrd et al, *Clin. Cancer Res.*, Vol. 11 (11), pages 4176-4181 (2005) (**EXHIBIT III**) state (see *Conclusions* in the Abstract section on page 4176): "Flavopiridol has modest, schedule-dependent clinical activity in relapsed CLL and warrants further investigation utilizing alternative schedules of administration." Also, on page 4180 in the same article, the authors state:"... [t]his agent remains a worthwhile therapy to develop."

EXHIBIT IV is an article by J. brown, *Clin. Cancer. Res.,* Vol. 11 (11), 3971 (2005). On page 3972 (left hand column, 8th line from bottom up) states: "These results, emerging from persistent and careful characterization by Byrd and colleagues, suggest significant activity of flavopiridol in refractory CLL."

EXHIBIT V is a 20-page copy from Iddb3, the data base on investigational drugs (June 1, 2005 update). The article states, on page 10: "Alvocidib's selectivity for cyclin-dependent kinases also makes it a potential therapeutic tool for the treatment of smooth muscle cell rich vascular lesions..... In vitro studies demonstrated that alvocidib can potentiate the

action of many cytotoxic agents including cisplatin, paclitaxel... and 5-fluorouracil."

EXHIBIT VI is a 14-page copy of an Iddb3 report on seliciclib ((R)-roscovitine) (June 1, 2005 update). On page 1, it states: "Seliciclib... is under development by Cyclacel Ltd for the potential treatment of various cancers and inflammatory diseases ... . Phase IIa trials in non-small-cell lung cancer (NSCLC) and breast cancer were initiated in January 2003. ... In March 2004, clinical trials in mantle cell lymphoma, multiple myeloma (MM) and lymphoid leukemia were initiated."

EXHIBIT VII is 4-page copy from an Iddb3 report on BMS-387032 (June 1, 2005 update). It states that Bristol-Myers Squibb outlicensed its rights to Sunesis in April 2004, and Sunesis is investigating BMS-387032 (now SNS-032) "for the potential iv or oral treatment of solid and hematological cancers."

Applicants thus believe that there is ample, well-documented evidence, already published as well as ongoing, that CDK inhibitors are indeed worthwhile targets in the study of cancer. Withdrawal of the 35 U.S.C. §112, first paragraph rejection is, therefore, respectfully requested.

VI. New claims 38-42 have been added. There is sufficient support on various pages in the specification. Thus, no new matter has been added.

There being no other rejections pending, Applicants believe that claims 1-42 are in allowable condition and such an action is earnestly solicited.

If the Examiner has any questions, the Examiner is invited to contact the undersigned.

September 22, 2005

Respectfully submitted,

Schering-Plough Corporation
2000 Galloping Hill Road
Patent Department, K-6-1,1990
Kenilworth, NJ 07033
Tel: (908) 298-5068
Fax: (908) 298-5388

Dr. Palaiyur S. Kalyanaraman
Attorney for Applicants
Reg. No. 34,634

Exhibit I

MOLECULAR AND CELLULAR BIOLOGY, Apr. 2001, p. 2755–2766 Vol. 21, No. 8
0270-7306/01/$04.00+0 DOI: 10.1128/MCB.21.8.2755–2766.2001

S and G_2 Phase Roles for Cdk2 Revealed by Inducible Expression of a Dominant-Negative Mutant in Human Cells

BING HU,[1,2,3] JAYASHREE MITRA,[1,2,3] SANDER VAN DEN HEUVEL,[4] AND GREG H. ENDERS[1,2,3]*

Departments of Medicine[1] and Genetics[2] and Cancer Center,[3] University of Pennsylvania, Philadelphia, Pennsylvania, and Massachusetts General Hospital Cancer Center, Charlestown, Massachusetts[4]

Received 8 November 2000/Accepted 17 January 2001

Cyclin-dependent kinase 2 (Cdk2) is essential for initiation of DNA synthesis in higher eukaryotes. Biochemical studies in *Xenopus* egg extracts and microinjection studies in human cells have suggested an additional function for Cdk2 in activation of Cdk1 and entry into mitosis. To further examine the role of Cdk2 in human cells, we generated stable clones with inducible expression of wild-type and dominant-negative forms of the enzyme (Cdk2-wt and Cdk2-dn, respectively). Both exogenous proteins associated efficiently with endogenous cyclins. Cdk2-wt had no apparent effect on the cell division cycle, whereas Cdk2-dn inhibited progression through several distinct stages. Cdk2-dn induction could arrest cells at the G_1/S transition, as previously observed in transient expression studies. However, under normal culture conditions, Cdk2-dn induction primarily arrested cells with S and G_2/M DNA contents. Several observations suggested that the latter cells were in G_2 phase, prior to the onset of mitosis: these cells contained uncondensed chromosomes, low levels of cyclin B-associated kinase activity, and high levels of tyrosine-phosphorylated Cdk1. Furthermore, Cdk2-dn did not delay progression through mitosis upon release of cells from a nocodazole block. Although the G_2 arrest imposed by Cdk2-dn was similar to that imposed by the DNA damage checkpoint, the former was distinguished by its resistance to caffeine. These findings provide evidence for essential functions of Cdk2 during S and G_2 phases of the mammalian cell cycle.

A substantial body of evidence indicates that DNA synthesis in higher eukaryotes is initiated by activation of cyclin-dependent kinase 2 (Cdk2) (52, 66). Cdk2 associates with cyclin E and is activated shortly before S phase. The actual onset of S phase correlates closely with induction of cyclin A and its binding to Cdk2. Transient transfection of a catalytically inactive form of Cdk2 arrests cells in G_1 (74). This arrest was prevented by coexpression of wild-type (wt) Cdk2 (Cdk2-wt) but not other Cdks, suggesting that the mutant abrogates the function of endogenous Cdk2 in a dominant-negative (dn) manner. Similarly, addition of Cdk2 inhibitors or antibodies directed against Cdk2 to *Xenopus* egg extracts (19), microinjection of antibodies directed against Cdk2, cyclin A, or cyclin E in mammalian cells (54, 56, 73), or mutation of cyclin E in *Drosophila* (12, 13, 35) can block initiation of DNA synthesis. Candidate substrates of Cdk2 action at the G_1-S transition include the retinoblastoma tumor suppressor protein (pRb), CDC6, and NPAT (32, 43, 57, 78, 81). Cdk2 is also implicated in duplication of centrosomes, another important event initiated at the G_1/S boundary (26, 41, 46).

Evidence of a more limited scope suggests additional potential roles for Cdk2 in later cell cycle events. The catalytic activity of Cdk2, derived largely from its association with cyclin A, peaks in late S and G_2 phases (55, 73). In some *Drosophila* tissues, mutation of cyclin A blocks mitotic entry in a cyclin B mutant background (36). In *Xenopus* egg extracts, Cdk2 complexes appear to be required for activation of Cdk1 (Cdc2), independently of Cdk2's role in DNA synthesis (23). In this setting, immunodepletion of Cdk2 or addition of $p21^{WAF1/CIP1}$ blocks activation of Cdk1. The $p21^{WAF1/CIP1}$ effect does not appear to result from direct binding to Cdk1, occurs even in the absence of nuclei, and can be rescued by addition of cyclin E-Cdk2 complexes. In HeLa cells, microinjection during S phase of antibodies directed against cyclin A can block cell division, without a gross effect on bromodeoxyuridine (BrdU) incorporation (56). This finding has been supported by two recent microinjection studies in human cells that have provided evidence that Cdk2 may be required to stabilize cyclin B (42) and/or to perform another step required to activate Cdk1 (21).

We have investigated the role of Cdk2 in human cell cycle progression by generating stable clones in which transcription of wt and dn forms of Cdk2 can be efficiently induced. This system permits flow cytometric and biochemical analysis of the effects of these proteins in cells that are proliferating exponentially or are synchronized at specific points in the cell cycle. Using these clones, we found that induction of Cdk2-wt had no apparent cell cycle effect, whereas induction of Cdk2-dn inhibited progression through several distinct phases of the cell cycle.

MATERIALS AND METHODS

Cell culture and transfection. Cells were cultured in Dulbecco's modified Eagle's medium (DMEM; Life Technologies) containing 10% fetal bovine serum (Life Technologies), penicillin (100,000 U/liter), streptomycin sulfate (100,000 U/liter), and glutamine (1 mM). Tetracycline (Tet; culture grade; Sigma) was added to the culture medium at 1 to 2 μg/ml to suppress expression of the inducible protein. To allow induction, cells were washed once with phosphate-buffered saline (PBS), treated with trypsin and EDTA, washed off the dish with DMEM, pelleted at 300 × *g* for 5 min, and replated in the medium without Tet. Semiconfluent U2-OS cells were transfected by the calcium phosphate method, for stable as well as transient transfection (62). For transient expression of

* Corresponding author. Mailing address: Penn/GI Division, 600 CRB, 415 Curie Blvd., Philadelphia, PA 19104-6144. Phone: (215) 898-0159. Fax: (215) 573-2024. E-mail address: endersgh@mail.med.upenn.edu.

Cdk2-wt prior to immunofluorescence, a cytomegalovirus (CMV) vector expressing β-galactosidase (β-Gal; 0.8 μg per 3.5-cm-diameter dish) was cotransfected with either a CMV vector without insert or the same vector expressing Cdk2-wt (2.5 μg) (18, 74). The following methods were used for transfection of other cell types: Lipofectin (2 μl per 6-cm-diameter culture dish; Life Technologies) for HCT 116 cells and Effectene (10 μl per 6-cm-diameter culture dish; Quiagen) for NIH 3T3 mouse fibroblasts. Cells were fixed in methanol-acetone and stained for β-Gal, BrdU, and DNA as described elsewhere (18, 49). For transient expression of Cdk2-wt prior to flow cytometry, a CMV vector expressing CD20 (1.6 μg per 6-cm-diameter dish) (74) was cotransfected with 5 μg of each plasmid.

Plasmid constructs and generation of stable clones. cDNAs encoding Cdk2-wt and Cdk2-dn (74) were tagged at the carboxy terminus with an eight-amino-acid peptide corresponding to sequences from the hemagglutinin (HA) epitope of influenza virus and cloned behind the Tet operon in plasmid pUHD10-3 (22). A U2-OS osteogenic sarcoma cell clone (U24 [29]) stably transfected with plasmid pUHD15.1, encoding a Tet-sensitive transcription factor (22), was cotransfected with each of the above plasmids and the puromycin-resistant plasmid pBabePuro (51) at a ratio 20:1 (wt/wt). Clones resistant to 1 μg of puromycin per ml were selected in the presence of Tet. Expression of the target protein was assessed by immunofluorescence (49) or by immunoblotting, using antibody 12CA5 directed against the HA tag. About 75% of clones in each transfection produced detectable target protein.

Cell synchronization. For hydroxyurea (HU) block and release, cells were replated as described above in medium containing 1 mM HU (Sigma) and cultured with or without Tet for 24 h. The cells were washed twice with PBS and cultured in fresh medium with or without Tet. For subsequent nocodazole block, cells were typically replated into nocodazole. In some experiments, nocodazole was added 12 h after the HU release, with similar results. For nocadazole block and release, cells were replated into medium containing 40 ng of nocodazole (Sigma) per ml with or without Tet for 24 h. Cells were gently washed twice with PBS, and the mitotic cells were washed off the plates by pipetting up and down a few times with DMEM. The cells were pelleted at 300 × *g* for 5 min and replated in medium with or without Tet. For serum starvation of 3T3 cells, cells were incubated in 0.1% serum for 66 h.

Caffeine treatment and irradiation. For flow cytometry experiments, cells were untreated or treated with caffeine (1 to 10 mM) for 30 min. Some cells were next exposed to 5-Gy irradiation at 2.9 Gy/min from a J. L. Shepard model 30 Mark I ^{137}Cs irradiator. Subsequently, cells were incubated with or without caffeine for another 24 h. Cells with or without Cdk2-dn induction were, similarly, left untreated or treated with 1 to 10 mM caffeine for 24 h. For DNA condensation experiments, cells were synchronized with HU and released from this inhibition for 4 h; 1 mM caffeine was added, and incubation was continued for another 8 h. Cells were then fixed with ice-cold methanol-acetone (1:1) and stained for DNA using bisbenzimide.

Flow cytometry. Cells were washed with PBS, treated with trypsin-EDTA, washed off the dish with PBS, and centrifuged at 1,500 × *g* for 5 min (4°C; Eppendorf Microfuge). The cells were resuspended in PBS, fixed by dropwise addition of a 3× volume of ice-cold ethanol (96%), and incubated for at least 2 h at 4°C before staining. Fixed cells were pelleted and stained at 37°C for 30 min with 0.5 ml of a solution containing 0.001% propidium iodide (Sigma) and 250 μg of RNase A per ml. The total cellular DNA content was determined using a Becton Dickinson flow cytometer and ModFit software. Cell aggregates were gated out of the analysis, based on the width of the propidium iodide fluorescence signal. Each profile was compiled from approximately 5,000 gated events. CD20 staining was as described previously (74). A plasmid expressing a farnesylated green fluorescent protein (Clontech) was to mark transfected cells in 3T3 experiments.

Cell extracts. Total cell extracts were prepared in E1A lysis buffer as described previously (49).

Antibodies. Immunoblotting and immunoprecipitation were performed as described previously (49). Separation of differentially phosphorylated forms of Cdk1 was performed on 12% polyacrylamide gels. For immunoblotting, we used 1:600 to 1:800 dilutions of a 200-μg/ml solution of antibodies directed against cyclin A (H-432 or BF683), cyclin E (C-19), cyclin B1 (GNS1), cyclin B1 (H-433), Cdk2 (M2), and Cdk1 (C-19 or 17), all from Santa Cruz Biotechnology. Antibody directed against a tyrosine 15-phosphorylated peptide of Cdk1 [phospho-Cdc2 (Tyr15); referred to here as K1Y15-P] was obtained from New England Biolabs. Antibody directed against Chk2 was kindly provided by S. Elledge (Howard Hughes Medical Institute, Baylor College of Medicine) (44). Immunoblotting of proteins containing the HA tag was done with a 1:40 dilution of monoclonal antibody 12CA5 (100 μg/ml). For immunoprecipitations, 50 to 200 μg of cell extract was incubated with 2 to 3 μg of antibody as described previously (49). For immunodepletion of HA-tagged proteins, 3 μg of anti-HA antibody (rat monoclonal clone 3F10; Roche) was used two times, each followed by precipitation with 60 μl of packed protein G-agarose beads (Life Technologies).

Kinase assays. Anti-cyclin A (H432), anti-cyclin B1 (GNS1), 12CA5, and anti-Cdk2 (M2) were used to immunoprecipitate active kinases. After immunoprecipitation, the beads were washed three times with E1A lysis buffer and once with 1× kinase buffer (25 mM HEPES buffer [pH 7.4], 1 mM phenylmethylsulfonyl fluoride, 0.1 mM sodium vanadate, 10 μg aprotinin/ml, 10 μg of leupeptin/ml) and then incubated with kinase reaction mix (5 μg of histone H1 [Sigma], 0.1 mM ATP, and 0.2 μCi of [γ-^{32}P]ATP in a total volume of 25 μl of 1× kinase buffer) at 30°C for 30 min. The reaction was stopped by addition of 25 μl of 2× sample buffer. The mixture was heated at 90°C for 3 min and centrifuged, and proteins in the supernatant were resolved by sodium dodecyl sulfate-polyacrylamide gel electrophoresis (10% gel).

Sequencing of integrated plasmids. Two primers close to the cloning site of pUDH10-3 vector were used to amplify integrated Cdk2-dn cDNAs. The upstream primer was 5′-ACCGGGACCGATCCAGCCT-3′, and the downstream primer was 5′-GCATTCTAGTTGTGGTTTGTCC-3′. The products were purified from agarose gels and directly sequenced by automated methods.

Southern blotting. Genomic DNA was purified from cells as described elsewhere (62). Briefly, 10 μg of each purified genomic DNA was digested overnight by *Eco*RI and then subjected to electrophoresis in 0.7% agarose. DNA was blotted onto a nylon membrane (Hybond-N+; Amersham) and detected by pUDH10-3 vector labeled by ^{32}P nick translation.

RESULTS

Generation of clones. To further define the role of Cdk2 in the human cell cycle, we generated cell lines in which expression of Cdk2-wt and Cdk2-dn could be rapidly and strongly induced. We cloned cDNAs for Cdk2-wt and Cdk2-dn into a Tet-regulated expression vector (the Tet-off system [22]). In the Cdk2-dn protein, an asparagine residue is substituted for the aspartic acid residue at position 145 (74). This aspartic acid residue is conserved in all protein kinases and has been implicated in orienting the beta and gamma phosphates of ATP for the phospho-transfer reaction (9, 33, 34). Each cDNA encoded a carboxy-terminal influenza HA epitope tag, to permit identification of the exogenous enzymes.

We transfected these constructs into a U2-OS clone (U24 [29, 49]) that expressed a Tet-sensitive transcription activator. We chose U2-OS cells because they have been shown in transient transfection studies to be efficiently arrested by Cdk2-dn (74). In addition, these cells have been shown to support efficient regulation of transcription using the Tet-off system (24, 29, 49). Puromycin-resistant colonies were selected in the presence of Tet, to repress transcription from the target vectors. Similar numbers of colonies were recovered from parallel plates transfected with target vector lacking an insert, suggesting that any leaky expression of the exogenous enzymes that may have occurred did not generally confer a selective disadvantage on clone growth or selection pressure for mutation of the host cells (data not shown). Consistent with this observation, we found little or no expression of the exogenous proteins in the uninduced state (Fig. 1). We selected clones with a range of expression of the exogenous proteins relative to the endogenous enzyme (Fig 1) and identified clones with comparable levels of expression of exogenous wt and dn proteins (e.g., dn.4 and wt.2 [Fig. 1]). Note that induction of Cdk2-dn (Fig. 1, dn.5 lanes) appeared to inhibit formation of the rapidly migrating, active form of Cdk2, suggesting inhibition of endogenous Cdk2 activity (25, 73). The effect of Cdk2-dn on endogenous Cdk2 activity is further addressed below.

Induction of Cdk2-dn imposes S and G_2/M phase arrests. In preliminary studies, we chose a clone with a moderate level of

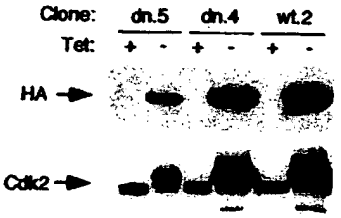

FIG. 1 Induction of Cdk2-wt and Cdk2-dn in U2-OS clones. The designated clones were cultured in the presence (+) or absence (−) of Tet for 3 days. Protein extracts were subjected to immunoblotting with monoclonal antibody 12CA5 directed against the HA epitope tag (top) or a polyclonal antibody directed against Cdk2 (bottom).

expression (dn.3) to assess whether induction of Cdk2-dn inhibited DNA synthesis, as judged by pulse tritiated thymidine incorporation. Tet withdrawal had no discernible effect on tritiated thymidine incorporation in vector-transfected clones (data not shown) (8, 49). In contrast, Tet withdrawal for 3 days in dn.3 yielded an 85% inhibition of tritiated thymidine incorporation relative to uninduced cells (data not shown). Next, we assessed by flow cytometry the effects of Tet withdrawal on total cellular DNA content in this clone over the same time course. Surprisingly, we observed an increase in the fraction of cells in S and G_2/M phases in cells maintained without Tet (data not shown) rather than the expected accumulation of cells in G_1 phase (74). The reduced thymidine incorporation that followed Cdk2-dn induction in dn.3 argued against acceleration of G_1 progression and indicated that the accumulation of cells in S and G_2/M phases was likely caused by cell cycle inhibition. Similar S and G_2/M arrests were obtained from a second clone (dn.2 [data not shown]).

We then examined whether this was a reproducible response in Cdk2-dn-expressing clones. We derived a new set of clones from an independent transfection and selected representative low- and high-expressing clones (dn.5 and dn.4, respectively) for analysis (Fig. 1). Tet withdrawal in each clone again yielded S and G_2/M arrests (Fig. 2). (We use the term "arrest," as opposed to "delay," throughout this report, without implying that the cells are necessarily permanently arrested.) In contrast, induction of Cdk2-wt had no discernible cell cycle effect (Fig. 2).

Cdk2-dn-mediated G_1 arrest. We sought to reconcile these results with the previously observed G_1 arrest mediated by transient transfection of Cdk2-dn in U2-OS cells (74). Because the S and G_2/M arrests were seen in every Cdk2-dn-expressing clone and the exogenous enzymes were consistently of the expected size, it seemed unlikely that the Cdk2-dn coding region had undergone rearrangement or mutation during plasmid amplification or integration into genomic DNA. We further excluded these possibilities by performing Southern blotting, PCR amplification, and DNA sequencing of the integrated plasmids from two clones (data not shown).

We noted that simply replating U2-OS cells, which was also done prior to the transient transfections, induces a moderate synchronization in G_1 phase (49) (data not shown). In addition, transient transfection is somewhat growth inhibiting (data not shown) and may contribute to cell synchronization in G_1. Another potential difference in these experimental settings is that analysis of the transiently transfected cells was gated to the

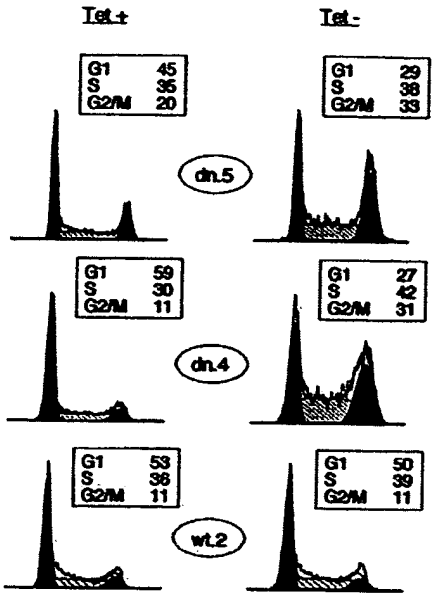

FIG. 2 Cdk2-dn induction preferentially imposes S and G_2/M arrests. Dn.5, dn.4, and wt.2 cells were grown in the presence (left) or absence (right) of Tet for 3 days, and the DNA content of the cells was assayed by flow cytometry. DNA content is displayed on the *x* axis, and cell number is shown on the *y* axis. For ease of presentation in all figures, DNA content profiles were normalized to the highest peak. G_1 and G_2/M fractions are shaded black, and S fractions are hatched. Boxed areas show the percentage of cells in each fraction.

1 to 5% of cells, with strongest staining for a cotransfected marker protein (74). We therefore reasoned that a G_1 arrest might be observed in the stable clones if Cdk2-dn was expressed to high levels during M and/or G_1 phases, perhaps mimicking the setting of transient transfection.

To test this notion, we synchronized cells from clones dn.5 and dn.4 in early mitosis, using the microtubule inhibitor nocodazole. We induced expression of the mutant protein during this period, then released the nocodazole block, and analyzed cellular DNA content at subsequent time intervals by flow cytometry. Cdk2-dn induction yielded a G_1 arrest in each clone (Fig. 3). The arrest in the high-expressing clone (dn.4) was as strong as that obtained following transient transfection (Fig. 3 and reference 74). Note that Cdk2-dn did not nonspecifically delay passage through all phases of the cell cycle, because there was no delay in progression through mitosis following release from the nocodazole-mediated arrest (Fig. 3). Furthermore, no mitotic delay was detected in cells examined 1.5 and 3 h after nocodazole release (data not shown). Immunoblotting confirmed that Cdk2-dn was expressed during the nocodazole block (data not shown).

Finally, we tested the effect of transient transfection on the cell cycle distribution of dn.5 cells. We found that cells successfully expressing the transfected marker CD20 were slower to progress through G_1 and S phases than either CD20-negative cells exposed to the transfection procedure or untransfected cells (data not shown). This phenomenon was observed in the presence or absence of Cdk2-dn induction, but it particularly enhanced the G_1/S arrest imposed by induction of Cdk2-dn (data not shown). We conclude that whereas tran-

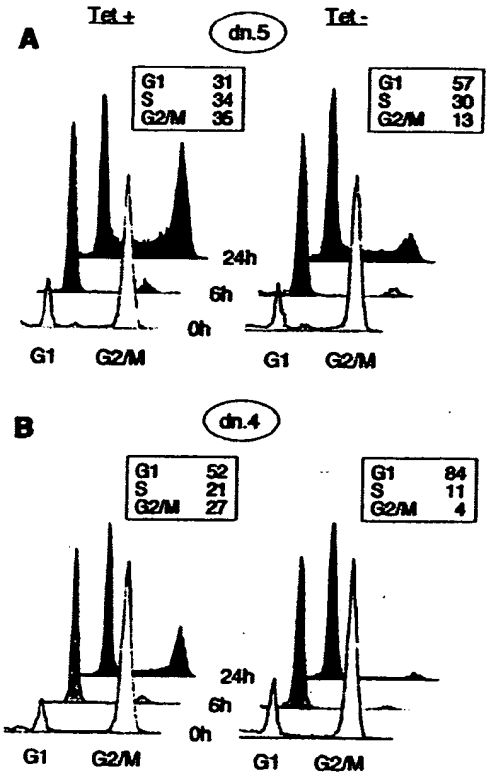

FIG. 3 Inhibition of progression through G_1 phase following induction of Cdk2-dn during a nocodazole block. Dn.5 (low expressor; A) and dn.4 (high expressor; B) cells were incubated with nocodazole for 24 h in the presence or absence of Tet. The mitotic cells were washed off the dish and replated in the absence of nocodazole (0 h; white profiles); cells were collected for flow cytometry at 6 h (grey profiles) and 24 h (black profiles) while maintaining the respective Tet conditions. Boxed areas show the percentage of cells in each fraction at 24 h.

sient transfection of Cdk2-dn revealed a bona fide role for Cdk2 in the G_1/S transition, these experimental conditions masked a more general propensity of Cdk2-dn to arrest progression through S and G_2/M phases in U2-OS cells.

Inhibition of S and G_2/M phase progression. To demonstrate directly that expression of Cdk2-dn results in S and G_2/M arrests and to identify favorable settings for biochemical analysis of Cdk2-dn's effects in synchronized cells, we performed experiments using cells synchronized in late G_1 and S phases with HU. We determined cellular DNA content at intervals following release of dn.4 cells from this block, with and without induction of Cdk2-dn. The results showed that induced cells were inhibited in passage through S and G_2/M phases (Fig. 4). In addition, we noted that 15% of cells with Cdk2-dn induction retained a G_1 DNA content, while fewer than 5% of uninduced cells did so following release, further confirming the ability of Cdk2-dn to inhibit G_1/S progression. In similar experiments, induction of the wt protein again had no marked effect on cell cycle progression (data not shown).

We considered the possibility that the apparent G_2/M arrest following induction of the mutant resulted from slow progression through S phase. However, in exponentially growing cells, cells of clones displaying low induced levels of the mutant showed little S-phase arrest, but still accumulated in G_2/M

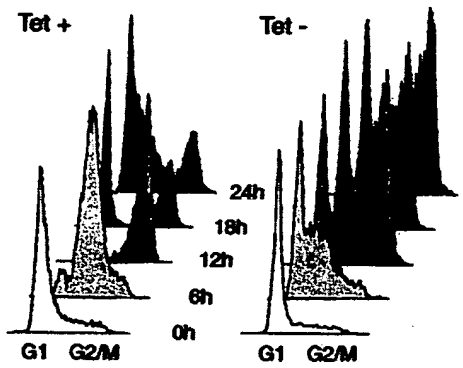

FIG. 4 Inhibition of cell cycle progression following induction of Cdk2-dn during an HU block. Dn.4 cells were incubated with HU for 24 h in the presence or absence of Tet. Cells were collected for flow cytometry at 6-h intervals after removal of HU (0 h).

(data not shown). We therefore repeated the HU experiment using dn.5, a clone with a lower expression level. As expected, induction of Cdk2-dn in this clone yielded only a modest S-phase arrest, compared to dn.4, but a prominent G_2/M arrest (Fig. 5). Likewise, a G_1 arrest was not seen in the clone with lower expression of Cdk2-dn (Fig. 5). We conclude that G_2/M is the phase most sensitive to Cdk2-dn expression.

DNA damage checkpoint pathways. Cdk2 is believed to be essential for the firing of DNA replication origins (2, 57, 70). Some regions of the mammalian genome are typically replicated early in S phase, and others are replicated late. It has been documented that in yeast, some origins preferentially fire in early S phase, whereas others fire late (68). The S-phase arrest observed upon induction of Cdk2-dn may therefore reflect a need for Cdk2 within S phase, to fire late-replicating origins (see Discussion). It is less clear what event(s) may be responsible for the accumulation of cells in G_2/M phase. Moreover, this is the cell cycle phase most sensitive to expression of Cdk2-dn. We therefore focused on characterizing further the point at which the G_2/M arrest occurs.

Given that Cdk2 has been implicated in initiation of DNA synthesis and that Cdk2-dn expression inhibits S-phase progression, we first asked whether the observed G_2/M arrest might result from activation of checkpoint pathways that block cell division in response to damaged or unreplicated DNA (16). Some cell death was seen after 3 days of induction of Cdk2-dn, but there was hardly any cell death during the experiments described here (data not shown). p53 is functional in U2-OS cells and is commonly induced by DNA damage (71). We found that p53 levels were unaffected by Cdk2-dn expression (data not shown). p21 levels were moderately increased, but no more so than by induction of Cdk2-wt (data not shown). Chk2 undergoes a shift in mobility on polyacrylamide gels in response to DNA damaging agents in some cells (44). A protein of the expected size that reacts with anti-Chk2 antibodies showed no mobility shift in response to Cdk2-dn expression but also showed no shift with irradiation (data not shown). Thus, these experiments did not provide evidence for Cdk2-dn-induced activation of checkpoint pathways that monitor DNA integrity or replication.

Caffeine is known to be a potent antagonist of checkpoint

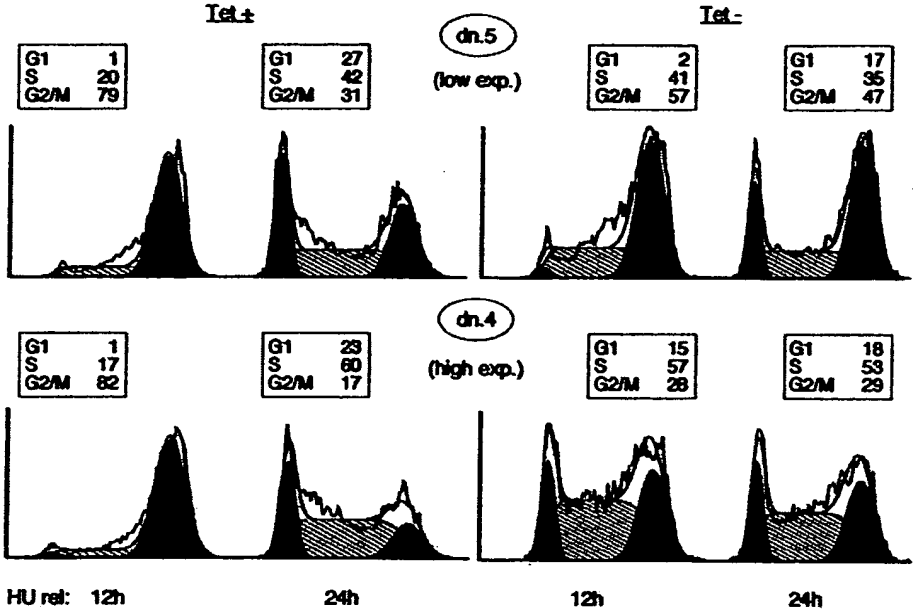

FIG. 5 Induction of lower levels of Cdk2-dn preferentially yields a G_2/M arrest, whereas higher levels also yield S and G_1 arrests. Dn.5 (low expressor) and dn.4 (high expressor) cells were incubated with HU for 24 h in the presence or absence of Tet. Cells were collected for flow cytometry 12 and 24 h after removal of HU. G_1 and G_2/M fractions are outlined in black, the S phase fraction is hatched, and the percentage of cells in each fraction is presented in a box above each profile.

pathways that monitor damaged and unreplicated DNA in mammalian cells (48, 64, 77). We therefore examined whether caffeine could rescue the S and G_2/M arrests mediated by Cdk2-dn. We focused on clones with high levels of Cdk2-dn expression for this analysis, because they display more distinct S and G_2/M arrests. As a positive control for caffeine's effects, we exposed uninduced cells to gamma irradiation. Representative flow cytometry results are shown in Fig. 6. Caffeine efficiently prevented the G_2/M arrest imposed by irradiation (Fig. 6, Tet +, Irr). In contrast, caffeine only slightly reduced the S and G_2/M fractions in cells with Cdk2-dn induction (Fig. 6, Tet −), less so than in control cells without induction or irradiation (Fig. 6, Tet +). Thus, the S and G_2/M arrests imposed by Cdk2-dn appear to be relatively resistant to the effects of caffeine.

In addition to its effects on DNA content, caffeine is capable of inducing premature DNA condensation in cells with unreplicated DNA (64, 77). Such an effect would not be evident by flow cytometry. To address this issue, we synchronized cells with HU, with or without Cdk2-dn induction, released the HU block, and examined whether caffeine addition during S phase could increase the fraction of cells with condensed nuclear DNA, assessed by fluorescence microscopy. The results are summarized in Table 1. Caffeine was able to induce premature DNA condensation in 15% of uninduced cells but only 2% of cells with Cdk2-dn induction. We conclude that the S and G_2/M arrests imposed by Cdk2-dn are not solely due to activation of caffeine-sensitive checkpoint pathways but may reflect disruption of events required for normal cell cycle progression.

Cdk2-dn associates efficiently with endogenous cyclins. To further characterize the mechanism by which Cdk2-dn exerted its effects, we analyzed the induced protein's association with

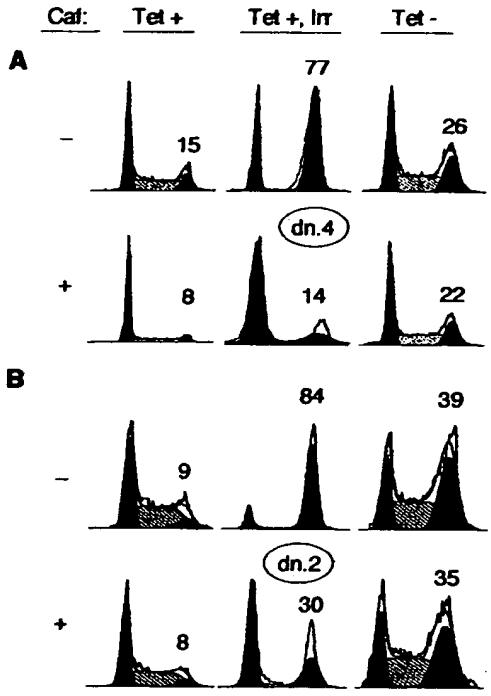

FIG. 6 Caffeine fails to rescue the S and G_2/M arrests imposed by Cdk2-dn. Dn. 4 (A) and dn.2 (B) cells were incubated in the presence or absence of Tet for 48 h. A third culture maintained in Tet was subjected to 5 Gy of gamma irradiation (Irr) at the end of this time period. Each culture was then incubated in the presence or absence of 1 mM caffeine (Caf) for an additional 24 h and collected for flow cytometry. The percentage of cells in the G_2/M fraction is given above each DNA profile.

TABLE 1. Caffeine does not mediate premature DNA condensation in cells with Cdk2-dn induction[a]

Transfection	Condensed nuclei (%)[b]	
	+Tet	−Tet
No caffeine	5.3 ± 0.9	3.2 ± 2.6
Caffeine	20 ± 2.0	5.1 ± 2.4

[a] Cells were synchronized with HU, released for 4 h, incubated with 1 mM caffeine for another 8 h, fixed, and stained with bisbenzimide (Hoechst).
[b] Mean ± standard deviation from three independent experiments.

known cyclin partners. Cyclin E expression is not markedly cell cycle regulated in U2-OS cells (49) (data not shown). We therefore used unsynchronized cells 24 h after induction of wt or dn enzymes to assay association with cyclin E. Immunoblotting with antibodies directed against the HA epitope tag demonstrated that the exogenous proteins were induced to similar levels (Fig. 7A). We immunoprecipitated the exogenous proteins through their HA tags and assayed their associated kinase activity using histone H1 as a substrate. The results confirmed that the wt enzyme was catalytically active whereas the mutant was not (Fig. 7A) (74).

Next, we compared the abilities of the induced enzymes to associate with endogenous cyclins. To estimate the fraction of endogenous cyclin E bound by the induced enzymes, we immunodepleted the induced proteins from the lysates using antibody directed against the HA tag and assayed the level of cyclin E remaining in the supernatant. Immunodepletion effectively removed most of the induced protein (Fig. 7B; compare lane 4 with lane 3 and lane 8 with lane 7). Although some cyclin E was nonspecifically lost from the supernatants due to the procedure itself (lanes 2 and 6), most cyclin E appeared to be bound to the exogenous proteins (lanes 4 and 8). These results suggest that the exogenous wt and dn proteins, respectively, associated with most of the endogenous cyclin E, consistent with their abundance relative to endogenous Cdk2. Consistent with this, cyclin E-associated kinase activity was inhibited by Cdk2-dn induction (data not shown). Because Cdk2-wt induction was without cell cycle effect, the results provide further evidence that the cell cycle inhibition mediated by Cdk2-dn is not due to sequestration of endogenous cyclins per se but also reflects a lack of Cdk2 kinase activity.

We then sought to extend these results by analyzing association of the exogenous enzymes with cyclin A and effects on cyclin A-associated kinase activity. Cyclin A expression and kinase activity are strongly cell cycle regulated in U2-OS cells, peaking in S and G_2 phases (49), and the increase in cyclin A-associated Cdk2 activity is primarily responsible for the peak in Cdk2 activity that occurs in late S/G_2 phases (55). To control for cell cycle position effects, we induced Cdk2-dn during synchronization of dn.4 cells with HU and prepared cell extracts at intervals following release from this block (see Fig. 4 for flow cytometry profiles of cells treated in this manner). Synchrony was lost in the uninduced cells beyond 20 h, and so we focused our analysis on earlier time points. Induction of Cdk2-dn had little impact on cyclin A expression, assessed either by direct immunoblotting (data not shown) or by immunoprecipitation of cyclin A followed by immunoblotting (Fig. 7C, top). However, cyclin A-associated kinase activity was strongly inhibited (Fig. 7C, middle). This correlated with binding of cyclin A to

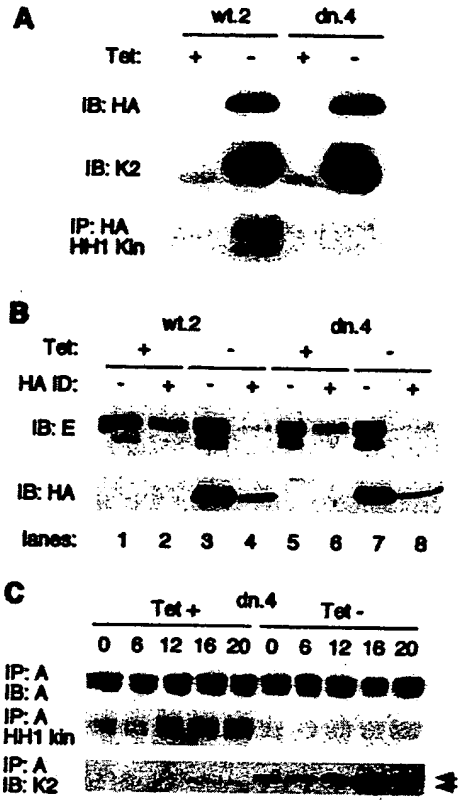

FIG. 7 Induced Cdk2-wt and Cdk2-dn each associate with the majority of endogenous cyclin A and E, but Cdk2-dn is catalytically inactive. (A) Induced Cdk2-dn is catalytically inactive, whereas induced Cdk2-wt retains catalytic activity. Cells from clones wt.2 and dn.4 were incubated in the presence or absence of Tet for 24 h. Whole-cell extracts were subjected to immunoblotting (IB) with an antibody directed against the HA tag (top), immunoblotting with an antibody directed against Cdk2 (K2; middle), and immunoprecipitation (IP) with an antibody directed against the HA tag, followed by in vitro kinase assays using histone H1 (HH1 Kin) as a substrate (bottom). (B) Induced Cdk2-wt and Cdk2-dn each associate with the majority of endogenous cyclin E. Two successive rounds of immunodepletion (ID) with the HA antibody were performed on the extracts described above. Cyclin E (top) and induced Cdk2 (wt or dn, using the anti-HA antibody; bottom) levels in the extracts were determined by immunoblotting before and after immunodepletion. (C) Induction of Cdk2-dn abolishes most of the endogenous cyclin A-associated kinase activity. Dn.4 cells were synchronized at the G_1/S border with HU. The HU was removed, and extracts were prepared from cells at the designated intervals. Cyclin A immunoprecipitates were subjected to immunoblotting with an anti-cyclin A antibody (top), examined for associated kinase activity, using histone H1 as a substrate (middle), or subjected to immunoblotting with an anti-Cdk2 antibody (bottom). Arrowheads, exogenous (upper band) and endogenous Cdk2.

the exogenous enzyme at the expense of the endogenous (Fig. 7C, bottom). In contrast, induction of Cdk2-wt in wt.2 under similar conditions had no substantial effect on cyclin A-associated kinase activity (data not shown). In conclusion, both Cdk2-wt and Cdk2-dn compete with the endogenous Cdk2 for cyclin binding, but Cdk2-dn lacks kinase activity and blocks the accumulation of cyclin A-associated kinase activity during S and G_2/M phases.

G_2/M arrest occurs prior to DNA condensation. To characterize further the point at which cells are arrested in the G_2/M period, we sought to determine whether Cdk2-dn-expressing

cells arrested before or after nuclear DNA condensation, a robust marker for prophase, the first stage of mitosis. We synchronized cells with HU, released cells from this block, and added nocodazole, to trap and quantitate cells reaching the mitotic spindle checkpoint. We fixed the cells 24 h after release from HU and stained nuclear DNA with bisbenzimide (Hoechst). A large fraction of U2-OS cells that reach prophase are arrested by nocodazole and show condensed nuclear DNA (65). Flow cytometry showed that most cells without induction were indeed arrested in the presence of nocodazole with a G_2/M DNA content (Fig. 8A, left) and that 30 to 40% of cells had fully condensed nuclei (Fig. 8B and C, left). In contrast, even though nearly half of the dn.4 cells and most of dn.5 cells with Cdk2-dn induction achieved a G_2/M DNA content (Fig. 8A, right), only 4 and 8%, respectively, had fully condensed nuclear DNA (Fig. 8B and C, right). These data indicate that the cells with induction of Cdk2-dn were arrested prior to prophase.

We next used this experimental format to examine whether the delay in progression to mitosis imposed by Cdk2-dn could be abrogated by overexpression of Cdk2-wt. Dn.4 cells were cotransfected with a vector expressing β-Gal and either a vector without insert or a vector expressing Cdk2-wt. As discussed previously, this experiment was complicated by the fact that the successfully transfected cells showed an increased fraction of cells arrested at G_1 phase and generally slower cell cycle progression; fewer cells progressed to fully condensed DNA under these experimental conditions (data not shown). We therefore scored the fraction of vector- or Cdk2-wt-transfected cells that showed any distinct nuclear condensation, identified by an examiner blinded to the treatment conditions as a marked reduction in nuclear size and/or loss of an oval shape. Cdk2-dn induction reduced the fraction of cells with nuclear condensation by 40% in the vector-transfected population, whereas inclusion of a Cdk2-wt cDNA insert in the transfection vector at least partially abrogated this effect (Table 2). Flow cytometry analyses of similarly treated cells indicated that Cdk2-wt transfection also modestly decreased the fraction of cells that retained G_1 and S phase DNA contents and increased the fraction of G_2/M cells (data not shown).

Regulation of Cdk1. We next examined the effect of Cdk2-dn induction on cyclin B levels and associated kinase activity. Cells were synchronized at the G_1/S and then G_2/M borders as before (Fig. 8), to minimize cell cycle position effects. We observed that cyclin B levels were reproducibly lower at each stage in cells with Cdk2-dn induction, consistent with recent evidence that hypophosphorylation of pRb and/or inhibition of Cdk2-cyclin A activity at the G_1/S transition may decrease cyclin B stability in U2-OS cells (42) (Fig. 9A). However, cyclin B levels actually fell as cells progressed toward G_2/M in the absence of Cdk2-dn induction, and the difference in cyclin B levels between uninduced and induced cells narrowed as cells progressed toward G_2/M (Fig. 9A). pRb was hyperphosphorylated, as judged by its migration on polyacrylamide gels, with or without Cdk2-dn induction in the G_1/S synchronized cells but migrated slightly more rapidly in the extract with Cdk2-dn induction (data not shown). pRb remained largely hyperphosphorylated, with or without Cdk2-dn induction, as the cells progressed toward G_2/M (data not shown).

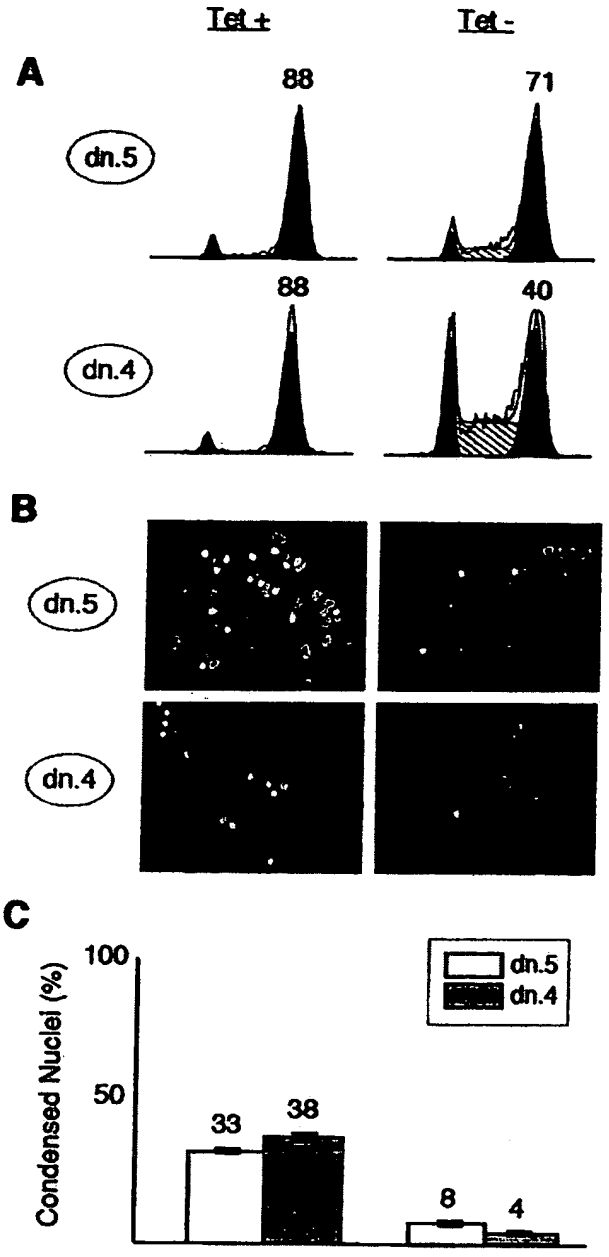

FIG. 8 Cdk2-dn arrests cells in G_2, prior to DNA condensation. Dn.5 and dn.4 cells were synchronized at the G_1/S border by incubation with HU for 24 h in the presence (left) or absence (right) of Tet. HU was then removed, and nocodazole was added; 24 h after HU release, portions of each culture were either collected for flow cytometry or fixed and stained with bisbenzimide. (A) Flow cytometry profiles. G_1 and G_2/M fractions are outlined in black, S phase fractions are hatched, and the percentage of cells in G_2/M is shown above that peak. (B) Representative fields with nuclear DNA stained by bisbenzimide. Interphase nuclei are broad, oval, and pale; early mitotic nuclei trapped by nocodazole are condensed, irregularly shaped, and bright. (C) Quantitation of the results in panel B, expressed as the percentage of nuclei in random high-power fields showing a condensed morphology. The bars depict mean numbers plus or minus ranges from two counts of more than 200 randomly chosen cells per condition. Similar results were obtained in a second experiment (not shown).

TABLE 2. Transfection of Cdk2-wt rescues the inhibition of DNA condensation mediated by Cdk2-dn induction[a]

Transfection	Condensed nuclei (%)[b]	
	+Tet	−Tet
Vector	66 ± 6	40 ± 10
Cdk2-wt	73 ± 2	65 ± 8

[a] Cells were transfected with vector or Cdk2-wt and incubated in medium with or without Tet. The cells were then synchronized with HU, released in the presence of nocodazole for 18 h, fixed, and stained with bisbenzimide.
[b] Mean ± standard deviations from three independent experiments.

In addition to the modestly lower cyclin B levels in the cells with Cdk2-dn induction, we observed accumulation of Cdk1 in a form that migrated more slowly on polyacrylamide gel electrophoresis (Fig. 9B). Inhibitory phosphorylation on threonine 14 and tyrosine 15 is known to reduce the electrophoretic mobility of Cdk1 (58). We therefore examined whether the slower-migrating form seen in cells with Cdk2-dn induction reacted with an antibody generated against peptide K1Y15-P. Immunoblotting with K1Y15-P antibody yielded a single major band that comigrated with the slower-migrating Cdk1-reactive species (Fig. 9B). Endogenous Cdk2 has an electrophoretic mobility greater than that of Cdk1 (58) (data not shown), but the HA tag on Cdk2-dn causes this protein to migrate at rate similar to that of Cdk1. To confirm that the slowly migrating species reactive with both anti-Cdk1 and anti-K1Y15-P antibodies was not derived from cross-reactivity with Cdk2-dn, we repeated the experiments following Cdk2-dn immunodepletion, using an antibody directed against the HA tag. Depletion of more than 90% of Cdk2-dn (see below) had no effect on the intensity of either the slower-migrating Cdk1-reactive band or the K1Y15-P-reactive band (data not shown). We conclude that these bands represent tyrosine-phosphorylated Cdk1.

The results suggested that Cdk1 activation was likely inhibited in cells with Cdk2-dn induction. Cdk1 was difficult to immunoprecipitate directly, as has been observed by others, but could be precipitated through associated cyclin B. We immunoprecipitated cyclin B from extracts prepared with and without Cdk2-dn induction. Immunoblotting with anti-Cdk1 and anti-K1Y15-P antibodies demonstrated the slowly migrating species, further confirming its identity as tyrosine-phosphorylated Cdk1 (Fig. 9B). We assayed kinase activity associated with the immunoprecipitates using histone H1 as a substrate. Cdk2-dn induction resulted in a strong reduction in cyclin B-associated kinase activity, even after normalizing for the amount of cyclin B immunoprecipitated (Fig. 9B). Similar results were obtained without prior synchronization with HU (data not shown). Somewhat less Cdk1 was present in the immunoprecipitates from Cdk2-dn-expressing cells than would be expected from the level of the protein present in the extracts. Because most of this Cdk1 appears to be tyrosine phosphorylated, an event requiring prior cyclin binding, we infer that the relative defect in immunoprecipitating Cdk1 is likely due to changes in recovery of the complexes or accessibility of the cyclin B epitope. Nonetheless, it is evident that the majority of Cdk1 associated with cyclin B in the cells with Cdk2-dn induction is in the slower migrating form (Fig. 9B). We conclude that the reduced levels of cyclin B-associated kinase activity result both from reduced cyclin B levels and from inhibitory phosphorylation of Cdk1.

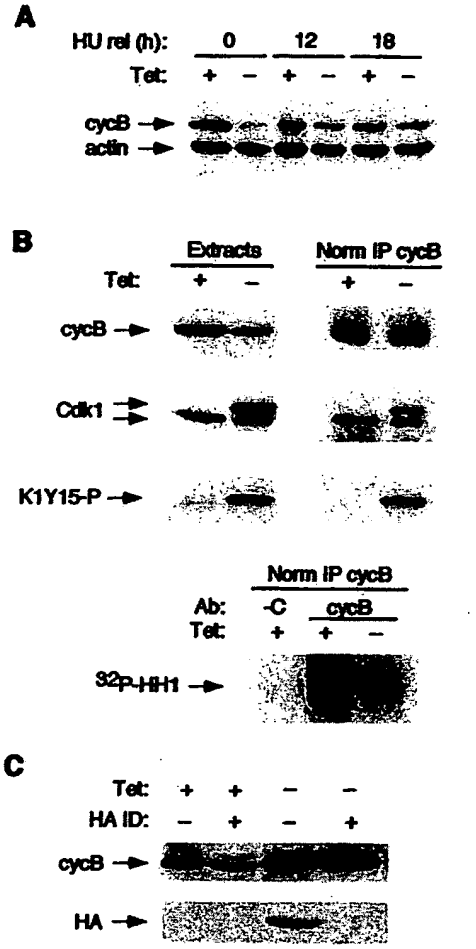

FIG. 9 Cdk2-dn-expressing cells arrest in G_2 phase with moderately reduced levels of cyclin B and greatly reduced activation of Cdk1. Dn.4 cells were synchronized with HU and then nocodazole, with or without Cdk2-dn induction, as described in the legend to Fig. 8. Protein extracts were subjected to immunoblotting, with or without the following immunoprecipitations. (A) Cyclin B (cycB) levels in S and G_2/M phases are moderately reduced by Cdk2-dn induction. Extracts were prepared from cells at the end of treatment with HU (0 h) and at 12 h and 18 h after release (rel) into nocodazole and subjected to immunoblotting for cyclin B and actin (loading control). Note that cyclin B levels are strongly reduced by Cdk2-dn induction during the G_1/S block but only moderately reduced, compared to uninduced cells, at the G_2/M block. (B) Cdk1 activation is inhibited by Cdk2-dn induction. (Top) Immunoblotting was performed on the 18-h extracts (left), normalized by protein content, or cyclin B immunoprecipitates (right), normalized for immunoprecipitated cyclin B (IP cycB), using anti-cyclin B, Cdk1, and K1Y15-P antibodies. (Bottom) Kinase activity associated with the normalized cyclin B immunoprecipitates was assayed using histone H1 (HH1) as a substrate. C denotes immunoprecipitation with a negative control antibody (Ab). (C) Cdk2-dn does not sequester cyclin B. Cdk-2dn was immunodepleted (ID) from the above extracts, and the levels of cyclin B (top) and Cdk2-dn (detected through its HA tag; bottom) remaining in the supernatant were assayed by immunoblotting.

We considered the possibility that sequestration of cyclin B by direct binding to Cdk2-dn might contribute to the defect in cyclin B-associated kinase activity. This scenario seemed un-

TABLE 3. Transfection of Cdk2-dn in serum-starved and restimulated 3T3 cells blocks DNA condensation after BrdU incorporation[a]

Ratio of expression plasmid to marker plasmid	BrdU-positive nuclei with condensed DNA (%)[b]	
	Vector	Cdk2-dn
1:1	77 ± 1	53 ± 9
2:1	75 ± 5	39 ± 4
4:1	78 ± 2	28 ± 1

[a] 3T3 cells were synchronized by serum starvation, restimulated with serum (0 h), and cotransfected (between 4 h and 10 h) with a plasmid expressing β-Gal and either an empty vector or one expressing Cdk2-dn. BrdU was added at 10 and 24 h, to ensure continuous labeling of cells in DNA synthesis. Nocodazole was added at 32 h and washed off at 48 h. The cells were fixed at 50 h. A least 100 β-Gal- and BrdU-positive cells were scored for each condition, to determine the fraction with condensed DNA (stained with bisbenzimide).

[b] Means ± standard deviation from four independent experiments for the 2:1 ratio; mean ± range from two independent experiments for the 1:1 and 4:1 ratios.

likely, because Cdk2-wt induction should also compete with Cdk1 for binding, yet Cdk2-wt induction had no demonstrable cell cycle effect. Moreover, induction of Cdk2-dn during a nocodazole block had no effect on progression through mitosis, a process dependent on cyclin B-Cdk1 activity. Consistent with this reasoning, we found that immunodepletion of Cdk2-dn from the extracts did not significantly reduce the level of cyclin B remaining in the supernatant, providing further evidence against sequestration of cyclin B by Cdk2-dn (Fig. 9C).

Taken together, these experiments indicate a requirement for Cdk2 in progression through S and G_2 phases of the human cell cycle, in addition to its previously described role at the G_1/S transition.

Other cell types. We then examined whether Cdk2-dn could impose S and/or G_2 arrests in other cell types. These experiments were complicated by the fact that transient transfection of Cdk2-dn appears to predispose to G_1 arrest, potentially outweighing S and G_2 arrests mediated in asynchronous cultures. We therefore performed experiments in 3T3 cells synchronized in G_1, allowing us to directly assess effects of Cdk2-dn on progression into replicative phases. 3T3 cells were deprived of serum for 66 h, yielding greater than 90% G_1/G_0 cells (data not shown). Serum was restored, and the cells were cotransfected with a marker plasmid expressing β-Gal and either an empty vector or one expressing Cdk2-dn. Continuous BrdU labeling was used to monitor S-phase progression. Nocodazole was added at 30 h (late S phase [data not shown]) and maintained until 48 h, to trap and quantitate cells reaching the spindle checkpoint. 3T3 cells arrest prior to prophase in response to spindle disruption, apparently due to an intact Chfr checkpoint (65). We therefore released cells from the nocodazole trap for 2 h prior to fixation and assessed the fraction of cells that were able to condense their DNA. Cdk2-dn yielded a dose-dependent reduction in the ability of BrdU-positive cells to undergo DNA condensation (Table 3). In similarly designed flow cytometry experiments in which nocodazole was omitted and cells were fixed 40 h after serum stimulation, Cdk2-dn-transfected cells showed a trend toward increased S-phase fractions and a statistically significant 50% increase in the G_2/M fraction (four independent experiments [data not shown]). These results suggest that Cdk2-dn can inhibit S- and G_2-phase progression in a nontransformed cell type. Preliminary experiments suggest that Cdk2-dn also mediates S and G_2 arrests in HCT 116 colorectal carcinoma cells synchronized with HU (data not shown).

DISCUSSION

Studies in diverse experimental systems have established that Cdk2 must be activated to initiate DNA synthesis in higher eukaryotes (52, 66). Similarly, increasing evidence suggests that inhibition of Cdk2 is necessary and sufficient to prevent S-phase entry in normal and neoplastic cells (29, 45, 49). Evidence that Cdk2 performs other functions within the replicative cycle has been limited. However, both human Cdk2 and Cdk1 are highly homologous to the single major Cdk in yeast, termed CDC28 in *Saccharomyces cerevisiae* and Cdc2 in *Schizosaccharomyces pombe* (17, 38, 53, 72). Either human protein can complement CDC28 mutants that arrest at the G_1/S or G_2/M transition (17, 38, 47, 53). In addition, recent evidence suggests that CDC28 may drive S-phase progression, including events of semiconservative DNA replication distinct from initiation (11). Based on these observations, Cdk2 may also be expected to regulate multiple steps of cell replication.

To address the role(s) of Cdk2 in the mammalian cell cycle, we generated U2-OS cell clones in which transcription of Cdk2-dn can be efficiently induced. We found that induction of Cdk2-dn could reproduce the G_1 arrest observed following its transient transfection (74). However, under standard growth conditions, induction of Cdk2-dn preferentially inhibited progression through S and G_2/M phases.

Specificity of the cell cycle effects. Do the arrests imposed by Cdk2-dn result from defective Cdk2 function? Several lines of evidence support this conclusion. In parallel experiments, induction of Cdk2-wt to levels as high as those achieved for Cdk2-dn did not cause discernible cell cycle effects. Based on the crystal structure of the enzyme, the mutation would not be expected to alter the enzyme's interfaces with known binding partners or substrates (9, 28). In agreement with this prediction, exogenous Cdk2-wt and Cdk2-dn both associated with the majority of cyclin A and E in the cell (Fig. 6), and thus far we have detected no major differences in the composition of wt or dn complexes immunoprecipitated from metabolically labeled cells or sedimented through glycerol gradients (data not shown). We also confirmed that Cdk2-dn did not bind to a significant fraction of cyclin B and did not inhibit progression through mitosis following release from a nocodazole block. Finally, transfection of Cdk2-wt could at least partially prevent the cell cycle arrests imposed by Cdk2-dn induction. A complex scenario can be envisioned in which Cdk2 normally plays no role in G_2/M progression, but Cdk2-dn inhibits the G_2/M transition by disrupting the function of an essential cyclin A-Cdk1 complex. In this scenario, both the exogenous Cdk2-wt and Cdk2-dn sequester cyclin A from Cdk1 and overexpression of Cdk2-wt artifactually complements the loss of cyclin A-Cdk1 kinase activity, by generating supraphysiologic levels of cyclin A-Cdk2 kinase activity. However, this scenario seems unlikely, because total cellular Cdk2 kinase activity remained near physiologic levels in the setting of Cdk2-wt induction (data not shown), probably because factors other than Cdk2 expression are limiting. In sum, our results suggest that the observed cell

cycle inhibition is due to abrogation of Cdk2 function rather than an artifact of Cdk2 overexpression or a gain of function from the Cdk2-dn mutation.

Could the effects of Cdk2-dn on cell cycle progression be mediated indirectly, through activation of DNA damage checkpoint pathways that respond to damaged or unreplicated DNA? Several observations argue against this possibility. p53 levels were not increased by Cdk2-dn expression, and p21 levels were no higher than in cells with Cdk2-wt induction. Migration of Chk2 was also not detectably altered, and caffeine did not rescue the cell cycle arrests. The observation that U2-OS cells are defective in the Chfr spindle checkpoint (65) suggests that this checkpoint pathway is also not involved in the Cdk2-dn-mediated G_2 arrest. We have not, of course, ruled out activation of other checkpoint pathways that might be insensitive to caffeine or that might proceed through biochemical events not examined here (61). However, the observation that Cdk2 inhibition can block Cdk1 activation in *Xenopus* egg extracts in the absence of nuclei (23) further supports the notion that Cdk2 plays a more direct role in mitotic entry.

S-phase arrest. Cdk2 has not previously been shown to be required for efficient S-phase progression in mammalian cells. Studies have revealed that origins fire at different points throughout S phase in yeasts, and some mammalian genes are preferentially replicated in late S phase, perhaps reflecting the use of late-firing origins (67, 68). Cdk2 can phosphorylate in vitro a number of substrates required for different steps of DNA replication (75). Thus, Cdk2 function may be required during S phase to activate late-firing origins and/or to drive other events of DNA replication (11).

Expression of phosphorylation-resistant pRb mutants during S phase delays DNA synthesis (6, 37, 79), an effect proposed to be mediated by inhibition of cyclin A expression. Consistent with this interpretation, our findings provide evidence that Cdk2 activity drives S-phase progression. On the other hand, it appears unlikely that the effects of Cdk2-dn are mediated through activation of pRb, because we observed only a slight reduction in pRb phosphorylation in HU-synchronized cells with Cdk2-dn induction, and pRb remained hyperphosphorylated throughout S phase following release from the chemical block.

E2F complexes are candidate targets for Cdk2 function during S phase. Phosphorylation by Cdk2 complexes abrogates the DNA binding activity of E2F-DP complexes in vitro (14, 39). Expression of E2F mutants defective for Cdk2 binding can delay progression through S phase, suggesting that inactivation of E2F by Cdk2 may be required to complete S phase (40). However, in our preliminary studies, transfection of a construct expressing a dn mutant of DP-1, the E2F heterodimerization partner, was unable to relieve S-phase inhibition imposed by Cdk2-dn (data not shown). Disruption of Cdk2 function in U2-OS cells through incubation with a peptide derived from the Cdk2 binding domain of E2F1 has been shown to result in apoptosis that is pronounced in serum-starved cells (5). We did not observe substantial cell death until Cdk2-dn had been induced for more than 3 days, perhaps because our cells were maintained continuously in serum.

G_2 arrest. An early experiment in mammalian cells that pointed to a possible role for Cdk2 within replicative phases of the cycle was the observation that microinjection of antibodies directed against cyclin A into S-phase HeLa cells could prevent subsequent cell division (56). This work has been extended by recent microinjection studies in which manipulation of Cdk2 function by several means was found to influence G_2/M progression (21, 42). Microinjection of either a phosphorylation-resistant pRb mutant, which repressed cyclin A expression, or $p27^{KIP1}$ in early-S-phase U2-OS cells decreased cyclin B stability (42). Further evidence suggested that cyclin A-Cdk2 complexes could stabilize cyclin B by phosphorylating and inactivating Cdh1, a specificity factor for proteolysis by the anaphase-promoting complex (42). Thus, this work suggests that Cdk2 may contribute to G_2/M progression by facilitating accumulation of cyclin B. In a separate study, microinjection of purified cyclin A-Cdk2 complexes in G_2-phase HeLa cells was found to accelerate entry into mitosis (21). Injection of cyclin A complexed to an inactive Cdk2 mutant, different from the mutant used in our studies, appeared to slightly delay mitotic entry. A stronger delay was observed following microinjection of the Cdk inhibitory domain of $p21^{WAF1/CIP1}$. This delay was not noted to alter the intensity of cyclin B immunofluorescent staining but may have been mediated by inhibition of Cdk1, because coinjection of Cdc25 could rescue the effect. Although these studies did not demonstrate directly that Cdk2 is required for entry into mitosis, the results are in good agreement with those presented here.

Several observations suggest that the G_2/M arrest observed in our U2-OS cell clones with Cdk2-dn induction occurs within G_2 rather than M phase: the arrested cells have uncondensed DNA, low levels of cyclin B-associated kinase activity, and high levels of tyrosine-phosphorylated Cdk1. Furthermore, induction of Cdk2-dn in nocodazole-arrested cells did not interfere with mitosis following removal of the drug. Induction of Cdk2-dn yielded moderately lower cyclin B levels, consistent with the microinjection results in these cells (42). However, we observed that cyclin B levels actually declined as U2-OS cells progressed from S through G_2/M in our experimental settings, in the absence of Cdk2-dn induction, raising doubt as to whether stabilization of cyclin B is a critical factor. Cells with Cdk2-dn induction appear to have an additional block to the activation of Cdk1, subsequent to cyclin B binding. These results point to a key role for Cdk2 in mediating entry into mitosis.

Is the defect in mitotic entry in U2-OS cells with Cdk2-dn induction the same as that present in the Cdk2-depleted *Xenopus* egg extracts and $p21^{WAF1/CIP1}$-injected HeLa cells? In the *Xenopus* egg extracts, Cdk2 depletion blocked activation of exogenous cyclin B and appeared to favor inhibitory phosphorylation of Cdk1, a process thought to follow cyclin B binding (23, 50). These results are consistent with our observations in U2-OS cells. The mitotic block in HeLa cells could be rescued with co-injection of Cdc25 or active cyclin B-Cdk1 complexes. Similarly, we have preliminary evidence that adenovirus-mediated expression of a Cdk1 mutant resistant to inhibitory phosphorylation (30) can rescue the G_2 block imposed by Cdk2-dn (data not shown). Thus, we believe that the major defect resulting from Cdk2 inhibition in each of these experimental systems is an inability to activate cyclin B-Cdk1 complexes. We suggest that inhibitory phosphorylation of Cdk1 is a default state that is overcome by the peak in Cdk2 kinase activity achieved during G_2 phase and/or release of Cdk2 complexes

from S-phase substrates. The notion that tyrosine phosphorylation of Cdk1 may limit normal cell cycle progression is supported by the observation that Cdk1 migrated in a slower-migrating form as synchronized leukemia cells traversed G_2 (10). Candidate targets of Cdk2 in Cdk1 regulation include CDC25B (10), CDC25C (7), Mik1 (1), Protein phosphatase 2A (27, 31), Pin1 (77), Plx1 (60), and Plkk 1 (60).

G_2 versus late S. We have used the standard operational definition that cells with fully replicated DNA, as judged by flow cytometry, are in G_2 or M phase. Whether such cells have actually completed S phase or, instead, retain small amounts of unreplicated DNA or DNA strand breaks cannot be determined. In fact, it has recently been demonstrated that approximately 1% of the genome is replicated within 90 min of mitosis in different mammalian cell types, within the period standardly defined as G_2 (76). The replication of specific sequences from autosomes and, in female cells, the inactivated X chromosome appears to occur preferentially at the end of S phase. If, indeed, Cdk2-dn preferentially arrests cells in late S phase, then the blocked steps would appear to be distinct from those performed earlier in S phase. This notion derives from the observation that clones expressing only moderate amounts of Cdk2-dn progress well through early and mid-S phase but still arrest in late S/G_2 (Fig. 5).

Implications. Our results provide strong evidence that Cdk2 is required not only for entry into the cell division cycle but also for efficient progression through S and G_2 phases. Our results imply that physiologic cell cycle inhibitors may mediate S and G_2 arrests by targeting Cdk2. For example, $p21^{WAF1/CIP1}$ is induced in response to irradiation and contributes to G_2 arrest (3, 15). During the arrest Cdk1 becomes tyrosine phosphorylated, an effect thus far ascribed to other events, such as direct Chk1-mediated inhibition of CDC25 (4, 20, 63). $p21^{WAF1/CIP1}$ is known to bind primarily to Cdk2 in this setting (59). Our results suggest that inhibition of Cdk2 by $p21^{WAF1/CIP1}$ may also foster tyrosine phosphorylation of Cdk1. In the same vein, recent experiments suggest that transient overexpression of cyclin E-Cdk2 can relieve the G_2/M arrest mediated by transforming growth factor β in Mv1Lu cells (80) and sustained overexpression can contribute to chromosomal instability (69).

ACKNOWLEDGMENTS

B.H. and J.M. contributed equally to this work.

This work was supported in part by a Research Scholar Award from the American Cancer Society (RPG 999-168-01-CCG) and by institutional funds provided to G.H.E. We also acknowledge use of facilities of the Penn Digestive Disease Center, supported by Center Grant P30 DK50306, and the Penn Cancer Center, supported by grants from the NCI and the Markey Charitable Trust.

We thank Amit Maity for help with the caffeine experiments.

REFERENCES

1. **Baber-Furnari, B. A., N. Rhind, M. N. Boddy, P. Shanahan, A. Lopez-Girona, and P. Russell.** 2000. Regulation of mitotic inhibitor Mik1 helps to enforce the DNA damage checkpoint. Mol. Biol. Cell **11**:1–11.
2. **Baum, B., H. Nishitani, S. Yanow, and P. Nurse.** 1998. Cdc18 transcription and proteolysis couple S phase to passage through mitosis. EMBO J. **17**: 5689–5698.
3. **Bunz, F., A. Dutriaux, C. Lengauer, T. Waldman, S. Shou, J. Brown, J. Sedivy, K. Kinzler, and B. Vogelstein.** 1998. Requirement for p53 and p21 to sustain G2 arrest after DNA damage. Science **282**:1497–1501.
4. **Chen, L., T. H. Liu, and N. C. Walworth.** 1999. Association of Chk1 with 14-3-3 proteins is stimulated by DNA damage. Genes Dev. **13**:675–685.
5. **Chen, Y. N., S. K. Sharma, T. M. Ramsey, L. Jiang, M. S. Martin, K. Baker, P. D. Adams, K. W. Bair, and W. G. Kaelin, Jr.** 1999. Selective killing of transformed cells by cyclin/cyclin-dependent kinase 2 antagonists. Proc. Natl. Acad. Sci. USA **96**:4325–4329.
6. **Chew, Y. P., M. Ellis, S. Wilkie, and S. Mittnacht.** 1998. pRB phosphorylation mutants reveal role of pRB in regulating S phase completion by a mechanism independent of E2F. Oncogene **17**:2177–2186.
7. **Clarke, P. R., I. Hoffmann, G. Draetta, and E. Karsenti.** 1993. Dephosphorylation of cdc25-C by a type-2A protein phosphatase: specific regulation during the cell cycle in Xenopus egg extracts. Mol. Biol. Cell **4**:397–411.
8. **Dai, C. Y., and G. H. Enders.** 2000. p16 INK4a can initiate an autonomous senescence program. Oncogene **19**:1613–1622.
9. **De Bondt, H. L., J. Rosenblatt, J. Jancarik, H. D. Jones, D. O. Morgan, and S. H. Kim.** 1993. Crystal structure of cyclin-dependent kinase 2. Nature **363**:595–602.
10. **De Souza, C. P., K. A. Ellem, and B. G. Gabrielli.** 2000. Centrosomal and cytoplasmic Cdc2/cyclin B1 activation precedes nuclear mitotic events. Exp. Cell Res. **257**:11–21.
11. **Duncker, B. P., P. Pasero, D. Braguglia, P. Heun, M. Weinreich, and S. M. Gasser.** 1999. Cyclin B-Cdk1 kinase stimulates ORC- and Cdc6-independent steps of semiconservative plasmid replication in yeast nuclear extracts. Mol. Cell. Biol. **19**:1226–1241.
12. **Duronio, R. J., A. Brook, N. Dyson, and P. H. O'Farrell.** 1996. E2F-induced S phase requires cyclin E. Genes Dev. **10**:2505–2513.
13. **Duronio, R. J., and P. H. O'Farrell.** 1995. Developmental control of the G1 to S transition in Drosophila: cyclin Eis a limiting downstream target of E2F. Genes Dev. **9**:1456–1468.
14. **Dynlacht, B. D., O. Flores, J. A. Lees, and E. Harlow.** 1994. Differential regulation of E2F *trans*-activation by cyclin-cdk2 complexes. Genes Dev. **8**:1772–1786.
15. **El-Deiry, W. S., T. Tokino, V. E. Velculescu, D. B. Levy, R. Parsons, J. M. Trent, D. Lin, W. E. Mercer, K. W. Kinzler, and B. Vogelstein.** 1993. *WAF1*, a potential mediator of p53 tumor suppression. Cell **75**:817–825.
16. **Elledge, S. J.** 1996. Cell cycle checkpoints: preventing an identity crisis. Science **274**:1664–1672.
17. **Elledge, S. J., and M. R. Spottswood.** 1991. A new human p34 protein kinase, CDK2, identified by complementation of a cdc28 mutation in Saccharomyces cerevisiae, is a homolog of Xenopus Eg1. EMBO J. **10**:2653–2659.
18. **Enders, G. H., J. Koh, C. Missero, A. K. Rustgi, and E. Harlow.** 1996. p16 inhibition of transformed and primary squamous epithelial cells. Oncogene **12**:1239–45.
19. **Fang, F., and J. W. Newport.** 1991. Evidence that the G1-S and G2-M transitions are controlled by different cdc2 proteins in higher eukaryotes. Cell **66**:731–742.
20. **Furnari, B., N. Rhind, and P. Russell.** 1997. Cdc25 mitotic inducer targeted by chk1 DNA damage checkpoint kinase. Science **277**:1495–1497.
21. **Furuno, N., N. den Elzen, and J. Pines.** 1999. Human cyclin A is required for mitosis until mid prophase. J. Cell Biol. **147**:295–306.
22. **Gossen, M., and H. Bujard.** 1992. Tight control of gene expression in mammalian cells by tetracycline-responsive promoters. Proc. Natl. Acad. Sci. USA **89**:5547–5551.
23. **Guadagno, T. M., and J. W. Newport.** 1996. Cdk2 kinase is required for entry into mitosis as a positive regulator of Cdc2-cyclin B kinase activity. Cell **84**:73–82.
24. **Harkin, D. P., J. M. Bean, D. Miklos, Y. H. Song, V. B. Truong, C. Englert, F. C. Christians, L. W. Ellisen, S. Maheswaran, J. D. Oliner, and D. A. Haber.** 1999. Induction of GADD45 and JNK/SAPK-dependent apoptosis following inducible expression of BRCA1. Cell **97**:575–586.
25. **Higashi, H., I. Suzuki-Takahashi, S. Saitoh, K. Segawa, Y. Taya, A. Okuyama, S. Nishimura, and M. Kitagawa.** 1996. Cyclin-dependent kinase-2 (Cdk2) forms an inactive complex with cyclin D1 since Cdk2 associated with cyclin D1 is not phosphorylated by Cdk7- cyclin-H. Eur. J. Biochem. **237**: 460–467.
26. **Hinchcliffe, E. H., C. Li, E. A. Thompson, J. L. Maller, and G. Sluder.** 1999. Requirement of Cdk2-cyclin E activity for repeated centrosome reproduction in xenopus egg extracts. Science **283**:851–854.
27. **Hoffmann, I., P. R. Clarke, M. J. Marcote, E. Karsenti, and G. Draetta.** 1993. Phosphorylation and activation of human cdc25-C by cdc2-cyclin B and its involvement in the self-amplification of MPF at mitosis. EMBO J, **12**:53–63.
28. **Jeffrey, P. D., A. A. Russo, K. Polyak, E. Gibbs, J. Hurwitz, J. Massague, and N. Pavletich.** 1995. Mechanism of cdk activation revealed by the structure of a cyclin A-cdk2 complex. Nature **376**:313–320.
29. **Jiang, H., H. S. Chou, and L. Zhu.** 1998. Requirement of cyclin E-Cdk2 inhibition in $p16^{INK4a}$-mediated growth suppression. Mol. Cell. Biol. **18**: 5284–5290.
30. **Jin, P., Y. Gu, and D. O. Morgan.** 1996. Role of inhibitory CDC2 phosphorylation in radiation-induced G2 arrest in human cells. J. Cell Biol. **134**:963–970.
31. **Kinoshita, N., H. Yamano, H. Niwa, T. Yoshida, and M. Yanagida.** 1993. Negative regulation of mitosis by the fission yeast protein phosphatase ppa2. Genes Dev. **7**:1059–1071.
32. **Kitagawa, M., H. Higashi, H. K. Jung, I. Suzuki-Takahashi, M. Ikeda, K. Tamai, J. Kato, K. Segawa, E. Yoshida, S. Nishimura, and Y. Taya.** 1996.

The consensus motif for phosphorylation by cyclin D1-Cdk4 is different from that for phosphorylation by cyclin A/E-Cdk2. EMBO J. 15:7060–7069.
33. Knighton, D. R., J. H. Zheng, L. F. Ten Eyck, V. A. Ashford, N. H. Xuong, S. S. Taylor, and J. M. Sowadski. 1991. Crystal structure of the catalytic subunit of cyclic adenosine monophosphate-dependent protein kinase. Science 253:407–414.
34. Knighton, D. R., J. H. Zheng, L. F. Ten Eyck, N. H. Xuong, S. S. Taylor, and J. M. Sowadski. 1991. Structure of a peptide inhibitor bound to the catalytic subunit of cyclic adenosine monophosphate-dependent protein kinase. Science 253:414–420.
35. Knoblich, J., K. Sauer, L. Jones, H. Richardson, R. Saint, and C. Lehner. 1994. Cyclin E controls S phase progression and its down-regulation during drosophila embryogenesis is required for the arrest of cell proliferation. Cell 77:107–120.
36. Knoblich, J. A., and C. F. Lehner. 1993. Synergistic action of Drosophila cyclins A and B during the G2-M transition. EMBO J. 12:65–74.
37. Knudsen, E. S., C. Buckmaster, T. T. Chen, J. R. Feramisco, and J. Y. Wang. 1998. Inhibition of DNA synthesis by RB: effects on G1/S transition and S-phase progression. Genes Dev. 12:2278–2292.
38. Koff, A., F. Cross, A. Fisher, J. Schumacher, K. Leguellec, M. Philippe, and J. M. Roberts. 1991. Human cyclin E, a new cyclin that interacts with two members of the CDC2 gene family. Cell 66:1217–1228.
39. Krek, W., M. E. Ewen, S. Shirodkar, Z. Arany, W. G. Kaelin, Jr., and D. M. Livingston. 1994. Negative regulation of the growth-promoting transcription factor E2F-1 by a stably bound cyclin A-dependent protein kinase. Cell 78:161–172.
40. Krek, W., G. Xu, and D. M. Livingston. 1995. Cyclin A-kinase regulation of E2F-1 DNA binding function underlies suppression of an S phase checkpoint. Cell 83:1149–1158.
41. Lacey, K. R., P. K. Jackson, and T. Stearns. 1999. Cyclin-dependent kinase control of centrosome duplication. Proc. Natl. Acad. Sci. USA 96:2817–2822.
42. Lukas, C., C. S. Sorensen, E. Kramer, E. Santoni-Rugiu, C. Lindeneg, J. M. Peters, J. Bartek, and J. Lukas. 1999. Accumulation of cyclin B1 requires E2F and cyclin-A-dependent rearrangement of the anaphase-promoting complex. Nature 401:815–818.
43. Lundberg, A. S., and R. A. Weinberg. 1998. Functional inactivation of the retinoblastoma protein requires sequential modification by at least two distinct cyclin-cdk complexes. Mol. Cell. Biol. 18:753–761.
44. Matsuoka, S., M. Huang, and S. Elledge. 1998. Linkage of ATM to cell cycle regulation by the Chk2 protein kinase. Science 282:1893–1897.
45. McConnell, B. B., F. J. Gregory, F. J. Stott, E. Hara, and G. Peters. 1999. Induced expression of $p16^{INK4a}$ inhibits both CDK4- and CDK2-associated kinase activity by reassortment of cyclin-CDK-inhibitor complexes. Mol. Cell. Biol. 19:1981–1989.
46. Meraldi, P., J. Lukas, A. M. Fry, J. Bartek, and E. A. Nigg. 1999. Centrosome duplication in mammalian somatic cells requires E2F and Cdk2-cyclin A. Nat.. Cell Biol. 1:88–93.
47. Meyerson, M., G. Enders, C.-L. Wu, L.-K. Su, C. Gorka, C. Nelson, E. Harlow, and L.-H. Tsai. 1992. A family of human cdc2-related protein kinases. EMBO J. 11:2909–2917.
48. Michael, W. M., R. Ott, E. Fanning, and J. Newport. 2000. Activation of the DNA replication checkpoint through RNA synthesis by primase. Science 289:2133–2137.
49. Mitra, J., C. Y. Dai, K. Somasundaram, W. S. El-Deiry, K. Satyamoorthy, M. Herlyn, and G. H. Enders. 1999. Induction of $p21^{WAF1/CIP1}$ and inhibition of Cdk2 mediated by the tumor suppressor $p16^{INK4a}$. Mol. Cell. Biol. 19:3916–3928.
50. Morgan, D. O. 1995. Principles of CDK regulation. Nature 374:131–134.
51. Morgenstern, J. P., and H. Land. 1990. Advanced mammalian gene transfer: high titre retroviral vectors with multiple drug selection markers and a complementary helper-free packaging cell line. Nucleic Acids Res. 18:3587–3596.
52. Nasmyth, K. 1996. Viewpoint: putting the cell cycle in order. Science 274: 1643–1645.
53. Ninomiya-Tsuji, J., S. Nomoto, H. Yasuda, S. I. Reed, and K. Matsumoto. 1991. Cloning of a human cDNA encoding a CDC2-related kinase by complementation of a budding yeast cdc28 mutation. Proc. Natl. Acad. Sci. USA 88:9006–9010.
54. Ohtsubo, M., A. M. Theodoras, J. Schumacher, J. M. Roberts, and M. Pagano. 1995. Human cyclin E, a nuclear protein essential for the G_1-to-S phase transition. Mol. Cell. Biol. 15:2612–2624.
55. Pagano, M., R. Pepperkok, J. Lukas, V. Baldin, W. Ansorge, J. Bartek, and G. Draetta. 1993. Regulation of the cell cycle by the cdk2 protein kinase in cultured human fibroblasts. J. Cell Biol. 121:101–111.
56. Pagano, M., R. Pepperkok, F. Verde, W. Ansorge, and G. Draetta. 1992. Cyclin A is required at two points in the human cell cycle. EMBO J. 11:961–971.
57. Petersen, B., J. Lukas, C. Sorensen, J. Bartek, and K. Helin. 1999. Phosphorylation of mammalian CDC6 by cyclin A/CDK2 regulates its subcellular localization. EMBO J, 18:396–410.
58. Poon, R. Y., M. S. Chau, K. Yamashita, and T. Hunter. 1997. The role of Cdc2 feedback loop control in the DNA damage checkpoint in mammalian cells. Cancer Res. 57:5168–5178.
59. Poon, R. Y. C., W. Jiang, H. Toyoshima, and T. Hunter. 1996. Cyclin-dependent kinases are inactivated by a combination of p21 and Thr-14/Tyr-15 phosphorylation after UV-induced DNA damage. J. Biol. Chem. 271:13283–13291.
60. Qian, Y. W., E. Erikson, and J. L. Maller. 1999. Mitotic effects of a constitutively active mutant of the *Xenopus* polo-like kinase Plx1. Mol. Cell. Biol. 19:8625–8632.
61. Ruffner, H., W. Jiang, A. G. Craig, T. Hunter, and I. M. Verma. 1999. BRCA1 is phosphorylated at serine 1497 in vivo at a cyclin-dependent kinase 2 phosphorylation site. Mol. Cell. Biol. 19:4843–4854.
62. Sambrook, J., E. Fritsch, and T. Maniatis. 1989. Molecular cloning: a laboratory manual, 2nd ed. vol. 1. Cold Spring Harbor Press, Cold Spring Harbor, N.Y.
63. Sanchez, Y., C. Wong, R. S. Thoma, R. Richman, Z. Wu, H. Piwnica-Worms, and S. J. Elledge. 1997. Conservation of the Chk1 checkpoint pathway in mammals: linkage of DNA damage to Cdk regulation through Cdc25. Science 277:1497–1501.
64. Schlegel, R., and A. B. Pardee. 1986. Caffeine-induced uncoupling of mitosis from the completion of DNA replication in mammalian cells. Science 232: 1264–1264.
65. Scolnick, D. M., and T. D. Halazonetis. 2000. Chfr defines a mitotic stress checkpoint that delays entry into metaphase. Nature 406:430–435.
66. Sherr, C. J. 1996. Cancer cell cycles. Science 274:1672–1677.
67. Shirahige, K., Y. Hori, K. Shiraishi, M. Yamashita, K. Takahashi, C. Obuse, T. Tsurimoto, and H. Yoshikawa. 1998. Regulation of DNA-replication origins during cell-cycle progression. Nature 395:618–621.
68. Simon, L., and H. Cedar. 1996. Temporal order of DNA replication., p. 387–408. *In* M. L. DePamphilis (ed.), DNA replication in eukaryotic cells. Cold Spring Harbor Laboratory Press, Cold Spring Harbor. N.Y.
69. Spruck, C. H., K. A. Won, and S. L. Reed. 1999. Deregulated cyclin E induces chromosome instability. Nature 401:297–300.
70. Stoeber, K., A. D. Mills, Y. Kubota, T. Krude, P. Romanowski, K. Marheineke, R. A. Laskey, and G. H. Williams. 1998. Cdc6 protein causes premature entry into S phase in a mammalian cell-free system. EMBO J. 17:7219–7229.
71. Stott, F., S. Bates, M. James, B. McConnell, M. Starborg, S. Brookes, I. Palmero, K. Ryan, E. Hara, K. Vousden, and G. Peters. 1998. The alternative product from the human CDKN2A locus, p14ARF, participates in a regulatory feedback loop with p53. EMBO J. 17:5001–5014.
72. Tsai, L.-H., E. Harlow, and M. Meyerson. 1991. Isolation of the human cdk2 gene that encodes the cyclin A- and adenovirus E1A-associated p33 kinase. Nature 353:174–177.
73. Tsai, L.-H., E. Lees, B. Faha, E. Harlow, and K. Riabowol. 1993. The cdk2 kinase is required for the G1-to-S transition in mammalian cells. Oncogene 8:1593–1602.
74. van den Heuvel, S., and E. Harlow. 1993. Distinct roles for cyclin-dependent kinases in cell cycle control. Science 262:2050–2054.
75. Weisshart, K., and E. Fanning. 1996. Roles of phosphorylation in DNA replication, p. 295-330. *In* M. DePamphilis (ed.), DNA replication in eukaryotic cells. Cold Spring Harbor Press, Cold Spring Harbor, N.Y.
76. Widrow, R. J., R. S. Hansen, H. Kawame, S. M. Gartler, and C. D. Laird. 1998. Very late DNA replication in the human cell cycle. Proc. Natl. Acad Sci. USA 95:11246–11250.
77. Winkler, K. E., K. I. Swenson, S. Kornbluth, and A. R. Means. 2000. Requirement of the prolyl isomerase Pin 1 for the replication checkpoint. Science 287:1644–1647.
78. Zarkowska, T., and S. Mittnach. 1997. Differential phosphorylation of the retinoblastoma protein by G1/S cyclin-dependent kinases. J. Biol. Chem. 272:12738–12746.
79. Zhang, H., M. Gavin, A. Dahiya, A. Postigo, D. Ma, R. Luo, J. Harbour, and D. Dean. 2000. Exit from G1 and S phase of the cell cycle is regulated by repressor complexes containing HDAC-Rb-hSWI/SNF and Rb-hSWI/SNF. Cell 101:79–89.
80. Zhang, H. S., A. A. Postigo, and D. C. Dean. 1999. Active transcriptional repression by the Rb-E2F complex mediates G1 arrest triggered by p16INK4a, TGFbeta, and contact inhibition. Cell 97:53–61.
81. Zhao, J., B. Dynlacht, T. Imai, T. Hori, and E. Harlow. 1998. Expression of NPAT, a novel substrate of cyclin E-CDK2, promotes S phase entry. Genes Dev. 12:456–461.

calcium phosphate coprecipitation technique. After 48 hours, transfected cells were washed with medium containing 2 mM EDTA and then with culture medium. Cells were then challenged with HIV-1 LAI (corresponding to 0.5 μg of p25, which is equivalent to about 40 particles per cell) for 6 hours in the absence or presence of inhibitors. Cells were first washed in medium containing 2 mM EDTA and then washed once with trypsin before incubation (5 min at 37°C) in 5 ml of trypsin. Cells were then replated in 75-cm² flasks containing fresh culture medium and incubated at 37°C for 24 hours. One-milliliter portions of each supernatant were then used to infect CEM cells (5 × 10⁶). The production of HIV-1 (as determined by ELISA of p25) in CEM cultures was measured by assaying culture supernatants 7, 9, and 11 days later. The expression of CD4 antigen on the cell surface of transfected cells was carried out 48 hours after trypsin treatment by FACS analysis with mAb OKT4. [P. R. Rao, M. A. Talle, P. C. Kung, G. Goldstein, *Cell Immunol.* 80, 310 (1983)]. The expression of human CD26 was determined after immunoprecipitation (see Fig. 4, legend).

33. Supported by grants from Institut Pasteur, Paris, and Agence Nationale de la Recherche sur le SIDA. C.C. and E.J. were supported by Association des Artistes contre le SIDA. We thank I. Marié and N. Robert for assistance; A. Laurent-Crawford, M. A. Rey-Cuillé, and D. Cointe for discussion during this work; and B. Bauvois for advice on the assay of DPP IV activity and critical reading of the manuscript. Monoclonal antibody IF7 was kindly provided by C. Morimoto, Dana-Farber Cancer Institute, Harvard Medical School, Boston. The pLXSN-CD4 plasmid was obtained from O. Schwartz, Institut Pasteur, Paris. Plasmid pKG5 expressing human CD26 was kindly provided by B. Fleischer, Universitat Mainz. Additional thanks go to R. Siraganian and B. R. G. Williams for critical reading of the manuscript. Special acknowledgments are forwarded to L. Montagnier for advice and continual support during the realization of this work.

1 October 1993; accepted 18 November 1993

Distinct Roles for Cyclin-Dependent Kinases in Cell Cycle Control

Sander van den Heuvel* and Ed Harlow

The key cell-cycle regulator Cdc2 belongs to a family of cyclin-dependent kinases in higher eukaryotes. Dominant-negative mutations were used to address the requirement for kinases of this family in progression through the human cell cycle. A dominant-negative Cdc2 mutant arrested cells at the G_2 to M phase transition, whereas mutants of the cyclin-dependent kinases Cdk2 and Cdk3 caused a G_1 block. The mutant phenotypes were specifically rescued by the corresponding wild-type kinases. These data reveal that Cdk3, in addition to Cdc2 and Cdk2, executes a distinct and essential function in the mammalian cell cycle.

Cell division is controlled by way of a complex network of biochemical signals that are similar in all eukaryotic cells. Together, these signals regulate specific transitions in the cell cycle. The best characterized transitions are those from G_1 to S phase and from G_2 to mitosis. In yeast, passage through both transition points is regulated by the same protein kinase, the product of the *CDC28* or *cdc2*$^+$ gene for *Saccharomyces cerevisiae* and *Schizosaccharomyces pombe*, respectively (*1*). The Cdc2-CDC28 catalytic subunit requires association with a cyclin regulatory subunit for kinase activity (*2*), and different cyclins are involved in the G_1/S transition (G_1 cyclins) and the G_2/M transition (mitotic cyclins). Multicellular eukaryotes appear to have developed a higher degree of regulation. They express multiple cyclins, like yeast, but also contain multiple catalytic subunits that can interact with these cyclins. Whereas $p34^{cdc2}$ is active and essential at the G_2/M transition (*3*, *4*), a closely related kinase, $p33^{cdk2}$, has been implicated in the initiation of DNA replication (*3*, *5*, *6*).

Twelve human protein kinases have been described that share extensive amino acid sequence identity with $p34^{cdc2}$ (*7*–*10*). These kinases are named temporarily after their amino acid sequence in the PSTAIRE-region (*11*), a domain that is conserved between yeast and human Cdc2. Alternatively, they are designated as cyclin-dependent kinases either when a cyclin partner is identified or when they complement yeast *cdc2-cdc28* mutations. In mammalian cells, Cdc2 associates mainly with A- and B-type cyclins; Cdk2 associates with cyclins A, E, and D; and Cdk4 (formerly PSK-J3), Cdk5 (previously PSSALRE), and Cdk6 (previously PLSTIRE) associate with D-type cyclins (*5*, *8*, *10*, *12*, *13*). Although Cdk3 has never been found in association with cyclins, because of high sequence identity with both Cdc2 and Cdk2 and the ability to complement *cdc28* mutations in yeast, it is classified as a cyclin-dependent kinase (*7*).

The existence of a family of Cdc2-related genes suggests that other kinases, in addition to Cdc2 and Cdk2, may regulate distinct steps in the cell cycle. To investigate the requirement for the other kinases in cell cycle progression, we examined the phenotypic consequences of the inactivation of each kinase. We generated dominant-negative mutations for each Cdc2-related kinase and expressed these mutant forms in human cells. When expressed at high levels, dominant-negative mutations inactivate the function of the wild-type protein by competing for essential interacting molecules (*14*). Data from previous structure-function studies predicted that the mutation of Asp^{145} in Cdk2 (Asp^{146} in Cdc2) might generate dominant-negative mutants. This residue is conserved in all protein kinases and is part of an amino acid stretch, KLAD*FGLAR (*11*) (* marks point of mutation), that is identical in all Cdc2-related genes (*7*, *15*). The equivalent Asp residue in 3′,5′-adenosine monophosphate (cAMP)–dependent kinase is known to be essential in the phospho-transfer reaction (*16*). On the basis of the crystal structure data, this residue presumably chelates Mg^{2+} and orients the β- and γ-phosphates of magnesium adenosine triphosphate (Mg^{2+}ATP) in the catalytic cleft of the enzyme (*17*). Moreover, an Asp to Asn point mutation at this position has been identified in one of the two dominant-negative mutant alleles that have been found for CDC28 in yeast (*18*). Finally, this residue is located outside the regions of cdc2 that are implicated in binding cyclin and $p13^{suc1}$ subunits (*19*).

To determine whether dominant-negative inhibition could lead to specific loss of function, we tested the effects of the Asp to Asn mutation in Cdc2 and Cdk2. For each kinase, four versions were generated: wild type (wt) and mutant, each untagged or modified with an influenza hemagglutinin (HA) epitope tag at the COOH-terminus to allow discrimination between endogenous and exogenous kinases (*20*). When expressed from the inducible *GAL4* promoter in yeast, wild-type tagged and untagged forms of Cdc2 and Cdk2 were able to rescue the *cdc28-4* allele at the nonpermissive temperature (36°C), indicating that the tagged kinases were functional (*21*). The corresponding mutant forms could not rescue *cdc28* mutations at the nonpermissive temperature. Moreover, these mutants interfered with proliferation when induced at the permissive temperature (*21*).

The wild-type and mutant kinases were cloned under the control of the cytomegalovirus (CMV) promoter and were transiently transfected into human U2OS osteosarcoma cells (*20*, *22*). The expression levels of the wild-type and mutant proteins were similar (Fig. 1, B and C). However, in vitro histone H1 kinase activity was only associated with the wild-type kinases (Fig. 1D). The epitope-tagged forms of both wild-type and mutant Cdc2 appeared to associate with

Massachusetts General Hospital Cancer Center, Charlestown, MA 02129.

*To whom correspondence should be addressed.

cyclins A and B1, like endogenous Cdc2. The equivalent forms of Cdk2 bound to cyclins E and A (23). Thus, the Asp to Asn mutation in Cdc2 and Cdk2 abolished their function as kinases but did not affect their ability to associate with cyclins.

If wild-type Cdk2 and Cdc2 are required at specific times in the cell cycle, overexpression of dominant-negative mutants should block cell cycle progression when their kinase activity is required. We evaluated such phenotypes in transient transfection assays by including an expression plasmid for the B cell surface marker CD20. Transfected cells were identified by CD20 staining, and the cell cycle profile of the CD20-positive cells was determined by flow cytometry (22). Within the same experiment, the G_1, S, and G_2/M populations varied by a few percent at most between samples that were independently transfected with the same plasmids. Four different human cell lines with high transfection efficiencies were used in these experiments: U2OS and Saos-2 osteosarcoma cells, C33A cervical carcinoma cells, and T98G glioblastoma cells.

Expression of mutant Cdk2 and mutant Cdc2 changed the cell cycle distribution. The Cdk2 mutant (Cdk2-dn) caused a large increase in the G_1 population, whereas the Cdc2 mutant (Cdc2-dn) led to an increased G_2/M population (Fig. 1A). Transfection of wild-type Cdc2 or Cdk2 did not affect the cell cycle distribution (24). However, the effect of the mutant kinase could be overcome in each case by the cotransfection of a plasmid expressing the corresponding wild-type kinase (Fig. 1A). Whereas the Cdk2-dn caused an effect in all cell lines tested, a Cdc2-dn effect was not observed in C33A cells (25).

Together, these data suggest that the arrests observed after the overexpression of mutant Cdk2 or Cdc2 are the result of specific inhibition of the activity of the endogenous wild-type kinases. The timing of the arrest is distinct for the Cdc2 and Cdk2 mutants and is consistent with the timing of activation of the endogenous kinases, as well as their predicted roles in cell cycle progression (3–6). It is unlikely that the effects are the result of nonspecific toxic effects because plasmids expressing the wild-type kinases gave no such change and could overcome the phenotype of the corresponding mutant. Therefore, we conclude that these mutants act in a dominant-negative fashion and create highly specific loss-of-function phenotypes.

If the effects of Cdk2 and Cdc2 mutants were the result of competition with the endogenous wild-type kinases for cyclin binding, the block should be overcome by overexpression of cyclins. Plasmids expressing cyclins A, B1, B2, C, D1, D3, and E were transfected to test this possibility (26). Rescue of the Cdk2 dominant-negative effect was observed when a reduced amount of the mutant, resulting in a less stringent arrest, was transfected in a 1:2 ratio with the cyclin D1 plasmid (Fig. 2). Cyclins A and E were both less efficient in rescuing the inhibition, but their effectiveness was proportional to the level of their expression. No effects were observed when cyclins B1, B2, C, and D3 were cotransfected with the Cdk2 mutant. In contrast, a reduction of the Cdc2 dominant-negative effect was only observed when either cyclin B1 or B2 was coexpressed (27).

Although the rescue of Cdk2 and Cdc2 mutants by different cyclins points to specificity for G_1 versus mitotic cyclins, the

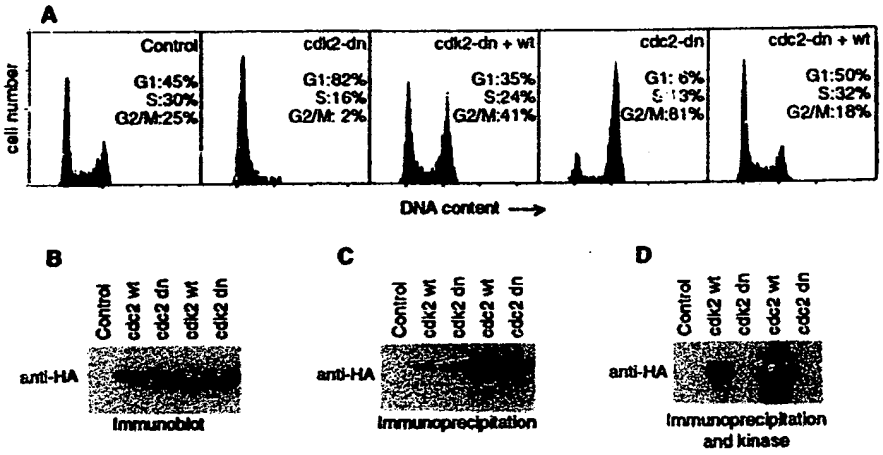

Fig. 1. Expression of mutant forms of Cdk2 and Cdc2 cause specific cell-cycle arrests. U2OS cells were transiently transfected with plasmids expressing the kinases indicated. Control cells are transfected with the CMV-neo-Bam vector. Dominant-negative (dn) and wild-type (wt) kinases were untagged in (A) whereas HA-tagged forms were expressed in (B), (C), and (D). (A) DNA histograms of CD20-positive cell populations in which relative DNA content is plotted against cell number. U2OS cells were transfected with 5 μg of pCMVCD20 plus 20 μg of CMV vector (control), 10 μg of CMVcdk2-dn and 10 μg of CMV vector (cdk2-dn), 10 μg of CMVcdk2-dn and 10 μg of CMVcdk2-wt (cdk2-dn + wt), 10 μg of CMVcdc2-dn and 10 μg of CMV vector (cdc2-dn), or 10 μg of CMVcdc2-dn and 10 μg of CMVcdc2-wt (cdc2-dn + wt). The cells were harvested 48 hours after the removal of DNA precipitates, stained for CD20 expression and DNA content, and analyzed by flow cytometry (33). (B) Expression levels of epitope-tagged mutant and wild-type Cdk2 and Cdc2 as determined by protein immunoblotting. Each lane contains 25 μg of total lysate from cells transfected with 20 μg of the CMV-neo-Bam vector (control) or 20 μg of CMV plasmids expressing the indicated genes. Proteins were separated by SDS-PAGE (polyacrylamide gel electrophoresis), immunoblotted, and probed with the anti-HA monoclonal antibody 12CA5 as described (33). Similar results have been obtained with U2OS and C33A cells. To be able to compare expression levels of the different kinases, we used the same experiment and exposure for Fig. 3, B through D, and Fig. 4. (C) Immunoprecipitation of epitope-tagged mutant and wild-type Cdk2 and Cdc2. The anti-HA tag monoclonal antibody 12CA5 was used to immunoprecipitate ^{35}S-labeled proteins from U2OS cells transfected with the indicated plasmids. Medium was replaced 42 hours after transfection by 3 ml of methionine-free DMEM supplemented with 0.5-mCi ^{35}S-protein labeling mix (NEN) per dish. The cells were lysed in E1A-lysis buffer, and 1/10 of each lysate was immunoprecipitated with 12CA5 and protein A beads as described (33). (D) In vitro histone H1 kinase activity associated with anti-HA immunoprecipitates. Transfections and immunoprecipitations were performed as in (C), but 200 μg of total cellular protein was used for each immunoprecipitation, followed by incubation of the immunoprecipitates in kinase buffer supplemented with 4 μg of histone H1 and 40-μCi [^{32}P]ATP at 30°C for 30 min as described (8).

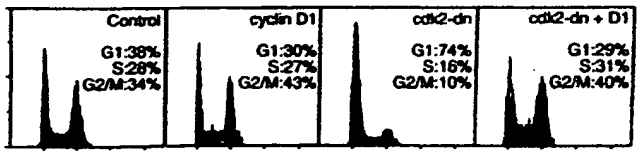

Fig. 2. Rescue of the Cdk2 dominant-negative phenotype by overexpression of cyclin D1. Saos-2 cells were transiently transfected with 2 μg of the CMVCD20 plasmid in combination with 24 μg of the CMV vector (control), 16 μg of cyclin D1 plasmid and 8 μg of the vector (D1), 8 μg of CMVcdk2-dn and 16 μg of vector (cdk2-dn), or 8 μg of CMVcdk2-dn and 16 μg of cyclin D1 plasmid. DNA histograms of CD20-positive Saos-2 cells are shown in which DNA content is plotted versus cell number as in Fig. 1. Cells were harvested 48 hours after the removal of DNA precipitates, stained, and analyzed by flow cytometry as in Fig. 1 and (22).

effect was highly dependent on the relative amount of the rescuing cyclin. Therefore, whereas the alleviation of the dominant-negative effects suggests that cyclin titration is at least part of the mechanism of inhibition, it does not necessarily reveal the cyclins that regulate the kinase in vivo. This restriction is substantiated by our inability to detect endogenous cyclin D1 in Saos-2 cells, although the Cdk2-dn effect could be rescued by cyclin D1 in these cells.

Because dominant-negative inhibition may uncover a requirement for other cyclin-dependent kinases in cell cycle progression, the corresponding Asp to Asn mutation was introduced into other candidate kinases, and both HA-tagged and -untagged forms were generated for each of the wild-type and mutant forms of these kinases. Plasmids expressing these kinases, driven by the CMV promoter, were transfected into several different human cell lines, and their expression and effects on cell cycle distribution were evaluated.

When the Cdk3 mutant was tested in these assays, it was also found to change the cell cycle profile (Fig. 3A), although its expression was found to be relatively low (Fig. 3D). The Cdk3 mutant resulted in an increased G_1 population in all 15 independent experiments in Saos-2 and C33A cells (mean ± SD, 24.2% ± 10.6%). Transfection of plasmids expressing wild-type Cdk3 did not have any noticeable effect.

We have supposed above that alteration of the flow cytometry profile by the dominant-negative mutants results from a block in cell cycle progression. However, another possibility is, in the case of Cdk3, that the mutant causes a G_1 increase as the consequence of the acceleration of S or G_2/M. To discriminate between these possibilities, we examined the effect of nocodazole on the Cdk3 dominant-negative phenotype. Nocodazole, which prevents spindle formation, causes cells that proceed through the cycle to accumulate in M phase. However, this drug should have no effect if the cells are already arrested in G_1. A substantial increase in the S and G_2/M populations was observed in control transfected cells when nocodazole was added 48 hours after transfection and cells were harvested 16 hours later. However, cells expressing the Cdk3-dn mutant did not accumulate in G_2/M (Fig. 3E). The lack of a nocodazole effect was specific for the Cdk3-dn– and CD20-positive cells because the same sample showed a large enrichment of cells at G_2/M when untransfected cells were included (Fig. 3E). Thus, the Cdk3 mutant causes a G_1 arrest and not acceleration of S or G_2/M.

Rescue experiments were performed to test the specificity of dominant-negative Cdk2 and Cdk3 because both mutants caused the accumulation of cells in G_1. The amount of mutant plasmid was reduced to lower the dominant-negative effect and make rescue as sensitive as possible. Whereas wild-type Cdk2 could efficiently overcome the dominant-negative effect of the Cdk2 mutant, wild-type Cdk3 could not (Table 1). In the converse experiment, wild-type Cdk3 neutralized the effect of the Cdk3 mutant, but wild-type Cdk2 did not (Table 1). The fact that dominant-negative Cdk3 causes a G_1 block that can be rescued by wild-type Cdk3 suggests that Cdk3 function is required for G_1 progression.

The same increase in the G_1 population could be obtained with amounts of the Cdk3 mutant 1/10 to 1/20 that of the Cdk2 mutant (28). Because a relatively low amount of the Cdk3 mutant caused a dominant-negative phenotype, the endogenous amount of this kinase might be low. An affinity-purified rabbit antiserum raised against the 10 amino acids of the COOH-terminus of Cdk3 readily detected 36- and 33-kD proteins from Cdk3-transfected cells

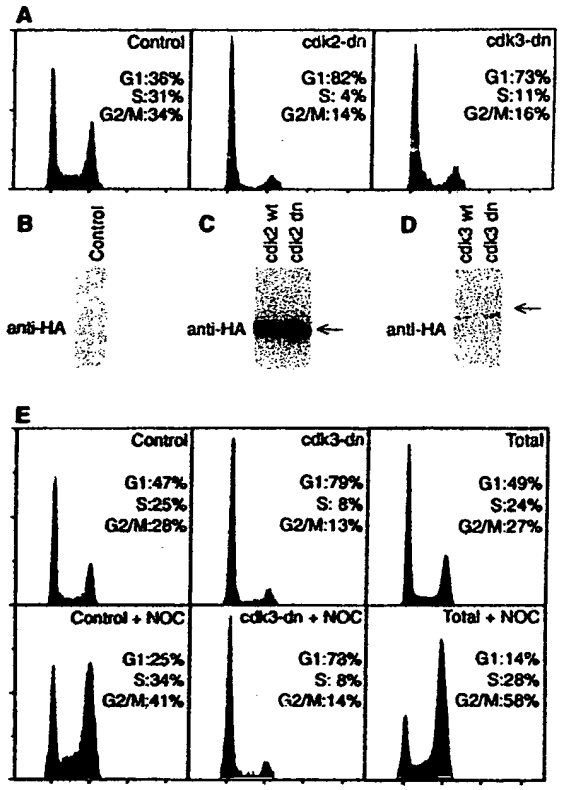

Fig. 3. Dominant-negative Cdk3 is expressed at a relatively low level but causes the accumulation of cells in G_1. (**A**) Saos-2 cells were transiently transfected with 5 μg of the CMVCD20 plasmid in combination with 20 μg of the CMV vector (control), 20 μg of CMVcdk2-dn (cdk2-dn), or 20 μg of CMVcdk3-dn (cdk3-dn). DNA histograms of CD20-positive Saos-2 cells are depicted as in Figs. 1 and 2. The cells were harvested 48 hours after the removal of DNA precipitates, stained, and analyzed by flow cytometry (22). The expression levels of epitope-tagged mutant and wild-type Cdk2 and Cdk3 were determined by protein immunoblotting. Arrows indicate the position of Cdk2 and Cdk3 proteins. Each lane contains 25 μg of total lysate from cells transfected with (**B**) 20 μg of the CMV-neo-Bam vector (control), (**C**) 20 μg of CMVcdk2-dn, or (**D**) 20 μg of Cdk3-dn. Proteins were separated by SDS-PAGE, immunoblotted, and probed with the HA monoclonal antibody 12CA5. To compare expression levels of the different kinases, the same experiment and exposure is used for each panel, as in Fig. 1B and Fig. 4. (**E**) Cells expressing Cdk3-dn are blocked in G_1. Forty-eight hours after transfection, cells were refed with fresh medium (upper panel) or fresh medium containing nocodazole (NOC) (50 ng/ml; lower panel). The cells were harvested, stained, and analyzed by flow cytometry 16 hours later. Saos-2 cells were transfected with 3 μg of CMVCD20 in combination with (left) 22 μg of CMV vector or (middle and right) 22 μg of CMVcdk3-dn. Left and middle histograms show the DNA content of the CD20-positive populations. Histograms at the right show the total population and include ≥90% untransfected cells. The middle and right histograms are derived from the same samples.

Table 1. Rescue of the Cdk2 and Cdk3 dominant-negative phenotype by coexpression of the corresponding wild-type kinases. Saos-2 cells were transiently transfected with 2 μg of the CMVCD20 vector in combination with either 20 μg of vector DNA or 10 μg of each plasmid indicated below. The cell cycle profile of CD20-positive cells (percentage of cells in each stage) was determined by flow cytometry (22). Each value is the mean ± SD of four independent experiments.

	Vector	Cdk2-dn + vector	Cdk2-dn + Cdk2-wt	Cdk2-dn + Cdk3-wt	Cdk3-dn + vector	Cdk3-dn + Cdk3-wt	Cdk3-dn + Cdk2-wt
G_1	43 ± 4	79 ± 5	38 ± 11	77 ± 5	66 ± 12	45 ± 7	55 ± 9
S	33 ± 4	14 ± 6	27 ± 3	15 ± 4	20 ± 8	26 ± 1	21 ± 2
G_2/M	24 ± 1	7 ± 3	35 ± 11	8 ± 3	14 ± 4	29 ± 6	24 ± 7

and proteins with the same mobility at much lower levels in untransfected normal human fibroblasts (WI38) and human tumor cell lines (29). The expression of the Cdk3 proteins was roughly two orders of magnitude lower than that of Cdk2, as determined from the signal obtained when Cdk2 and Cdk3 immunoprecipitations were immunoblotted and probed with an anti-PSTAIRE monoclonal antibody. To date, we have been unable to detect cyclins associated with Cdk3 in experiments in which Cdk2- and Cdc2-associated cyclins were readily detected. However, cotransfection with cyclins D1 or E could largely overcome the dominant-negative Cdk3 effect, which is an indication that Cdk3 requires a cyclin partner for its function (27).

Transfection of plasmids encoding wild-type or mutant forms of Cdk4, Cdk5, Cdk6, and PCTAIRE-1 had no noticeable effect on the cell cycle distribution of transfected C33A, Saos-2, U2OS, or T98G cells (Fig. 4). Moderate (Cdk6) to very high levels of each kinase were found in transfected cells (Fig. 4). In several cases, we tested for redundancy by cotransfection of related kinases. For example, Cdk4 and Cdk6 share 71% identity in amino acid sequence (7); however, cotransfection of the Cdk4 and Cdk6 mutants did not affect cell cycle distribution. Neither did combinations involving three or four of these mutant kinases. In this assay system, we cannot identify an essential role for the Cdk4, Cdk5, Cdk6, or PCTAIRE-1 kinases in cell cycle progression, but experiments in other systems will be required to evaluate such functions. Kinase activity associated with Cdk5 has been detected solely in terminally differentiated neuronal cells, suggesting that its function is unrelated to cell division (30).

Data from this and other studies suggest that different catalytic subunits have evolved in higher eukaryotes to control distinct cell cycle events (3–6). In addition to Cdc2 and Cdk2, Cdk3 appears to be one of such catalytic subunits. The phenotype of the dominant-negative Cdk3 mutant suggests that cellular Cdk3 executes a G_1 regulatory function. Several observations support this conclusion: (i) The effects of dominant-negative cyclin-dependent kinases were highly specific. The phenotypes of mutant Cdc2 and Cdk2 are distinct and consistent with their presumed functions, and mutant forms of several closely related kinases did not have any cell cycle effect. (ii) Coexpression of wild-type Cdk3 efficiently reversed the effect of mutant Cdk3. (iii) Growth arrest by dominant-negative Cdk3 was observed at relatively low expression levels, in agreement with the low amount of the endogenous protein. (iv) Overexpression of G_1 cyclins can overcome the effect of dominant-negative Cdk3. (v) In previous work, Cdk3 was shown to be the only kinase in addition to Cdk2 and Cdc2 that could rescue yeast *cdc28* mutations (7). Together, our data suggest that the Cdk2 and Cdk3 kinases play essential and independent roles in G_1/S progression.

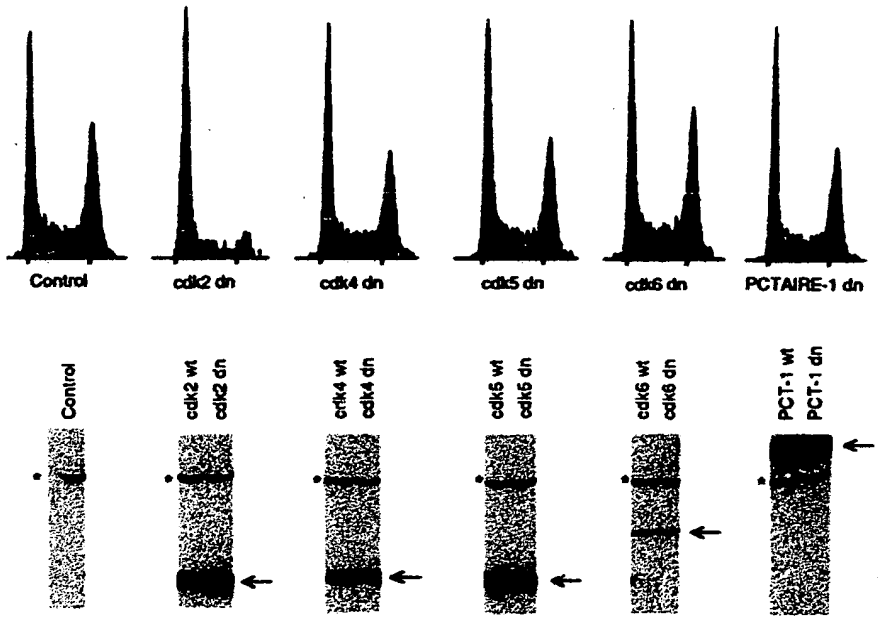

Fig. 4. Expression of mutant Cdk4, Cdk5, Cdk6, or PCTAIRE-1 (PCT-1) does not result in significant changes in cell cycle distribution. The top panel contains DNA histograms from CD20-positive C33A cells. DNA content is displayed versus cell number, as in Fig. 1. C33A cells were transiently transfected with 5 μg of pCMVCD20 in combination with 20 μg of plasmid DNA expressing the kinases indicated. The cells were harvested 48 hours after the removal of DNA precipitates, stained, and analyzed by flow cytometry (22). The lower panel shows the expression levels of epitope-tagged mutant and wild-type kinases as determined by protein immunoblotting. Arrows indicate the positions of each kinase. Asterisks indicate a cellular protein recognized by the 12CA5 antibody. Each lane contains 25 μg of total lysate from transfected C33A cells. Proteins were separated by SDS-PAGE, immunoblotted, and probed with the anti-HA monoclonal antibody 12CA5. To compare expression levels of the different kinases, the same exposure was used for each panel, as in Figs. 1B and 3, B through D.

REFERENCES AND NOTES

1. L. H. Hartwell *et al.*, *Science* 183, 46 (1974); P. Nurse and Y. Bissett, *Nature* 292, 558 (1981); S. I. Reed and C. Wittenberg, *Proc. Natl. Acad. Sci. U.S.A.* 87, 5697 (1990).
2. G. Draetta, *Trends Biochem. Sci.* 15, 378 (1990); S. L. Forsburg and P. Nurse, *Annu. Rev. Cell Biol.* 7, 227 (1991); J. Pines and T. Hunter, *New Biol.* 2, 389 (1990).
3. F. Fang and J. W. Newport, *Cell* 66, 731 (1991).
4. J. P. Th'ng *et al.*, *ibid.* 63, 313 (1990); K. Riabowol *et al.*, *ibid.* 57, 393 (1989).
5. L.-H. Tsai, E. Lees, B. Faha, E. Harlow, K. Riabowol, *Oncogene* 8, 1593 (1993).
6. M. Pagano *et al.*, *J. Cell Biol.* 121, 101 (1993).
7. M. Meyerson *et al.*, *EMBO J.* 11, 2909 (1992).
8. L.-H. Tsai *et al.*, *Nature* 353, 174 (1991).
9. S. K. Hanks, *Proc. Natl. Acad. Sci. U.S.A.* 84, 388 (1987); J. Ninomiya-Tsuji, S. Nomoto, H. Yasuda, S. I. Reed, K. Matsumoto, *ibid.* 88, 9006 (1991); S. J. Elledge and M. R. Spottswood, *EMBO J.* 10, 2653 (1991); Y. Lapidot-Lifson *et al.*, *Proc. Natl. Acad. Sci. U.S.A.* 89, 579 (1992).
10. Y. Xiong, H. Zhang, D. Beach, *Cell* 71, 505 (1992).
11. Abbreviations for the amino acid residues: A, Ala; C, Cys; D, Asp; E, Glu; F, Phe; G, Gly; H, His; I, Ile; K, Lys; L, Leu; M, Met; N, Asn; P, Pro; Q, Gln; R, Arg; S, Ser; T, Thr; V, Val; W, Trp; and Y, Tyr.
12. J. Pines and T. Hunter, *Nature* 346, 760 (1990); G. Draetta and D. Beach, *Cell* 54, 17 (1988); J. Pines and T. Hunter, *ibid.* 58, 833 (1989); J. Rosenblatt, Y. Gu, D. O. Morgan, *Proc. Natl. Acad. Sci. U.S.A.* 89, 2824 (1992); A. Koff *et al.*, *Science* 257, 1689 (1992); E. Lees, B. Faha, V. Dulić, S. I. Reed, E. Harlow, *Genes Dev.* 6, 1874 (1992); V. Dulić, E. Lees, S. I. Reed, *Science* 257, 1958 (1992); H. Matsushime *et al.*, *Cell* 71, 323 (1992).
13. M. Meyerson and E. Harlow, *Mol. Cell. Biol.*, in press.
14. I. Herskowitz, *Nature* 329, 219 (1987).
15. S. K. Hanks, A. M. Quinn, T. Hunter, *Science* 241, 42 (1988).
16. S. S. Taylor *et al.*, *Trends Biochem. Sci.* 18, 84 (1993).
17. D. R. Knighton *et al.*, *Science* 253, 407 (1991); D. R. Knighton *et al.*, *ibid.*, p. 414; H. L. DeBondt *et al.*, *Nature* 363, 595 (1993).
18. M. D. Mendenhall, H. E. Richardson, S. I. Reed, *Proc. Natl. Acad. Sci. U.S.A.* 85, 4426 (1988).
19. B. Ducommon, P. Brambilla, G. Draetta, *Mol. Cell. Biol.* 11, 6177 (1991); B. Ducommon *et al.*, *EMBO J.* 10, 3311 (1991).
20. Point mutations were introduced by in vitro mutagenesis. The DNA clones containing the open reading frames for each kinase were inserted into the Bam HI site of the pSelect vector (Promega), denatured, annealed to two different primers, and used for DNA synthesis, ligation, and transformation. One primer that contained a single mismatch in the middle was specific for each kinase and overlapped with most of the KLADFGL (*11*) encoding sequence. The DNA clones containing mutations were identified by DNA sequencing after a second transformation. A 7–amino acid epitope tag (YDVPDYA) was inserted just before the stop codon of each kinase, either by in vitro mutagenesis or by polymerase chain reaction (PCR). DNA sequencing was used to confirm the sequence of the tag. The complete open reading frame of the clones generated

Treatment of Relapsed Chronic Lymphocytic Leukemia by 72-Hour Continuous Infusion or 1-Hour Bolus Infusion of Flavopiridol: Results from Cancer and Leukemia Group B Study 19805

John C. Byrd,[1] Bercedis L. Peterson,[2] Janice Gabrilove,[3] Olatoyosi M. Odenike,[4] Michael R. Grever,[1] Kanti Rai,[5] Richard A. Larson,[4] and the Cancer and Leukemia Group B

Abstract **Purpose:** [redacted]

Patients and Methods: Patients with previously treated CLL were enrolled in two sequentially done phase II studies. Patients in the first trial received flavopiridol (50 mg/m^2/d) as a continuous infusion (CI) for 72 hours every 2 weeks. Patients in the second trial received flavopiridol 50 mg/m^2 as a 1-hour bolus (IVB) daily for 3 days repeated every 3 weeks. Patients received up to 12 (CI cohort) or 8 (IVB cohort) cycles of therapy.

Results: Fifteen patients were enrolled in the 72-hour CI phase II trial; 6 (40%) had intermediate-risk (Rai stage I or II) and 9 (60%) had high-risk (Rai stage III and IV) stages. No responses were noted in this group; 27% had stable disease and 73% had progressive disease. Thirty-six patients were enrolled in the second IVB trial; with 13 (36%) having intermediate and 23 (64%) having high-risk disease. Four patients (11%) had partial responses, 19 (53%) had stable disease, and 13 (36%) had progressive disease. The progression-free survival for responders in the IVB trial was 3, 3, 9, and 19 months. The median progression-free survival was 2 months (95% confidence interval (95% CI), 1.8-3.8) for patients in the CI trial and 3 months (95% CI, 2.5-7.4) for the IVB trial. The median overall survival was 27 months (95% CI, 20-42) for the CI trial and 24 months (95% CI, 18-31) for the IVB trial. Toxicity was manageable and included mainly myelosuppression, infections, diarrhea, and fatigue.

[redacted]

Chronic lymphocytic leukemia (CLL) is one of the most common types of adult leukemia but is incurable with current therapies including fludarabine, rituximab, and alemtuzumab. Developing new therapies for patients with CLL, particularly those with fludarabine-refractory disease or p53 mutations and/or deletions, remains a high priority.

The broad cyclin-dependent kinase inhibitor flavopiridol (National Service Center 649890) may be one such therapy. Studies from several laboratories noted that flavopiridol effectively induces apoptosis in both CLL cell lines and human CLL cells *in vitro* at concentrations attainable in the clinic (1-3). Additionally, flavopiridol seems to be a p53-independent agent and down-modulates select antiapoptosis genes including *mcl-1* and *XIAP* (1-3). These preclinical studies provide justification for pursuing clinical studies of flavopiridol in CLL.

A variety of different schedules of administration have been explored with flavopiridol including 72-hour continuous infusion (CI; refs. 4, 5), 24-hour CI (6), and a 1-hour bolus (IVB; ref. 7). The 1-hour IVB schedule recommended for phase II studies was 50 mg/m^2 administered on days 1, 2, and 3 (7). The trials all have generally short duration neutropenia, diarrhea, cytokine release syndrome (8), and fatigue. No significant clinical activity has been observed using 72-hour infusion flavopiridol as a single agent for solid tumors and mantle cell lymphoma (9-13). Modest activity in mantle cell lymphoma (12% partial response rate; ref. 14) has been noted with the 1-hour 50 mg/m^2 × 3 days schedule. Herein, results

Authors' Affiliations: [1]Division of Hematology-Oncology, Department of Medicine, The Ohio State University, Columbus, Ohio; [2]Cancer and Leukemia Group B, Statistical Center, Duke University Medical Center, Durham, North Carolina; [3]Division of Neoplastic Diseases, Mount Sinai Hospital, New York, New York; [4]Department of Medicine, The University of Chicago, Chicago, Illinois; and [5]Divisions of Hematology and Oncology, Long Island Jewish Medical Center, New Hyde Park, New York

Received 11/9/04; revised 3/9/05; accepted 4/15/05.

Grant support: National Cancer Institute (CA31946) to the Cancer and Leukemia Group B (Richard L. Schilsky, M.D., Chairman), the Sidney Kimmel Cancer Research Foundation (J.C. Byrd), Leukemia and Lymphoma Society of America (J.C. Byrd), and D. Warren Brown Foundation (J.C. Byrd). J.C. Byrd is a clinical scholar of the Leukemia and Lymphoma Society of America. The content of this manuscript is solely the responsibility of the authors and does not necessarily represent the official views of the National Cancer Institute.

The costs of publication of this article were defrayed in part by the payment of page charges. This article must therefore be hereby marked *advertisement* in accordance with 18 U.S.C. Section 1734 solely to indicate this fact.

Requests for reprints: John C. Byrd, Division of Hematology-Oncology, The Ohio State University, Starling Loving Hall, Room 302, Columbus, OH 43210. Phone: 614-293-9321; E-mail: byrd-3@medctr.osu.edu.

of a Cancer and Leukemia Group B trial that pursued two sequential studies examining the efficacy of single agent flavopiridol utilizing the 72-hour CI and 1-hour IVB schedules in CLL are described.

Materials and Methods

Subjects. Patients were enrolled in this multicenter trial done by the Cancer and Leukemia Group B after approval by local institutional review boards. All patients gave written informed consent. Patients were required to have histologically documented CLL as defined by the modified National Cancer Institute (NCI) guidelines (15) and to require therapy according to these same criteria. Patients with stage I and II disease had symptomatic lymphadenopathy. Patients had all received at least one prior chemotherapy regimen but not greater than three regimens. Patients may have received one prior nonradiolabeled antibody treatment (e.g., Campath-1H or rituximab) in addition to the maximum limit of three chemotherapy treatments. Required clinical features included age older than 17 years, symptomatic by the NCI 96 criteria (15), and not pregnant. The serum creatinine and total bilirubin levels were required to be less than or equal to 1.5 times the normal value.

Pretreatment evaluation. All patients underwent pretreatment screening that included history, physical examination, laboratory, and X-ray studies before entry into the trial. These tests included a complete blood count with differential, electrolytes, blood urea nitrogen, creatinine, total protein, albumin, calcium, phosphate, lactate dehydrogenase, uric acid, total bilirubin, alanine aminotransferase, aspartate aminotransferase, immunoglobulins, direct antiglobulin test, chest X-ray, and bone marrow aspirate and biopsy.

Treatment and dose modifications. All patients received allopurinol 300 mg/d beginning 1 day before initiation of treatment and continued during the first 2 weeks of therapy. The first trial (n = 15 patients) administered flavopiridol (50 mg/m^2) daily for 3 consecutive days by continuous infusion every 2 weeks. Patients could discontinue therapy for stable disease without improvement after four treatments. Otherwise, patients continued therapy in the absence of progression or toxicity that prohibited further treatment for a maximum of 12 treatments of flavopiridol. The second trial (n = 36 patients) given flavopiridol (50 mg/m^2) as a 1-hour IVB daily for 3 consecutive days repeated every 3 weeks. Patients could discontinue therapy for stable disease without improvement after two treatments. Otherwise, patients continued therapy in the absence of progression or toxicity that prohibited further treatment for a maximum of eight treatments of flavopiridol.

If treatment was tolerated with grade 2 or less diarrhea or fatigue that resolves within 5 days and no other grade 3 toxicity, then the dose of flavopiridol remained constant. If grade 3 or 4 diarrhea developed, then diarrhea treatment with cholestipol (5 grams orally every 6 hours) and loperamide (4 mg every 4 hours while awake) was initiated immediately and prophylaxis was administered with subsequent treatments. For grade 3 diarrhea, the dose was not reduced unless this recurred despite prophylaxis. Patients developing grade 4 diarrhea had a 33% dose reduction (i.e., to 2 days of therapy), but were reescalated to full dose on subsequent cycles if severe diarrhea did not recur. Patients experiencing fatigue were not re-treated until this symptom has resolved to grade 2 or less. Patients experiencing grade 3 or 4 fatigue for greater than 5 days had a 33% dose reduction. If recurrent grade 3 or fatigue persisted at this lower dose, a second dose reduction occurred and patients received 1 day of therapy (50 mg/m^2 for 1 day; total dose, 50 mg/m^2). If recurrent fatigue persisted at this dose, the patient was removed from protocol therapy. Grade 3 or 4 hematologic toxicity mandated a 33% dose reduction. For renal, pulmonary, hepatic, and other toxicities of grade 3 and greater related to flavopiridol, therapy was discontinued.

Assessment of toxicity and response. Hematologic toxicity was graded according to the modified NCI criteria for CLL (15) and nonhematologic toxicity was graded according to the NCI Common Toxicity Criteria. Patients were assessed for disease response with a detailed clinical evaluation (physical exam with lymph node, liver, and spleen measurement) and complete blood count with differential after four and eight treatments in the CI schedule and after three and six cycles of therapy in the IVB schedule. Criteria for response used the Revised NCI-sponsored Working Group Guidelines (15). As specified by these guidelines, a response had to be maintained for a period of 2 months. Response duration was defined in responders from the time the response was first noted until progression or last follow-up. Progression-free survival was defined similarly, except that follow-up began for all patients from the time of initiation of treatment. Progression was defined using the NCI 96 criteria (15). Survival time was measured from the time of initial treatment until the time last seen alive (censored) or death (event). Survival probabilities for progression free survival and overall survival were estimated using the method of Kaplan-Meier (16). The SEs for these estimates were obtained using the variance estimate as previously described (17).

Results

Patient characteristics. Fifteen patients, nine of whom were fludarabine-refractory, were enrolled and treated in the 72-hour CI trial between March 01, 1999 and October 11, 2000, after which time further enrollment was discontinued due to lack of efficacy. Thirty-six patients, 18 of whom were fludarabine refractory, were then enrolled and treated in the 1-hour IVB schedule of flavopiridol between November 27, 2000 and June 18, 2002. The pretreatment features of the patients enrolled in the two studies are summarized in Table 1.

Response to treatment and treatment outcome. All patients were evaluable for response and toxicity assessments. Among the 15 patients enrolled in the 72-hour CI trial, there were no complete or partial responses. Four patients (27%) had stable disease and 11 (63%) had progressive disease. No patients completed all 12 courses of therapy with a median of 3.5 treatments taken (range 1-10). No evidence of acute tumor lysis was observed. The median progression-free survival for the entire group was 2 months (95% confidence interval, 2-4), as depicted in Fig. 1. Thirteen patients have died; the median survival is 27 months (95% confidence interval, 20-42), as depicted in Fig. 2.

Among the 36 patients enrolled in the 1-hour IVB trial, there were no complete response; 4 (11%) showed partial response, 19 (53%) had stable disease, and 13 (36%) had progressive disease. All four patients who responded had fludarabine refractory CLL. Seven patients completed all eight planned courses of therapy (median, 3; range, 1-8). One patient had evidence of tumor lysis syndrome with an increase in potassium to 5.8 mmol/L and phosphate to 5.3 mg/dL accompanied by a drop in WBC from 267 $\times$ 10^9/L to 62 $\times$ 10^9/L baseline to day 3 of therapy. This patient had concomitant grade 3 diarrhea, was managed medically with hydration and urine alkalination, and did not require dialysis. This patient attained a partial response that was maintained for 3 months. The time to progression for each of the four responders was 3, 3, 9, and 19 months. The median progression-free survival for the entire group was 3 months (95% confidence interval, 3-7) as depicted in Fig. 1. Twenty-three (64%) of the patients have died after a median survival of 24 months (95% confidence interval, 18-31) as depicted in Fig. 2.

Toxicity. The toxicities observed in each of the two trials are summarized in Table 2. Overall, patients experienced one or more grade 3 and 4 toxicities; 20% and 27% for the CI trial and

Table 1. Pretreatment characteristics of patients enrolled in CI and IVB studies

	72-hour CI trial, *N* = 15	1-hour IVP trial, *N* = 36
Median age (range)	63 (47-80)	61 (37-81)
Stage		
Rai intermediate risk	40%	36%
Rai high risk	60%	64%
% Female	27%	33%
Performance status		
0	53%	34%
1	47%	60%
2	0%	6%
Median number of prior therapies (range)	2 (1-3)	2 (1-5)
% Fludarabine refractory	60%	50%
Median (range) leukocyte count ($\times 10^9$/L)	15.7 (1-33.1)	16.4 (0.7-96.6)
Median (range) hemoglobin count (g/dL)	11.3 (7.9-17.4)	11.1 (5.9-16.0)
Median (range) platelet count ($\times 10^9$/L)	80 (9-209)	85 (11-339)
% with splenomegaly	67%	47%
% with hepatomegaly	29%	18%
% with adenopathy	80%	86%

39% and 33% for the IVB trial. Common grade 3 and 4 toxicities in both studies included granulocytopenia, anemia, infection, diarrhea, and fatigue. There were no grade 5 toxicities in the CI trial. The fatal myocardial infarction found in one patient in the IVB trial was not treatment related as the patient developed progressive disease on day 17 of cycle 5 with a rapidly enlarging spleen. He was admitted for small bowel obstruction and subsequently suffered a fatal myocardial infarction.

Discussion

In this study, we have observed that the cyclin-dependent kinase inhibitor flavopiridol, when administered as a 72-hour CI every 2 weeks, has no clinical activity in previously treated CLL. In contrast, flavopiridol by IVB daily for 3 consecutive days every 3 weeks showed modest activity, with 4 patients (11%) attaining a partial response, 19 (53%) having stable disease, and only 13 (36%) having progressive disease as their best response. Although the four responding patients had fludarabine-refractory disease, the overall survival of the entire group of patients is longer than the large alemtuzumab phase II trial (18), likely reflective of a less heavily treated population. Unfortunately, this study did not include genetic studies for interphase cytogenetics, p53 mutational status, V_H mutational status, or ZAP-70 expression. Future investigation of flavopiridol should include these. With both schedules of administration, toxicity was modest, mainly consisting of reversible myelosuppression, diarrhea, infection, and fatigue. Overall, these studies suggest that flavopiridol in CLL is highly schedule dependent with predictable toxicity with clinical

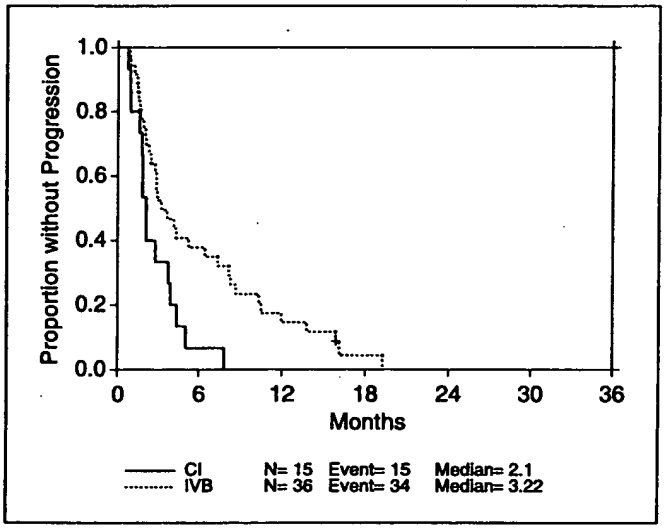

Fig. 1. Progression-free survival for all patients with previously treated CLL treated with flavopiridol by 72-hour CI (*black line*, $n = 15$) and 1-hour IVB daily for 3 consecutive days (*dotted line*, $n = 36$) in Cancer and Leukemia Group B 19805.

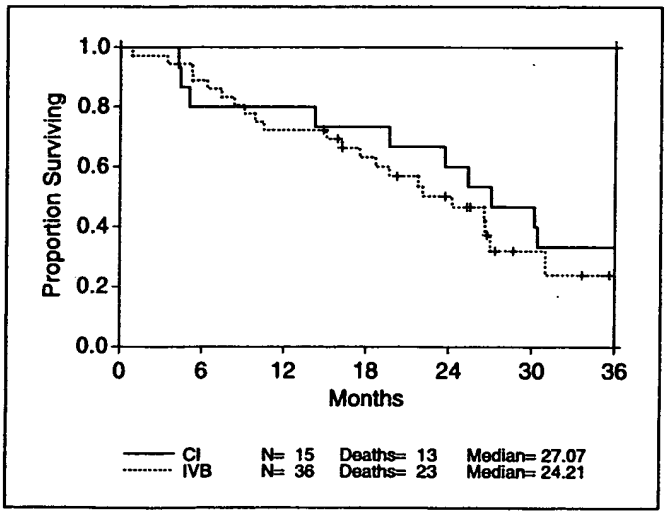

Fig. 2. Overall survival for all patients with previously treated CLL treated with flavopiridol by 72-hour CI (*black line*, $n = 15$) and 1-hour IVB daily for 3 consecutive days (*dotted line*, $n = 36$) in Cancer and Leukemia Group B 19805.

Table 2. Number (%) of patients with toxicity during treatment

Toxicity	Grade 1, *n* (%)	Grade 2, *n* (%)	Grade 3, *n* (%)	Grade 4, *n* (%)
Neutropenia				
CI	1 (7)	1 (7)	1 (7)	4 (27)
IVB	4 (11)	2 (6)	9 (25)	9 (25)
Thrombocytopenia				
CI	4 (27)	1 (7)	3 (20)	1 (7)
IVB	6 (17)	9 (25)	6 (17)	2 (6)
Anemia				
CI	0 (0)	0 (0)	0 (0)	0 (0)
IVB	10 (28)	10 (28)	2 (6)	1 (3)
Infection				
CI	1 (7)	2 (13)	3 (20)	0 (0)
IVB	0 (0)	3 (8)	7 (19)	2 (6)
Diarrhea				
CI	2 (13)	2 (13)	1 (7)	0 (0)
IVB	10 (28)	11 (31)	13 (36)	0 (0)
Cough				
CI	0 (0)	0 (0)	0 (0)	0 (0)
IVB	0 (0)	0 (0)	1 (3)	0 (0)
Dyspnea				
CI	0 (0)	1 (7)	0 (0)	0 (0)
IVB	0 (0)	2 (6)	1 (3)	0 (0)
Fatigue				
CI	4 (27)	2 (13)	0 (0)	0 (0)
IVB	17 (47)	8 (22)	4 (11)	0 (0)
Weight loss				
CI	1 (7)	0 (0)	1 (7)	0 (0)
IVB	0 (0)	0 (0)	0 (0)	0 (0)
Pain				
CI	3 (20)	1 (7)	0 (0)	0 (0)
IVB	4 (11)	3 (8)	0 (0)	0 (0)
	4 (27)	1 (7)	0 (0)	0 (0)
	2 (6)	1 (3)	0 (0)	0 (0)
Maximum toxicity (per patient)				
CI	1 (7)	6 (40)	3 (20)	4 (27)
IVB	2 (6)	6 (17)	14 (39)	12 (33)

activity. Indeed, the efficacy observed in the 72-hour CI (13) and 1-hour IVB (14) studies of mantle cell lymphoma mimics that observed in CLL. Further schedule optimization might therefore lead to improved efficacy of single agent flavopiridol in lymphoid diseases.

Despite the remarkable activity of flavopiridol *in vitro* with both short and long exposures, one must ask why more clinical activity was not observed in this trial. Indeed, pharmacokinetic data from the 72-hour phase I and II CI studies done by others attained plasma drug concentrations (200-400 nmol/L) that induced apoptosis *in vitro* (4, 5, 12, 19). Although no pharmacokinetic studies were done in this trial, studies done to date have shown relatively consistent pharmacokinetics across different patient populations (4, 5, 12, 19). One explanation for poor concordance between the promising *in vitro* results and disappointing clinical results may be due to increased flavopiridol drug binding to human plasma proteins as compared with protein in the FCS typically used for *in vitro* studies with this agent. Based on poor results in the 72-hour and 24-hour trials done by Aventis Pharmaceuticals in fludarabine-refractory CLL (20)[7] our group investigated the possibility that differential protein binding could exist between these two culture media. These studies showed that substitution of human plasma for FCS *in vitro* resulted in a decrease in free drug level from 63-100% to 5-8%, with an increase in 1-hour and 24-hour LC_{50} values from 670 and 120 nmol/L to 3,510 and 470 nmol/L, respectively (21). This increase in the *in vitro* LC_{50} may be critical, as the 24-hour LC_{50} of 470 nmol/L has not been achieved *in vivo* with the 72-hour CI schedule (12, 22). Additionally, the 1-hour LC_{50} concentration for CLL cells in human serum was not obtained in the solid tumor phase I trial exploring this schedule (7). Thus, the CI or IVB dosing schedule may not achieve pharmacologically effective drug concentrations of flavopiridol, thereby explaining the absence of activity in the CI schedule and the marginal activity with the IVB schedule described herein.

[7] Jose Ramon-Suarez, personal communication.

Where does the development of flavopiridol in CLL go from here? Given the novel mechanism of action of this agent and the ability of flavopiridol to induce apoptosis independent of p53 dysfunction, this agent remains a worthwhile therapy to develop. One strategy includes combining the 1-hour or 24-hour schedule of administration with other therapeutic agents to generate synergy in previously described tumor systems *in vitro* (23–27). This is currently being pursued by several investigators with fludarabine, rituximab, and other targeted therapies such as the histone deacetylase inhibitor depsipeptide. Another strategy would be to further optimize the schedule of administration of flavopiridol given the schedule dependence observed to date. Based on the pharmacokinetic studies described above related to differential protein binding in FCS and human serum, pharmacokinetic modeling from the Aventis 24-hour CI study suggested that a 30-minute IVB followed by a 4-hour CI schedule could attain a concentration of flavopiridol that induces apoptosis in primary CLL cells. Based on this modeling, an NCI-sponsored clinical study has been initiated in fludarabine refractory CLL. In this study, a 30 mg/m^2 dose is administered as a bolus followed by a second 30 mg/m^2 4-hour dose (total 60 mg/m^2 per week) every week for 4 consecutive weeks followed by a 2-week observation period with 10 mg/m^2 incremental increases in the IVB and 4-hour dose with subsequent cohorts. A preliminary report of this study has included responses and a dose-limiting toxicity of acute tumor lysis syndrome (28). Based on these promising results, other trials in lymphoid malignancies, acute leukemia, and solid tumors are now being pursued utilizing this novel schedule. Alternative schedules of administration or combinations with other drugs may be required to fully exploit the benefits of flavopiridol in lymphoid malignancies.

Appendix 1

The following institutions participated in this study:

Cancer and Leukemia Group B Statistical Center, Durham, North Carolina—Stephen George, Ph.D., supported by CA33601.

Christiana Care Health Services, Inc., CCOP, Wilmington, Delaware—Stephen Grubbs, M.D.., supported by CA45418.

Dartmouth Medical School, Norris Cotton Cancer Center, Lebanon, New Hampshire—Marc S. Ernstoff, M.D., supported by CA04326.

Duke University Medical Center, Durham, North Carolina—Jeffrey Crawford, M.D., supported by CA47577.

Illinois Oncology Research Association, Peoria, Illinois—John W. Kugler, M.D., supported by CA35113.

Mount Sinai Medical Center, Miami, Florida—Rogerio Lilenbaum, M.D., supported by CA45564.

Mount Sinai School of Medicine, New York, New York—Lewis R. Silverman, M.D., supported by CA04457.

North Shore-Long Island Jewish Medical Center, Manhasset, New York—Daniel R. Budman, M.D., supported by CA35279.

Roswell Park Cancer Institute, Buffalo, New York—Ellis Levine, M.D., supported by CA02599.

Southeast Cancer Control Consortium, Inc., CCOP, Goldsboro, North Carolina—James N. Atkins, M.D., supported by CA45808.

The Ohio State University Medical Center, Columbus, Ohio—Clara D. Bloomfield, M.D., supported by CA77658.

University of California at San Diego, San Diego, California—Stephen L. Seagren, M.D., supported by CA11789.

University of California at San Francisco, San Francisco, California—Alan P. Venook, M.D., supported by CA60138.

University of Chicago Medical Center, Chicago, Illinois—Gini Fleming, M.D., supported by CA41287.

University of North Carolina at Chapel Hill, Chapel Hill, North Carolina—Thomas C. Shea, M.D., supported by CA47559.

University of Illinois MBCCOP, Chicago, Illinois—Lawrence E. Feldman, M.D., supported by CA74811.

University of Maryland Greenebaum Cancer Center, Baltimore, Maryland—Martin Edelman, M.D., supported by CA31983.

University of Minnesota, Minneapolis, Minnesota—Bruce A. Peterson, M.D., supported by CA16450.

University of Missouri/Ellis Fischel Cancer Center, Columbia, Missouri—Michael C. Perry, M.D., supported by CA12046.

University of Nebraska Medical Center, Omaha, Nebraska—Anne Kessinger, M.D., supported by CA77298.

University of Tennessee Memphis, Memphis, Tennessee—Harvey B. Niell, M.D., supported by CA47555.

Walter Reed Army Medical Center, Washington, District of Columbia—Joseph J. Drabeck, M.D., supported by CA26806.

Washington University School of Medicine, St. Louis, Missouri—Nancy Bartlett, M.D., supported by CA77440.

References

1. Kitada S, Zapata JM, Andreeff M, et al. Protein kinase inhibitors flavopiridol and 7-hydroxy-staurosporine down-regulate antiapoptosis proteins in B-cell chronic lymphocytic leukemia. Blood 2000;96:393–7.
2. Byrd JC, Shinn C, Waselenko JK, et al. Flavopiridol induces apoptosis in chronic lymphocytic leukemia cells via activation of caspase-3 without evidence of bcl-2 modulation or dependence on functional p53. Blood 1998;92:3804–16.
3. Konig A, Schwartz GK, Mohammad RM, et al. The novel cyclin-dependent kinase inhibitor flavopiridol down-regulates Bcl-2 and induces growth arrest and apoptosis in chronic B-cell leukemia lines. Blood 1997;90:4307–12.
4. Thomas JP, Tutsch KD, Cleary JF, et al. Phase I clinical and pharmacokinetic trial of the cyclin-dependent kinase inhibitor flavopiridol. Cancer Chemother Pharmacol 2002;50:465–72.
5. Senderowicz AM, Headlee D, Stinson SF, et al. Phase I trial of continuous infusion flavopiridol, a novel cyclin-dependent kinase inhibitor, in patients with refractory neoplasms. J Clin Oncol 1998;16:2986–99.
6. Schwartz GK, O'Reilly E, Ilson D, et al. Phase I study of the cyclin-dependent kinase inhibitor flavopiridol in combination with paclitaxel in patients with advanced solid tumors. J Clin Oncol 2002;20:2157–70.
7. Tan AR, Headlee D, Messmann R, et al. Phase I clinical and pharmacokinetic study of flavopiridol administered as a daily 1-hour infusion in patients with advanced neoplasms. J Clin Oncol 2002;20:4074–82.
8. Messmann RA, Ullmann CD, Lahusen T, et al. Flavopiridol-related proinflammatory syndrome is associated with induction of interleukin-6. Clin Cancer Res 2003;9:562–70.
9. Aklilu M, Kindler HL, Donehower RC, et al. Phase II study of flavopiridol in patients with advanced colorectal cancer. Ann Oncol 2003;14:1270–3.
10. Schwartz GK, Ilson D, Saltz L, et al. Phase II study of the cyclin-dependent kinase inhibitor flavopiridol administered to patients with advanced gastric carcinoma. J Clin Oncol 2001;19:1985–92.
11. Stadler WM, Vogelzang NJ, Amato R, et al. Flavopiridol, a novel cyclin-dependent kinase inhibitor, in metastatic renal cancer: a University of Chicago phase II consortium study. J Clin Oncol 2000;18:371–5.
12. Shapiro GI, Supko JG, Patterson A, et al. A phase II trial of the cyclin-dependent kinase inhibitor flavopiridol in patients with previously untreated stage IV non-small cell lung cancer. Clin Cancer Res 2001;7:1590–9.
13. Lin TS, Howard OM, Neuberg DS, et al. Seventy-two hour continuous infusion flavopiridol in relapsed

and refractory mantle cell lymphoma. Leuk Lymphoma 2002;43:793–7.
14. Kouroukis CT, Belch A, Crump M, et al. Flavopiridol in untreated or relapsed mantle-cell lymphoma: results of a phase II study of the National Cancer Institute of Canada clinical trials group. J Clin Oncol 2003;21:1740–5.
15. Cheson BD, Bennett JM, Grever M, et al. National Cancer Institute-sponsored working group guidelines for chronic lymphocytic leukemia: revised guidelines for diagnosis and treatment. Blood 1996;87:4990–7.
16. Kaplan EL, Meier P. Nonparametric estimation from incomplete observations. J Am Stat Assoc 1958;43: 457–81.
17. Peto RPM, Armitage P. Design and analysis of randomized clinical trials requiring prolonged observation of each patient II. Analysis and examples. Br J Cancer 1977;35:1–39.
18. Keating MJ, Flinn I, Jain V, et al. Therapeutic role of alemtuzumab (Campath-1H) in patients who have failed fludarabine: results of a large international study. Blood 2002;99:3554–61.
19. Rudek MA, Bauer KS Jr, Lush RM III, et al. Clinical pharmacology of flavopiridol following a 72-hour continuous infusion. Ann Pharmacother 2003;37:1369–74.
20. Flinn IW, Byrd JC, Barlett N, et al. Flavopiridol administered as a 24-hour continous infusion in chronic lymphocytic leukemia lacks clinical activity. Leuk Res. In press 2005.
21. Shinn C, Larsen D, Suarez JR, et al. Flavopiridol sensitivity of chronic lymphocytic leukemia (CLL) cells *in vitro* varies based upon species specific drug protein binding. Blood 2000;96:294b.
22. Innocenti F, Stadler WM, Iyer L, et al. Flavopiridol metabolism in cancer patients is associated with the occurrence of diarrhea. Clin Cancer Res 2000;6: 3400–5.
23. Bible KC, Kaufmann SH. Cytotoxic synergy between flavopiridol (NSC 649890, L86-8275) and various antineoplastic agents: the importance of sequence of administration. Cancer Res 1997;57:3375–80.
24. Matranga CB, Shapiro GI. Selective sensitization of transformed cells to flavopiridol-induced apoptosis following recruitment to S-phase. Cancer Res 2002; 62:1707–17.
25. Schwartz GK, Farsi K, Maslak P, et al. Potentiation of apoptosis by flavopiridol in mitomycin-C-treated gastric and breast cancer cells. Clin Cancer Res 1997;3: 1467–72.
26. Yu C, Krystal G, Dent P, et al. Flavopiridol potentiates STI571-induced mitochondrial damage and apoptosis in BCR-ABL-positive human leukemia cells. Clin Cancer Res 2002;8:2976–84.
27. Dai Y, Rahmani M, Grant S. Proteasome inhibitors potentiate leukemic cell apoptosis induced by the cyclin-dependent kinase inhibitor flavopiridol through a SAPK/JNK- and NF-κB-dependent process. Oncogene 2003;22:7108–22.
28. Byrd JC, Lin TS, Dalton JT, et al. Flavopiridol administered as a pharmacologically-derived schedule demonstrates marked clinical activity in refractory, genetically high risk, chronic lymphocytic leukemia (CLL). Blood 2004;104:476a.

Chronic Lymphocytic Leukemia: A Niche for Flavopiridol?

□□Commentary on Byrd et al., p. 4176

Jennifer R. Brown

Cyclin-dependent kinases (cdks) are key regulators of orderly progression through the cell cycle and of RNA transcription. Inhibition of their activity *in vitro* can cause cell cycle arrest at the G_1-S or G_2-M boundaries (1, 2). Flavopiridol, a synthetic flavone related to a natural product of the bark of a plant native to India, has generated intense interest as the first cdk inhibitor to enter clinical trials. Flavopiridol selectively inhibits multiple cdks by blocking ATP binding and by blocking their phosphorylation by cdk7 (1, 2). Flavopiridol also decreases cyclin D1 levels (3) and inhibits gene transcription by blocking cdk9, which phosphorylates RNA polymerase II (4).

Initial observations in cell culture found that flavopiridol at 150 to 200 nmol/L is cytostatic, causing reversible cell cycle arrest (5). Flavopiridol is also cytotoxic to both cycling and noncycling A549 lung cancer cells, however (6, 7). Hematopoietic cells, including B cell lines and chronic lymphocytic leukemia (CLL) cells *in vitro*, are particularly susceptible to early apoptosis induced by flavopiridol, with LC_{50} 1.15 μmol/L at 4 hours and 100 to 400 nmol/L at 24 hours of exposure (8, 9). Solid tumor cell lines often require prolonged exposure to higher flavopiridol concentrations (0.5-1 μmol/L for 24-72 hours) for equivalent cytotoxicity (6, 7).

The observation that the cytotoxicity of flavopiridol is enhanced by prolonged exposure *in vitro* led to two phase I clinical trials of a 72-hour continuous infusion every 2 weeks (10, 11). The maximum tolerated dose was 40 to 50 mg/m^2/day continuous infusion for 3 days, with a dose-limiting toxicity of secretory diarrhea. Pharmacokinetic data showed mean steady-state plasma concentrations of >270 nmol/L, similar to the *in vitro* concentration required for cdk inhibition (10–12). Objective responses were noted in renal cell and gastric cancer, and minor responses in non-Hodgkin's lymphoma, renal cell, and colon cancer.

These encouraging phase I results led to phase II studies of this dose and schedule in gastric, lung, colon, and renal cell cancers (13–16). No objective responses were observed in gastric, lung, or colon cancers, and only two responses (6%) in renal cell cancer, despite steady-state flavopiridol concentrations >200 nmol/L in the gastric, lung, and renal cell studies (13, 15, 17). The same schedule in mantle cell non-Hodgkin's lymphoma also produced no objective responses and led to early termination of the study (18). Efforts to identify biological activity of flavopiridol found no change in the number of peripheral blood mononuclear cells (13) and no inhibition of stimulated proliferation of peripheral blood mononuclear cells *in vitro* (14).

The lack of biological activity of flavopiridol in a 72-hour continuous infusion was clearly discordant with its *in vitro* potency in inducing cdk inhibition and cell cycle arrest at concentrations achieved *in vivo*. Inducing cytotoxicity in solid tumor cell lines *in vitro* has often required significantly higher flavopiridol concentrations, however (2, 5). Furthermore, in HL60 xenografts, 72-hour continuous infusion flavopiridol has little or no activity, whereas daily i.v. bolus flavopiridol potently inhibits the xenografts, leading to prolonged complete remissions (19). The continuous infusion schedule produced mean steady-state concentrations of 427 nmol/L, whereas the bolus schedule achieved peak concentrations of 7 μmol/L at 2 minutes, declining to 0.1 μmol/L by 8 hours (19). The bolus schedule had potent effects on hematopoietic tissues, inducing dose-dependent leukopenia, atrophy of lymphoid organs, and inhibition of mitogen stimulation of peripheral blood mononuclear cells (19).

A phase I human study of 1 hour i.v. bolus flavopiridol identified the maximum tolerated dose as 50 mg/m^2/day for 3 days, with dose-limiting toxicity now grade 4 neutropenia (20). The median peak plasma concentration on this schedule was 3.2 μmol/L, approaching that in the xenograft model (21). Although no objective responses were observed, 24% of patients had stable disease (20). A phase II study of flavopiridol with this dose and schedule in mantle cell non-Hodgkin's lymphoma resulted in 11% partial responses and 71% stable disease, with some evidence of additional transient lymph node regressions (22). These results are significantly improved over the 72-hour continuous infusion and suggest some level of activity.

The rationale for studying flavopiridol in CLL is high. In CLL, lymphocytes accumulate at least in part due to a defect in apoptosis. Flavopiridol induces apoptosis in CLL cells *in vitro* in a p53-independent, caspase-dependent manner (9), and has been reported to decrease expression of antiapoptotic proteins including Mcl-1 and X-linked inhibitor of apoptosis (23, 24). If flavopiridol can induce cell death *in vivo* in the absence of p53, it could become an effective therapy for CLL patients with poor prognostic features, particularly mutations of 17p and the p53 pathway.

In this issue of *Clinical Cancer Research*, Byrd et al. report the results of two sequential phase II studies of flavopiridol in previously treated CLL, done by the Cancer and Leukemia Group B. The first study, using 50 mg/m^2/day continuous infusion over 72 hours, resulted in no objective responses and only 27% stable disease. The second study, using the 50 mg/m^2/day bolus over 1 hour for 3 days, resulted in 11% partial responses and 53% stable disease. All four responding patients in this study had fludarabine-refractory disease. One patient

Authors' Affiliation: Department of Medical Oncology, Dana-Farber Cancer Institute, Boston, Massachusetts

Received 4/15/05; accepted 4/15/05.

The costs of publication of this article were defrayed in part by the payment of page charges. This article must therefore be hereby marked *advertisement* in accordance with 18 U.S.C. Section 1734 solely to indicate this fact.

Requests for reprints: Jennifer R. Brown, Department of Medical Oncology, Dana-Farber Cancer Institute, 44 Binney Street, Boston, MA 02115. Phone: 617-632-4894; Fax: 617-582-7909; E-mail: jbrown2@partners.org.

who had a partial response developed acute tumor lysis syndrome, which was successfully managed medically.

Thus, similar to what was seen in mantle cell non-Hodgkin's lymphoma, Byrd et al. find that flavopiridol has minor activity in CLL when given by i.v. bolus but not by continuous infusion. The observation of tumor lysis syndrome is particularly notable and suggests the potential for greater efficacy than seen in this study. It is unfortunate that no pharmacokinetic data are available to correlate with response and tumor lysis. However, prior experience with flavopiridol shows that the i.v. bolus schedule results in significantly higher peak concentrations (20, 21). Why these higher concentrations are apparently needed for biological activity is unclear, given that low concentrations inhibit cdk activity and lead to cell cycle arrest *in vitro*. Possible explanations include inhibition of activity in human plasma, possibly due to plasma protein binding, unusual drug metabolism or an endogenous inhibitor, or the need for higher concentrations to reach an unknown target required for cytotoxicity *in vivo*. Preliminary data from the authors of these trials and others does in fact suggest that 92% to 95% of flavopiridol is protein-bound in human plasma, but not in fetal calf serum used *in vitro*, resulting in an increase in the LC_{50} for CLL cells *in vitro* from 0.67 to 3.5 μmol/L at 1 hour, and from 0.12 to 0.47 μmol/L at 24 hours (12, 25). These concentrations have not been reliably achieved in clinical studies, suggesting that increased protein binding may at least contribute to the dose and schedule dependence of flavopiridol activity *in vivo*.

Byrd et al. have gone on to test this hypothesis in relapsed CLL patients in a subsequent phase I study using flavopiridol given in a 30-minute bolus dose followed by a 4-hour infusion, designed based on pharmacokinetic modeling to achieve and sustain micromolar concentrations for several hours (25). As reported at the American Society of Hematology meeting last December (26), a remarkable 41% response rate was observed in 22 evaluable patients; eight of nine responders had fludarabine-refractory disease, bulky lymph nodes, and either 11q or 17p deletion. Concomitant with this activity, however, was significant tumor lysis syndrome, which proved to be the dose-limiting toxicity, resulting in one patient death, multiple patients requiring dialysis, and all patients requiring aggressive inpatient medical management. This dramatic improvement in tumor response with a pharmacokinetically designed schedule suggests that tumor response and tumor lysis are directly tied to achieved drug concentrations, but confirmation of this hypothesis will await the full publication of this study and its accompanying pharmacokinetic data.

These results, emerging from persistent and careful characterization by Byrd and colleagues, suggest significant activity of flavopiridol in refractory CLL. Many questions remain unanswered, however, and finding the answers will greatly enhance our insight into mechanisms of drug response and cell death in CLL and possibly other cancers. For example, will individual pharmacokinetic variables correlate with likelihood of tumor lysis and tumor response? Do genetic polymorphisms in flavopiridol glucuronidation, previously described to impact the incidence of diarrhea (17), also affect drug concentration, tumor lysis, and tumor response? Is plasma protein binding the sole reason why higher than expected flavopiridol concentrations are required for activity? What is the critical target required for flavopiridol-induced apoptosis in CLL cells *in vitro*, and is it targeted in responding patients? Does this target explain the apparent rapidity of CLL cell death and tumor lysis seen in the most recent trial? Is flavopiridol effective in high-risk CLL patients with 17p deletion or p53 mutation, and does its putative target explain this effectiveness? The answers to these questions will not only provide significant insight into the fundamental biology of CLL, but are also particularly critical for further clinical development of flavopiridol, which will require optimizing its safety as well as its efficacy.

Finding a niche for flavopiridol in CLL therapy may depend on developing predictors of which patients are most likely to develop tumor lysis syndrome, or optimizing the dosing schedule to maintain activity with increased safety. If these prove difficult but significant disease response is confirmed in subsequent studies, particularly in high-risk patient populations, flavopiridol could prove useful for clearance of residual disease following chemotherapy. Alternatively, lower doses of flavopiridol may be able to sensitize CLL cells to the effects of chemotherapy without inducing life-threatening tumor lysis (27, 28). Combination regimens studied thus far have found significant but likely manageable toxicity, with more activity than in studies of single-agent flavopiridol (2, 29, 30).

Pharmacokinetically designed schedules of flavopiridol administration are currently being tested in the treatment of other malignancies (2). In mantle cell lymphoma, the older i.v. bolus schedule showed activity similar to that seen in CLL (22). Given that mantle cell lymphoma overexpresses cyclin D1, and flavopiridol decreases levels of cyclin D1, the rationale for studying an optimized schedule in mantle cell lymphoma is high. In solid tumors, although few responses have been seen in phase II trials, prolonged stable disease has been observed and correlates with higher plasma concentrations of flavopiridol (15). Furthermore, higher flavopiridol concentrations not yet reached in clinical trials are likely required *in vitro* for cytotoxicity in solid tumors, possibly due to a different target than in CLL. Chemotherapy may be able to sensitize solid tumors to the effects of flavopiridol *in vitro* (27, 28), and tumor responses have been seen in phase I studies of flavopiridol in combination with gemcitabine and paclitaxel (2, 30). Ongoing and future research will be required to determine whether flavopiridol has a role in the therapy of solid tumors. Although much work remains to be done in CLL as well as in other malignancies, the development of flavopiridol to date suggests that systematic pharmacokinetic and mechanistic analysis in human studies is essential to identify the true potential of new drug candidates, even novel therapies for which a putative target is thought to be known *in vitro*.

References

1. Senderowicz AM, Sausville EA. Preclinical and clinical development of cyclin-dependent kinase modulators. J Natl Cancer Inst 2000;92:376–87.
2. Shapiro GI. Preclinical and clinical development of the cyclin-dependent kinase inhibitor flavopiridol. Clin Cancer Res 2004;10:4270–5s.
3. Chao SH, Price DH. Flavopiridol inactivates P-TEFb and blocks most RNA polymerase II transcription *in vivo*. J Biol Chem 2001;276:31793–9.
4. Bible KC, Kaufmann SH. Flavopiridol: a cytotoxic flavone that induces cell death in noncycling A549 human lung carcinoma cells. Cancer Res 1996;56:4856–61.
5. Shapiro GI, Koestner DA, Matranga CB, Rollins BJ. Flavopiridol induces cell cycle arrest and p53-independent apoptosis in non-small cell lung cancer cell lines. Clin Cancer Res 1999;5:2925–38.
6. Carlson B, Lahusen T, Singh S, et al. Down-regulation of cyclin D1 by transcriptional repression in MCF-7

human breast carcinoma cells induced by flavopiridol. Cancer Res 1999;59:4634–41.
7. Kaur G, Stetler-Stevenson M, Sebers S, et al. Growth inhibition with reversible cell cycle arrest of carcinoma cells by flavone L86-8275. J Natl Cancer Inst 1992; 84:1736–40.
8. Konig A, Schwartz GK, Mohammad RM, Al-Katib A, Gabrilove JL. The novel cyclin-dependent kinase inhibitor flavopiridol downregulates Bcl-2 and induces growth arrest and apoptosis in chronic B-cell leukemia lines. Blood 1997;90:4307–12.
9. Byrd JC, Shinn C, Waselenko JK, et al. Flavopiridol induces apoptosis in chronic lymphocytic leukemia cells via activation of caspase-3 without evidence of bcl-2 modulation or dependence on functional p53. Blood 1998;92:3804–16.
10. Thomas JP, Tutsch KD, Cleary JF, et al. Phase I clinical and pharmacokinetic trial of the cyclin-dependent kinase inhibitor flavopiridol. Cancer Chemother Pharmacol 2002;50:465–72.
11. Senderowicz AM, Headlee D, Stinson SF, et al. Phase I trial of continuous infusion flavopiridol, a novel cyclin-dependent kinase inhibitor, in patients with refractory neoplasms. J Clin Oncol 1998;16:2986–99.
12. Rudek MA, Bauer KS Jr, Lush RM III, et al. Clinical pharmacology of flavopiridol following a 72-hour continuous infusion. Ann Pharmacother 2003;37: 1369–74.
13. Schwartz GK, Ilson D, Saltz L, et al. Phase II study of the cyclin-dependent kinase inhibitor flavopiridol administered to patients with advanced gastric carcinoma. J Clin Oncol 2001;19:1985–92.
14. Stadler WM, Vogelzang NJ, Amato R, et al. Flavopiridol, a novel cyclin-dependent kinase inhibitor, in metastatic renal cancer: a University of Chicago Phase II Consortium Study. J Clin Oncol 2000;18:371–5.
15. Shapiro GI, Supko JG, Patterson A, et al. A phase II trial of the cyclin-dependent kinase inhibitor flavopiridol in patients with previously untreated stage IV non-small cell lung cancer. Clin Cancer Res 2001;7: 1590–9.
16. Aklilu M, Kindler HL, Donehower RC, Mani S, Vokes EE. Phase II study of flavopiridol in patients with advanced colorectal cancer. Ann Oncol 2003; 14:1270–3.
17. Innocenti F, Stadler WM, Iyer L, et al. Flavopiridol metabolism in cancer patients is associated with the occurrence of diarrhea. Clin Cancer Res 2000;6: 3400–5.
18. Lin TS, Howard OM, Neuberg DS, Kim HH, Shipp MA. Seventy-two hour continuous infusion flavopiridol in relapsed and refractory mantle cell lymphoma. Leuk Lymphoma 2002;43:793–7.
19. Arguello F, Alexander M, Sterry JA, et al. Flavopiridol induces apoptosis of normal lymphoid cells, causes immunosuppression, and has potent antitumor activity *in vivo* against human leukemia and lymphoma xenografts. Blood 1998;91:2482–90.
20. Tan AR, Headlee D, Messmann R, et al. Phase I clinical and pharmacokinetic study of flavopiridol administered as a daily 1-hour infusion in patients with advanced neoplasms. J Clin Oncol 2002;20: 4074–82.
21. Zhai S, Figg WD, Headlee D, et al. Pharmacokinetics (PK) of flavopiridol IV bolus in patients with refractory neoplasms. Clin Cancer Res 2000;6:4529s.
22. Kouroukis CT, Belch A, Crump M, et al. Flavopiridol in untreated or relapsed mantle-cell lymphoma: results of a phase II study of the National Cancer Institute of Canada Clinical Trials Group. J Clin Oncol 2003;21: 1740–5.
23. Pepper C, Thomas A, Hoy T, Fegan C, Bentley P. Flavopiridol circumvents Bcl-2 family mediated inhibition of apoptosis and drug resistance in B-cell chronic lymphocytic leukaemia. Br J Haematol 2001;114: 70–7.
24. Kitada S, Zapata JM, Andreeff M, Reed JC. Protein kinase inhibitors flavopiridol and 7-hydroxy-staurosporine down-regulate antiapoptosis proteins in B-cell chronic lymphocytic leukemia. Blood 2000;96: 393–7.
25. Shinn C, Larsen D, Suarez JR, et al. Flavopiridol sensitivity of chronic lymphocytic leukemia (CLL) cells *in vitro* varies based upon species specific drug protein binding. Blood 2000;96:294b.
26. Byrd JC, Lin TS, Dalton JT, et al. Flavopiridol administered as a pharmacologically-derived schedule demonstrates marked clinical activity in refractory, genetically high risk, chronic lymphocytic leukemia (CLL). Blood 2004;104:101a.
27. Bible KC, Kaufmann SH. Cytotoxic synergy between flavopiridol (NSC 649890, L86-8275) and various antineoplastic agents: the importance of sequence of administration. Cancer Res 1997;57:3375–80.
28. Matranga CB, Shapiro GI. Selective sensitization of transformed cells to flavopiridol-induced apoptosis following recruitment to S-phase. Cancer Res 2002; 62:1707–17.
29. Lin TS, Fischer B, Moran ME, et al. Phase I dose escalation study of flavopiridol in combination with fludarabine and rituximab: Activity in indolent B-cell lymphoproliferative disorders and mantle cell lymphoma. Blood 2004;104:683a.
30. Schwartz GK, O'Reilly E, Ilson D, et al. Phase I study of the cyclin-dependent kinase inhibitor flavopiridol in combination with paclitaxel in patients with advanced solid tumors. J Clin Oncol 2002;20: 2157–70.

Exhibit V

http://www.iddb3.com/iddb3/iddb3_2/reports.display?id=3472&template=Drug&i_query_id=5383441

alvocidib	
Company	National Cancer Institute
Highest Dev Status	Phase 2 Clinical
Indications	Esophagus tumor Stomach tumor Chronic lymphocytic leukemia Multiple myeloma Lymphoma Prostate tumor Cancer Solid tumor Lung tumor Colon tumor
Actions	Anticancer, chemosensitizer CDK inhibitor Transcription factor inhibitor Angiogenesis inhibitor Cell cycle inhibitor
Reason for update on 01-Jun-2005	
1 reference added [605112]	

Summary

Alvocidib (flavopiridol, HMR-1275, MDL-107826A, NSC-649890; structure shown) is a synthetic flavonoid inhibitor of cyclin-dependent kinases which is under development by the National Cancer Institute (NCI) for the potential treatment of cancer. Phase II trials of alvocidib as a montherapy were underway by February 2002 [440299], and by September 2003, phase II trials in combination with cytotoxics, including docetaxel and irinotecan, and immunotherapeutics, including trastuzumab and rituximab (all qv) had been initiated [510232].

Aventis Pharma (formerly Hoechst Marion Roussel) was previously collaborating with the NCI for the development of alvocidib [279466], however, by February 2004, Aventis had terminated its involvement [521627].

MONOTHERAPYIn June 2003, phase II data on alvocidib were presented at the 39th ASCO meeting in Chicago, IL. A total of 34 patients with chemotherapy-naive advanced renal cell carcinoma were given a 1-h bolus of alvocidib on days 1 to 3 of a 21-day cycle. From 33 evaluable patients there was 1 complete response, 2 partial responses (1 confirmed and 1 unconfirmed) and 13 cases of stable disease. Median overall survival was 9 months (95% CI: 8 to 14). The overall probability of not failing treatment by 6 months was 23% (95% CI: 8 to 37%). Most common grade 3 to 4 toxicities were diarrhea (33%), tumor pain (13%), anemia (9%), dyspnea (9%) and fatigue (9%). The response criteria of the study was not met; however, alvocidib may have biological activity against renal cell carcinoma [492181].

Data from a phase II trial in patients with metastatic androgen-independent prostate cancer were also presented at the 39th ASCO meeting. Patients (n = 36) were given alvocidib (50 mg/m2/day) for three consecutive 24-h infusions every 2 weeks. Due to toxicity the dose was reduced to 40 mg/m2/day. Grade 3 and 4 adverse events included thrombus, nausea, diarrhea and fatigue. Four

patients received at least ten courses of treatment, 12 received six courses and 11 received two or fewer courses. A transient decrease in PSA was noted in 11 patients, four had stable disease, 23 had disease progression and 13 withdrew early due to toxicities [493537].

In May 2002, clinical data were presented at the 38th ASCO annual meeting in Orlando, FL. Seven patients with acute relapsed or refractory acute leukemia were treated with alvocidib as a 1-h infusion on days 1, 2 and 3. Serum was obtained on days 0, 3 and 6 and were used to treat bovine aortic endothelial cells for 72 h. Inhibition of cell growth was detected in all seven patients on days 3 and 6 after therapy, with mean inhibition recorded at 32% [452248], [450989].

A phase II study of alvocidib in patients with previously untreated metastatic malignant melanoma was also presented in May 2002, at the 38th ASCO annual meeting in Orlando, FL. Alvocidib was administered intravenously at a dose of 50 mg/m2 over 1 h daily for 3 days, every 3 weeks to 17 patients. There were no responses in 16 out of the 17 evaluable patients, but seven patients had stable disease after two cycles, ranging in duration from 1.8 to 9.2 months, with a median of 2.8 months. Most non-hematologic toxicities were grade I or II except for diarrhea (grade III in three patients, grade IV in one patient), nausea (grade III in one patient), motor neuropathy (grade III in one patient), tumor pain (grade III in one patient), cough (grade III in one patient) and dyspnea (grade III in two patients). All hematologic and biochemical toxicities were grade I or II. Gastrointestinal toxicity was the most common problem; two patients had dose reductions as a result of this adverse event [452758].

In December 2001, clinical data on alvocidib in mantle cell lymphoma (MCL) were presented at the 43rd ASH meeting in Orlando, FL. A total of 25 evaluable patients were treated in cycles of 50 mg/m2/day for 3 days every 3 weeks; 3 patients achieved a partial response and 12 patients achieved stable disease. This progression-delaying activity suggested that alvocidib should be combined with other chemotherapy [433007]. In September 2004, further data were presented at the 16th EORTC-NCI-AACR meeting in Geneva, Switzerland. At this time 72% of patients had demonstrated stable disease and 12% had partial responses [561351].

By July 1999, the compound had entered phase II trials for gastric cancer and leukemia, and phase I/II trials for esophageal tumor and non-small cell lung cancer (NSCLC) [277372], [331850], [325929]. Phase I trials for prostate and colon cancer have also been reported [279466].

By May 1999, a phase II trial was underway to examine the efficacy of the compound in fludarabine-refractory chronic lymphocytic leukemia (CLL). At this time, phase I/II studies were also planned in patients with CLL to examine 5 day bolus and 24 h continuous infusion treatment schedules, as well as higher doses of the compound in combination with diarrhea prophylaxis [325929]. By May 2001, optimized infusion regimen studies were ongoing [409257].

Results from a phase II trial at Memorial Sloan-Kettering Cancer Center, reported in May 1998, indicated that alvocidib had some activity against gastric cancer. However, some patients given a continuous 72 h infusion of the drug at 50 mg/m2/day, experienced unexpected toxicity, including thromboembolism, diarrhea and dyspnea. One patient on the trial died from what were described as 'unclear' reasons [288659], [402046].

By November 1997, a phase II trial had commenced in patients with high or intermediate-grade lymphoma or multiple myeloma at the University of Chicago Medical Center [272937], [277372].

In April 2005, phase I clinical data on alvocidib were presented at the 96th AACR meeting in Anaheim, CA. Alvocidib (37.5 to 80 mg/m2/day) was administered to children (aged < 22 years; n = 25) with refractory solid tumors or lymphomas as a 1 h intravenous infusion daily for 3 consecutive days every 21 days. Dose escalation was conducted until dose-limiting toxicities (DLTs) and the maximum tolerated dose (MTD) was reached. DLTs were grade 4 neutropenia and grade 3 diarrhea and the MTD was 62.5 mg/m2/day [597566].

In June 2004, phase I data were presented at the 40th ASCO meeting in New Orleans, LA. Nine patients with refractory chronic lymphocytic leukemia were administered alvocidib (cohort 1 = 60 mg/m2/dose, cohort 2 = 80 mg/m2/dose) as a 30 minute iv bolus followed by a 4 hour continuous iv infusion, once a week. Two patients in cohort 1 achieved an NCI 96 partial response lasting over 5 months. Grade 3 and 4 toxicity was observed (neutropenia, thrombocytopenia, dyspnea, edema and diarrhea), but most adverse events were grade 1 or 2 severity (fatigue, nausea and anorexia); tumor lysis was also seen in 3 patients in cohort 2 and resulted in one death [541126]. Similar data were presented in December 2004 at the 46th ASH meeting in San Diego, CA. The dose-limiting toxicity (DLT) was neutropenic fever. Patients in the 80 mg/m2/dose group exceeded the maximum tolerated dose, with hyper-acute tumor lysis syndrome as the DLT. After the establishment of an in-patient management plan to prevent life-threatening TLS, 14 patients were evaluable, with several cases of TLS observed, but no further deaths. A total of ten patients achieved a partial response, of which eight were fludarabine refractory and nine had unfavorable cytogenics. Remissions were durable and seven patients remained in remission for more than 12 months. No opportunistic infections were observed [576672].

In June 2003, phase I data on alvocidib were presented at the 39th ASCO meeting in Chicago, IL. A total of 29 patients received alvocidib at doses ranging from 40 to 140 mg/m2 as a 24 h iv infusion once weekly for a total of eight weeks. Gastrointestinal events were the most commonly reported adverse events. Dose-limiting toxicities preventing further dose escalation were observed at the 120 mg/m2 dose level and consisted mainly of pain at tumor sites that could not be controlled by analgesics. There were minimal grade 3 to 4 adverse events. The maximum tolerated dose recommended for further study was 80 mg/m2. Of 25 patients evaluable for response, one patient on the 60 mg/m2 dose had a partial response. There were seven cases of stable disease [491293].

In August 2002, phase I data were presented at the 1st Targeted Therapies meeting in Washington DC. A 72 h continuous infusion of alvocidib was administered to 76 patients. The dose-limiting toxicity was diarrhea, and other effects included an increase in C reactive protein, decrease in albumin and increase in plasma IL-6. In another study, 55 patients received 1 h infusions of the drug. The MTD was 37.3 mg/m2/day, five times, and toxicities were nausea, vomiting and neutropenia. Levels up to 2 to 3 microM were reached with a half-life of 3.6 h. No major responses were observed, although the trials were not designed to examine the cytostatic potential of the drug [463418]. Similar data were presented in August 2003 at the Second Targeted Therapies in Cancer meeting in Washington DC [505048].

In May 2002, phase I data on alvocidib in patients with solid tumors were presented at the 38th ASCO meeting in Orlando, FL. A total of twenty patients with advanced cancers were given weekly doses of alvocidib (40 to 100 mg/m2) for 4 consecutive weeks. Dose limiting toxicities manifested as reversible grade III abdominal pain and multiple colon ulcers in two patients at the 100 mg/m2 dose and in one patient as abdominal distension at the 40 mg/m2 dose. The mean Cmax and AUC were 718 nmol/l and 19699 nmol at 80 mg/m2 and 924 nmol/l and 22086

nmolh/l at 100 mg/m2, respectively. Although no tumor shrinkage was observed, five patients had stable disease over 90 days. The 80 mg/m2 dose of alvocidib was recommended for further evaluation [451829].

Results of a phase I trial evaluating a 1-h infusion per day for 5 days of alvocidib every 3 weeks were presented at the 36th ASCO Annual Meeting (New Orleans, May 2000). This showed that concentrations of 4 microM were achieved with acceptable toxicity [369760]. Similar data were presented in August 2003 at the Second Targeted Therapies in Cancer meeting in Washington DC [505048].

By 1996, an initial phase I trial had commenced, evaluating alvocidib in 22 patients with refractory neoplasms. Alvocidib was administered by continuous iv infusion for 72 h every 2 weeks. Dose levels/day were 4, 8, 12, 16, 21, 28 and 35 mg/m2. In one patient at the highest dose level, grade III diarrhea was observed. Other toxicities included transaminitis, grade II diarrhea, grade II fever, pleuritic chest pain, polyarthralgias and grade I fatigue. In addition, tumor cells from a patient with refractory chronic lymphocytic leukemia were exposed ex vivo, with increasing concentrations of alvocidib for 14 h; dose-dependent cdk2 inhibition-associated apoptotic changes were seen at 100 nM or higher concentrations. Dose-escalation studies continued in an attempt to define a non-gastrointestinal maximum tolerated dose and by the end of the study, 49 patients had been treated [203645].

An additional phase I study on the 72-h continuous infusion schedule, undertaken at the University of Wisconsin, gave an MTD of 40 mg/m2/day x 3 [325767]. Dose-limiting toxicities (DLTs) of this trial were secretory diarrhea and hypotension in the presence of antidiarrheal prophylaxis. A shorter infusion phase I study saw transient neutropenia as the DLT [391557].

COMBINATION THERAPYIt was announced in May 2005 at the 41st ASCO meeting in Orlando, FL, that a phase II trial for gemcitabine refractory metastatic pancreatic cancer was being planned [601684].

As of March 2004 a phase I trial of alvocidib in combination with bortezomib (qv) was underway with patients with refractory B-cell malignancies [531873].

In August 2003, studies to investigate combination therapy with trastuzumab (qv) or imatinib (qv) were being planned [505048].

In June 2004, phase I data from a trial combining alvocidib with irinotecan and cisplatin were presented at the 40th ASCO meeting in New Orleans, LA. A total of 26 patients were enrolled to receive weekly doses of irinotecan (60 mg/m2 to 65 mg/m2) and cisplatin (10 to 30 mg/m2) followed 7 h later by alvocidib (50 mg/m2) for 3 consecutive weeks as part of a 4-week cycle.In the first cohort of patients receiving cisplatin at 10mg/m2, grade 3/4 neutropenia occurred by week 3,
necessitating an alternate schedule of 2 weeks on and 1 week off. Cisplatin escalation proceeded with dose-limiting toxicity of neutropenia only reached when cisplatin was given at 30 mg/m2 and irinotecan was given at 65 mg/m2. From seven patients with gastroesophageal cancers there were five partial responses and a minor and partial response in two out of three patients with cholangiocarcinoma [542832].

In June 2004, phase I data from a trial combining alvocidib and docetaxel were presented at the 40th ASCO meeting in New Orleans, LA. Patients with solid tumors received a once weekly

dose of docetaxel (35 mg/m2) as a 30-min iv infusion followed 4h later by alvocidib (20 to 70 mg/m2) delivered as an 1-h infusion. The drugs were delivered for 3 consecutive weeks as part of a 4-week cycle. From 18 evaluable patients there were two partial responses, one from a breast cancer patient and one from an ovarian cancer patient. Stable disease was observed in two breast cancer patients, two pancreatic cancer patients and one gastric cancer patient. There were no dose-liniting toxicities up to 60 mg/m2 of alvocidib [543800]. Further data were presented in May 2005 at the 41st ASCO meeting in Orlando, FL. Out of 27 evaluable patients, two dose-limiting toxicities were observed: grade 3 mucositis at 70 mg/m2; and grade 4 neutropenia at 80 mg/m2. Pharmacokinetic analysis showed a Cmax ranging from 1.3 to 4.2 microM. In terms of efficacy, there were 5 partial responses and 10 stable disease [601684].

In May 2003, clinical data on alvocidib were presented at the 39th ASCO meeting in Chicago, IL. Alvocidib was combined with docetaxel in a phase I, safety and tolerability trial; the drug (40 to 120 mg/m2 iv infusion over 1 h, weekly or biweekly) was administered with docetaxel (75 mg/m2) to stage IIIB or IV NSCLC patients in a 21-day cycle. Eleven patients completed two cycles of drug therapy; dose-limiting toxicity (DLT) was observed at doses of alvocidib over 100 mg/m2. The MTD for biweekly administration was 80 mg/m2 combined with docetaxel (75 mg/m2). For weekly administration the MTD was 60 mg/m2 plus docetaxel. Grade 3 and 4 adverse events included neutropenia, diarrhea, nausea and fatigue. One patient died from septic shock/necrotizing enterocolitis. The mean elimination half-life over all dose groups was 13 h. In the biweekly treatment group, one patient achieved a partial response while the disease of four patients stabilized. At this time, a phase II/III study comparing alvocidib (60 mg/m2) plus docetaxel (75 mg/m2) with docetaxel alone was ongoing [491399], [491483], [493380], [493055]. As of March 2004, this trial was still ongoing [531873].

In June 2003, phase I data on alvocidib in combination with irinotecan were presented at the 39th ASCO meeting in Chicago, IL. A total of 38 evaluable patients with various solid tumors received weekly doses of irinotecan (100 to 125 mg/m2) followed 7 h later by a 1 h iv infusion of alvocidib (10 to 70 mg/m2), for 4 out of 6 weeks. At an irinotecan dose of 100 mg/m2 and a alvocidib dose of 70 mg/m2, grade 3 dose limiting toxicities were neutropenia (n = 2) and diarrhea (n = 1). The maximum tolerated doses were 100 mg/m2 of irinotecan and 60 mg/m2 of alvocidib. There were three confirmed partial responses in gastric, esophagus and colorectal cancer patients who had received prior irinotecan therapy. Two patients with adrenocortical cancer had prolonged stable disease (8.1 and 15.4 months). From the 38 evaluable patients, overall one-year survival was 54%. For the subset with colorectal cancer (n = 25), who had received prior irinotecan and/or oxaliplatin therapy, the one-year survival was 64% [491983].

In July 2003, data were presented at the 94th AACR meeting, Washington, DC, from a study to modulate cytarabine resistance ex vivo by combining cytarabine with 6 potential resistance modifiers, including alvocidib. The single agents and their combinations were studied ex vivo in blast cells isolated from 10 children with de novo AML using the 4-day total cell kill MTT assay. Cytarabine was tested in 6 different concentrations, the modulators were tested at a low concentration (inducing on average 10% cell kill as a single agent) and a high concentration (inducing on average 30% cell kill as a single agent). Nearly additive and moderately synergistic interactions were observed between cytarabine/alvocidib (median CI = 0.93 (n = 10) and CI = 0.82 (n = 8)) [484162].

In May 2003, clinical data on a combination of alvocidib, 5-FU and leucovorin in patients with advanced malignancies were presented at the 39th ASCO meeting in Chicago, IL. Patients (n = 24) were given alvocidib (40 to 100 mg/m2 over 24-h on day 1) plus 5-FU (350 mg/m2/day, 1-h

infusion on days 2 to 5) plus leucovorin (20 mg/m2/day on days 2 to 5). The mean time on the study was 1.5 months. Toxicities included diarrhea, fatigue, nausea, anorexia and anemia. One patient achieved a partial response, while 13% of the remaining patients had stable disease [493085].

By June 2002, further clinical trials of alvocidib in combination with docetaxel (qv) or irinotecan (qv) were planned [454720], [455054]. At this time, NDA/MAA submissions for alvocidib with docetaxel for lung cancer were planned for 2005. NDA/MAA submissions for alvocidib with irinotecan for colorectal cancer were planned for 2005 or 2006 [455004].

In May 2002, phase I data on alvocidib in combination with paclitaxel and carboplatin were presented at the 38th ASCO meeting in Orlando, FL. Patients with previously untreated advanced non-small cell lung cancer received three cycles of paclitaxel (175 mg/m2 over 3h) and carboplatin (AUC = 5 over 1 h) on day 1 and alvocidib (30 to 160 mg/m2) on day 2, with the cycle repeated every 3 weeks. The combination was safe up to a dose of 70 mg/m2 of alvocidib given as a 24 h iv infusion. No clear relationship was observed between alvocidib dose level and the occurrence of adverse events. The AUC and Cmax of alvocidib tended to increase with total dose of alvocidib in a less than dose-linear manner. From 12 evaluable patients partial response was observed in eight patients or six patients according to RECIST or WHO criteria, respectively [451830]. A preclinical study was also presented at the 38th ASCO meeting of the combination of alvocidib and docetaxel in a murine adenocarcinoma model. It was found that the compounds enhanced antitumor activity when compared to the single administration of the agents [452088], [470726].

Another phase I study of alvocidib in combination with irinotecan was also presented at the 38th ASCO meeting in Orlando, FL, in May 2002. Alvocidib could be given safely as a weekly 1-h infusion following irinotecan (100 mg/m2) up to 60 mg/m2. Dose escalation of alvocidib with 125 mg/m2 irinotecan was continuing [451832].

In April 2002, phase I data on alvocidib in combination with cisplatin were presented at the 93rd AACR meeting in San Francisco, CA. 25 Patients with advanced solid tumors received either a fixed dosage of cisplatin (30 mg/m2) with escalating amounts of alvocidib or, a fixed dosage of alvocidib with escalation of cisplatin. The MTD was established as 60 mg/m2 cisplatin and 100 mg/m2 alvocidib. Severe toxicities were nausea, vomiting, dehydration and diarrhea. Dose-limiting toxicities were abdominal pain, nausea, vomiting, dehydration and diarrhea. Stable disease was seen in 28% of patients however, there were no objective responses [445967].

In March 2001, results from a phase Ib trial on alvocidib in combination with paclitaxel and cisplatin in patients with solid tumors were presented at the 92nd AACR meeting in New Orleans, LA. Escalating doses of cisplatin (30 to 75 mg/m2) were administered to fixed doses of paclitaxel (175 mg/m2) and alvocidib (80 mg/m2), cycled every 21 days, with cisplatin being given on day 2, prior to alvocidib. The MTD for this sequence-dependent combination was 175 mg/m2 of paclitaxel on day 1 followed by 50 mg/m2 of cisplatin and 80 mg/m2 of alvocidib on day 2. Clinical responses were seen in patients with esophageal and lung cancer who had failed prior therapy with cisplatin, as well as in patients with esophageal cancer who had failed prior therapy with paclitaxel and paclitaxel and cisplatin [404471].

By June 1998, phase I trials of alvocidib in combination with paclitaxel in patients with solid tumors had been completed. Results showed that alvocidib enhances the effects of paclitaxel. A fixed dose of paclitaxel over 24 h, followed by escalating doses of alvocidib over 24 h, was

administered to 15 patients. One patient showed a pathological complete response, and another showed improvement in bone lesions. Reduction of the paclitaxel dose duration to 3 h resulted in no dose-limiting toxicities [289180], [291439].

In phase I trials in combination with standard therapy in NSCLC patients, in total 66% of patients demonstrated some therapeutic effect with the combination therapy, compared to 15% obtained with the standard therapy alone. No overlapping toxicity profile was observed [409257].

PRECLINICAL DATAIn April 2005, preclinical data on alvocidib were presented at the 96th AACR meeting in Anaheim, CA. Out of 46 primary cancer cell samples isolated from the ascites or pleural fluid of cancer patients, alvocidib was effective in 43 samples with LD50 values of 20 to 70 nM, and was able to induce cell death in cells that were resistant to other drugs such as cisplatin and taxol. Three cell samples demonstrated resistance to alvocidib (LD50 > 100 nM) and also cross-resistance to other chemotherapy agents [597511].

In March 2004, preclinical data on alvocidib were presented at the 95th AACR meeting in Orlando, FL. Blockade of the PI3K survival pathway using LY-294002 (qv) facilitated the apoptotic effects of alvocidib [530124]. Alvocidib was active in cisplatin-resistant as well as topoisomerase II- and MRP1-resistant lung cancer cell lines. Alvocidib also potentiated the antitumor activity of cisplatin but not docetaxel (qv) in various cell lines [530125]. HA14-1 (qv) interacted synergistically with alvocidib to induce mitochondrial injury and apoptosis in human myeloma cells through a free radical- and JNK-dependent mechanism [530126]. In a human CML cell line, K562, a combination of alvocidib, homoharringtonine and STI-571 (both qv) inhibited cell growth and clonogenicity to an extent that was greater than the sum of all the three agents used alone [530129]. Augmentation of SN-38 (qv) induced apoptosis by alvocidib required an intact p53 to induce apoptosis and this may have depended on posttranslational modifications of p53 by alvocidib on SN-38-treated cells [530220]. Increased apoptosis resulting from treatment of human breast cancer cells with docetaxel followed by alvocidib may have been due to alvocidib-mediated downregulation of the Mcl-1, Bcl-xL, XIAP and survivin, as well as repression of docetaxel-induced A2K levels and activity [530236].

In November 2003, preclinical data on alvocidib were presented at the 15th AACR-NCI-EORTC meeting in Boston, MA. Alvocidib was shown to interact synergistically with TRAIL to induce apoptosis in human leukemia cells through a mechanism involving XIAP downregulation [514834].

In November 2003, preclinical data on alvocidib were presented at the AHA meeting in Orlando, FL. Vascular smooth muscle cells were incubated with alvocidib in the 100 nM to 1 microM range. There were marked increases in several inflammatory cytokines. At a dose of 1 microM, alvocidib abrogated IL-1beta-stimulated increases in the mRNA of inflammatory cytokines. mRNA from cytokines which were not stimulated by IL-1beta were not affected. Alvocidib inhibits activation of NFkappaB and specific leukocyte recruiting cytokines [514331].

In July 2003, data were presented at the 94th AACR meeting, Washington, DC, from a study which investigated the in vitro radiosensitizing effect of alvocidib and the underlying molecular mechanisms in a murine ovarian cancer cell line, OCA-I. Alvocidib inhibited cell growth in a dose-dependent manner and enhanced cell radiosensitivity assessed by the clonogenic cell survival assay. A dose of 300 nM doubled radiosensitivity. Clonogenic cell survival after split-dose radiation showed that alvocidib inhibited repair from radiation damage. The drug downregulated expression of Ku70 and Ku86 proteins that play a role in DNA repair processes.

Flow cytometry analysis showed that alvocidib (300 nM) accumulated the cells in G1 and G2 phases, with a significant reduction in the S-phase component. Alvocidib downregulated cyclin D1, cyclin E protein levels and also inhibited phosphorylation of Rb protein, consistent with the observed cell cycle arrest. Among the cdks tested, cdk-9 was significantly downregulated by alvocidib suggesting that alvocidib may modulate cellular transcription processes. Alvocidib on its own induced apoptosis in the OCA-I cells, whereas in combination with radiation exerted no further increase in apoptosis [484116].

Further data were presented in July 2003, at the AACR meeting from a study evaluating the potential role and mechanism of alvocidib in modulating radiation, chemotherapy, and chemoradiation sensitivity in vitro. H460 human lung carcinoma cells were treated with docetaxel, alvocidib and radiation or a combination of these agents. Alvocidib enhanced the effects of docetaxel and radiation, and also enhanced the effects of the combination of docetaxel and radiation. The degree of enhancement was time-dependent. Maximum percent chemoradiation enhancement and apoptosis was observed when the cells were treated with the sequence of docetaxel, radiation, alvocidib. A moderate increase in the redistribution of cells into the G1 phase by alvocidib (43.5%) was observed compared with control (37.3%) and a significant redistribution of cells (41.2%) into the radiosensitive G2/M phase by docetaxel was observed compared with control (13.6%). Alvocidib blocked p27 expression, induced p21 expression and induced caspase-8 expression. Radiation also induced p21 expression. When 24-h alvocidib was followed by 1-h docetaxel, the alvocidib-induced p21 expression was inhibited, while docetaxel followed by alvocidib did not inhibit p21 expression [484120].

Additional preclinical data presented in July 2003 at AACR 2003, described the effect of flavopiridol on the murine GL261 glioma cell line. Treatment with flavopiridol at 300 nM for 72 h was cytotoxic; treatments for 14 h or 24 h also induced similar levels of cytotoxicity by 72 h. Flavopiridol inhibited the migration of GL261 cells on the extracellular matrix protein fibronectin at 24 h of treatment. Following flavopiridol treatment, GL261 cells showed increased expression of MDM2 and decreased expression of p53 and the cell cycle proteins p21, p27, cdk4, and cyclin D1 by western blotting. Syngeneic C57BL mice implanted with GL261 glioma cells intracranially showed a response to flavopiridol treatment (5 mg/kg ip qd on days 7 to 11). Tumor volumes in all drug treated groups were smaller compared with their respective control groups [484219].

In May 2003, preclinical data were presented at the 39th ASCO meeting, Chicago, IL. Flavonoid enhanced tumor response to radiotherapy in animals and in vitro. Animals who received alvocidib modestly increased their times-to-tumor progression, demonstrating that the drug affects multiple factors including inhibition of cellular repair, cell cycle redistribution and inhibition of tumor angiogenesis. The drug appeared to be both cytostatic and cytotoxic in mouse models of solid and lymphoma tumors. At the molecular level, it was reported that alvocidib increased cell sensitivity to radiation which was associated with drug-induced downregulation of Ku70 and Ku80 proteins that play a role in DNA repair processes [491325], [493380].

In January 2003, preclinical data on alvocidib were presented at the Apoptosis conference in Luxembourg. Viability studies were performed and significant neuroprotection was achieved when cells were pretreated 24 h before with alvocidib. The drug also prevented colchicine-induced apoptosis and resulted in significant prevention of microtubule disruption and inhibition of caspase 3 activity when used to pretreat cell cultures [480878].

In May 2001, results from a preclinical study of alvocidib in combination with irinotecan were

presented at the 37th ASCO meeting in San Francisco, CA. It was shown that it improved the response to irinotecan in a murine HCT-116 colon tumor xenograft model. Tumor regression and cures were achieved with the combination, in a schedule-dependent manner, compared to irinotecan alone, which did not result in any cures. It was stated, that at this time, a phase I trial of weekly irinotecan, followed by alvocidib 7 h later, was underway [409916]. In september 2004, preclinical data were presented at the 16th EORTC-NCI-AACR meeting in Geneva, Switzerland. Srp20, a gene that is transcriptionally induced during apoptosis by combination treatment of SN-38 (qv) followed by alvocidib, affected drug sensitivity. Studies suggested that transcriptional upregulation of pre-m-RNA splicing factor, Srp20, may be a mechanism by which alvocidib induces apoptosis or augments the effects of the compounds irinotecan (qv) and SN-38. Increased Srp20 expression may result in altered splicing of genes that mediate the process of apoptosis [563113].

In human gastric cancer xenografts tumors, a combination of alvocidib and Taxotere (qv) was more effective than either agent alone. In fact, the effect of alvocidib alone was similar to placebo [455004].

In May 2002, preclinical data on alvocidib were presented at the 38th ASCO meeting in Orlando, FL. Radiotherapy (4 Gy/day) followed by alvocidib (7.5 to 10 mg/kg) potentiated tumor shrinkage in mice bearing HCT-116 human colon cancer xenografts, as compared to radiotherapy alone [452229].

In April 2002, preclinical data on alvocidib were presented at the 93rd AACR meeting in San Francisco, CA. Alvocidib inhibited the growth of five head & neck small cell carcinoma cell lines in a time- and dose-dependent manner [446456]. Another study indicated that pretreatment of U251 glioma cells for 2 h with alvocidib reduced clonogenic survival compared to radiation alone. This pretreatment did not redistribute cells into a more radiosensitive phase of the cell cycle [446690]. Another study indicated that alvocidib and UCN-01 (qv) significantly reduced survivin abundance compared with either drug alone [447640]. Furthermore, alvocidib-induced disruption of STAT-3/DNA interactions, which occurred with some degree of selectivity when assayed in cells isolated from AML patients receiving alvocidib therapy, may represent the mechanism through which the drug induces cytotoxicity [446310].

In March 2001, preclinical data on alvocidib were presented at the 92nd AACR meeting in New Orleans, LA. In vitro data suggests the potential use of alvocidib in the treatment of glioblastomas. In glioblastoma cell lines (300 nM for 72 h), p53-independent apoptosis was observed, [404736]. In vivo tests for this indication are underway at Kaplan Comprehensive Cancer Center. Other data demonstrated how alvocidib disrupts the interaction of the transcription factor STAT-3 with DNA. Proteins downstream of STAT-3 (including the anti-apoptotic protein MC-1) were shown to be downregulated at the transcriptional level after treatment of human non-small cell lung carcinoma A549 cells with alvocidib. Further, most alvocidib-treated, G2-arrested cells did not express cyclin A and so cyclin A, being overexpressed in a number of malignancies, may be a target for alvocidib-based therapy [403729], [404565].

Data on alvocidib in combination therapies were also presented at the same meeting. Gemcitabine (10 nM) followed by alvocidib (100 nM) significantly enhanced apoptosis in breast cancer cell lines, MCF-7 and MDA-MB231 [404740]. A combination of alvocidib with PKC activators (eg, PMA or bryostatin (qv)) in myeloid leukemia cell lines, induced apoptosis in over 50% of cells. In colon cancer xenografts, alvocidib administered 7 or 16 h post administration of

irinotecan (qv) resulted in tumor regression of 86 +/- 9% and 82 +/- 5%, respectively, compared to 40 +/- 25% when cells were treated with irinotecan alone [403729], [404742]. The combination of trastuzumab and alvocidib was also explored in SKBR3 breast cancer cell lines; the combination synergistically altered several pathways leading to enhanced cell cycle arrest [404376].

Preclinical data presented at the 40th annual American Society of Hematology meeting, December 1998, suggest the potential use of alvocidib to treat HHV-8-associated malignancies, such as Kaposi's sarcoma, Castleman's disease and primary effusion lymphoma [309009].

Alvocidib's selectivity for cyclin-dependent kinases also make it a potential therapeutic tool for the treatment of smooth muscle cell rich vascular lesions. In a study presented at the 1999 American Cardiology meeting, alvocidib (75 nmol/l) resulted in near complete inhibition of basic fibroblast growth factor- and thrombin-induced proliferation in human aortic smooth muscle cells. Cyclin-dependent kinase activity was inhibited, as was induction of cell cycle-related proteins cyclin D1, PCNA and retinoblastoma protein. MAP kinase activation was unaffected [315119].

At the 9th International Conference of the Inflammation Research Association in November 1998, alvocidib was described as not very specific and failing to block the cell cycle in fibroblasts, whilst maintaining antitumor activity [306060].

Preclinical toxicology studies in rats and dogs demonstrated dose-related leukopenia and drug-related lesions in the thymus, spleen and bone marrow. The gastrointestinal and bone marrow toxicity was dose limiting [178579].

In November 2000, reports from the NCI-EORTC-AACR 11th Symposium described the ability of alvocidib to inhibit CDK9/cyclin T complex associated with the PTEFb transcriptional regulator [391557].

Preclinical studies have demonstrated that alvocidib reduced TUNEL-positive cells by 90%, leaving the cells histologically normal following a stroke [355744].

Alvocidib has shown potent activity against every CDK that has been studied, and also inhibits other protein kinases, with IC50 values in the range of 0.4 microM (CDKs), 145 microM (PKA) and 6 microM (PKC) [289180]. The compound also induces caspase-3 activation [379340]. Alvocidib causes arrest in G1 and G2 by direct inhibition of Cdk2, Cdk4 and Cdk1 and by downregulation of cyclins D1, D3 and B [454720].

In vitro studies have demonstrated that alvocidib can potentiate the action of many cytotoxic agents including cisplatin, mitomicin C, paclitaxel, cytarabine, topotecan, doxorubicin, etoposide and 5-fluorouracil [289180]. In vitro pharmacokinetic studies have shown that it undergoes hepatic biotransformation to its corresponding glucoronide by uridine diphosphate glucoronosyltransferases [283791].

ADDITIONAL INFORMATIONAlvocidib was originally derived by the NCI in a screen of synthetic analogs of a natural product isolated from the plant Dysoxylum binectariferum [289180], [325767].

Analysts Merrill Lynch predicted in September and November 2000, that the product would be

launched by 2003, with sales of Euro 50 million in that year, rising to Euro 100 million in 2004 [383742], [391426]. In April 1999, ABN Amro predicted annual sales of DM 100 million in 2002 [328676]. In March 2001, Commerzbank Securities predicted sales of Euro 100 million in 2003, rising to Euro 250 million in 2004 [412599], while Morgan Stanley Dean Witter predicted sales of Euro 25 million in 2003, rising to Euro 300 million in 2006 and Euro 600 million in 2007 [412600]. In May 2001, Morgan Stanley Dean Witter's sales predictions remained unchanged [412602].

Development Status

Detailed status for Aventis Pharma AG

Indication	Country	Status	Reference	Date
Chronic lymphocytic leukemia	US	Discontinued	521627	05-02-2004
Colon tumor	US	Discontinued	521627	05-02-2004
Esophagus tumor	US	Discontinued	521627	05-02-2004
Lung tumor	US	Discontinued	521627	05-02-2004
Prostate tumor	US	Discontinued	521627	05-02-2004

Detailed status for National Cancer Institute

Indication	Country	Status	Reference	Date
Cancer	US	Phase 1 Clinical	203645	01-12-1996
Chronic lymphocytic leukemia	US	Phase 2 Clinical	331850	14-07-1999
Colon tumor	US	Phase 1 Clinical	279466	01-09-1997
Esophagus tumor	US	Phase 2 Clinical	331850	14-07-1999
Lung tumor	US	Phase 2 Clinical	331850	14-07-1999
Lymphoma	US	Phase 2 Clinical	277372	11-02-1998
Multiple myeloma	US	Phase 2 Clinical	277372	11-02-1998
Prostate tumor	US	Phase 2 Clinical	493537	01-06-2003
Solid tumor	US	Phase 1 Clinical	396524	01-12-2000
Stomach tumor	US	Phase 2 Clinical	288659	12-06-1998

Licensing

Summary	Reference
Hoechst Marion Roussel Inc	
By September 1997, Hoechst (now Aventis Pharma) had a collaborative agreement with the NCI to develop flavopiridol [279466]. However, Aventis had discontinued development by February 2004 [521627].	279466

Chemistry

Structure

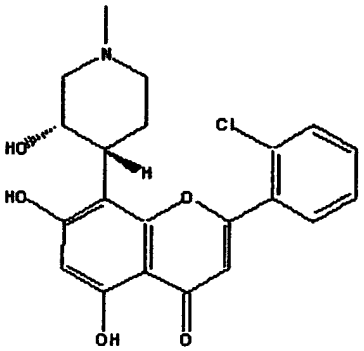

Confidence Level : 1

Compound names associated with this drug	
Name	Type
146426-40-6	CAS RN
L-868275	Research Code
L-868276	Analogue
MDL-107826A	Research Code
NSC-649890	Research Code
flavopiridol	
131740-09-5	CAS RN
alvocidib	USAN, INN
HMR-1275	Research Code

Literature Evaluation

There are two evaluations of this drug.

Hui-Kang Wang, University of North Carolina at Chapel Hill, NC, USA

5 June 2001

IntroductionFlavopiridol (also known as 5,7-Dihydroxy-8-(4-N-methyl-2-hydroxypyridyl)-6'-chloroflavone, HMR-1275, L-868275 or NSC-649890) is a novel semisynthetic flavone analog of the alkaloid, rohitukine, a leading compound from an Indian tree, Dysoxylum binectariferum [411768]. It was recently identified as a novel antineoplastic agent in the primary screen conducted by Aventis Pharma (formerly Hoechst Marion Roussel) and the Developmental Therapeutics Program, National Cancer Institute. Flavopiridol is the first cyclin-dependent kinase (CDK) inhibitor in early clinical trials for the potential treatment of renal, prostate, gastric and colon cancers, and non-Hodgkin's lymphoma.

CDKs are thought to be common cellular targets of flavopiridol and regulate the passage of cells through the cell cycle. Flavopiridol inhibits CDK1,-2, -3 and -4, causes both G1 and G2 cell cycle arrest and, in some cases, induces apoptosis [118256], [159704], [348164]. The flavopiridol-induced decline in cyclin D1 expression is an early event that is specific and, at least in part, due to the transcriptional repression of the cyclin D1 promoter [388848]. In addition to the CDKs, some other potential targets have also been explored. Flavopiridol downregulates bcl-2 mRNA and Bcl-2 protein expression within 24 h [286602] and interacts with multidrug resistance protein 1 (MDR1) in a potent way [411683]. Flavopiridol may also have anti-angiogenic as well as direct antiproliferative effects [360600]. A 60-kDa protein, cytosolic aldehyde dehydrogenase (ALDH)-1, which was present in non-small cell lung carcinoma

(NSCLC) cells and bound well to immobilized flavopiridol, was identified as another cellular target of flavopiridol [411732]. Furthermore, flavopiridol has recently been shown to inhibit other intracellular targets, notably PTEFb [38867], glycogen phosphorylase [413046], and DNA [413047]. This suggests that flavopiridol may not be a pure CDK inhibitor and that multi-targets may be involved.

Synthesis and SARTwo US patents covering the syntheses of key intermediates for preparing flavopiridol and its analogs have been awarded to Aventis and Bristol-Myers Squibb (US-05908934 and US-06225473, respectively). A US patent has been awarded to Bristol-Myers Squibb for thio- and oxoflavopiridols (US-05849733). These flavopiridol analogs, which contain a sulfur or oxygen atom linker between a chromone ring and the hydrophobic side chain, are selective cyclin-dependent kinase 1 (CDK1) inhibitors with IC50 values of 110 and 130 nM, respectively [388424]. The modifications of the 3-hydroxy-1-methylpiperidinyl group (D ring) of flavopiridol and their effect on CDK inhibitory activity have been studied [411733]. Inverting the hydroxyl substituent from cis to trans form results in > 1000-fold loss in activity against both CDK4/cyclin D and CDK1/cyclin B kinases. Both the presence and the position of the nitrogen moiety on the D ring are critical requirements for CDK inhibitory activity. The isocoumarin rings are not effective flavone replacements.

PharmacologyFlavopiridol is reported to have cytotoxic activity against a wide range of cancer cell lines, including HCT8 ileocecal adenocarcinoma, T98G glioblastoma, MCF-7 breast adenocarcinoma, HL-60 leukemia cells [250846], head and neck squamous cell carcinomas [388857], various ovarian cancers [307450], esophageal adenocarcinomas (SKGT-2, SKGT-4, and SKGT-5), epidermoid carcinoma (HCE-4) cells [388855], human chronic lymphocytic leukemia [286615], hematopoietic cell lines [286600], human umbilical vein endothelial cells [307451], seven non-small cell lung cancers [411680], bladder cancer [388854], and MDA-MB-435 breast cancer cells [411681].

In vivo, flavopiridol has demonstrated antitumor activity against several tumor xenografts, including prostate cancer [250839], head and neck squamous cell carcinomas [388857], and hematopoietic neoplasia [286595].
Combined administration of flavopiridol with other antineoplastic agents is highly schedule-dependent. Flavopiridol enhanced the cytotoxic effect of mitomycin C by promoting drug-induced apoptosis in both gastric and breast cancer cells. Scheduling studies suggested that mitomycin C followed by flavopiridol or simultaneous treatment is superior to flavopiridol followed by mitomycin C [279010]. Cisplatin was the only agent that resulted in schedule-independent synergy when combined with flavopiridol. Synergy was more pronounced for paclitaxel, cytarabine, topotecan (Hycamtin; SmithKline Beecham plc), doxorubicin and etoposide when the agents were administered before flavopiridol rather than concomitant with or following flavopiridol [265644]. The synergistic effect of flavopiridol on paclitaxel-treated cells is due to an enhancement of caspase activation [411682].

Recently, a US patent that covers flavopiridol and its salts for inhibiting neuronal cell damage or neuronal cell death was granted to Columbia University, New York (US-06087366).

MetabolismBesides flavopiridol, two metabolites (monoglucuronides with the glucuronide in positions 5 and 7 of the flavonoid core) were detected by high-performance liquid chromatography (HPLC) in bile and perfusate, respectively, by using an isolated perfused rat liver system. It is suggested that glucuronidation is the major mechanism of hepatic flavopiridol biotransformation. Metabolites are mainly excreted into bile but also released into systemic

circulation [307452].

ToxicityDiarrhea is the dose-limiting toxicity [411769]. It is likely to be multifactorial in origin and may involve interactions with endogenous secretagogues, eg, acetylcholine and bile acids [411722]. Other toxicities include nausea/vomiting, anorexia, and fatigue [411769]. In addition, some patients experienced grade 3 or 4 vascular thrombotic events, including myocardial infarction, transient neurological ischemic attacks, deep vein thrombosis and pulmonary emboli [407096], [411684].

Clinical DevelopmentPhase IA phase I trial was conducted by the National Institutes of Health (NIH). Flavopiridol was given as a 72-h infusion every 2 weeks. The MTD of infused flavopiridol was 50 mg/m2/day x 3, with dose-limiting secretory diarrhea at 62.5 mg/m2/day x 3. The MTD was 78 mg/m2/day x 3 in combination with antidiarrheal prophylaxis (ADP), with dose-limiting hypotension at 98 mg/m2/day x 3. Based on chronic tolerability, the recommended phase II dose without ADP is 50 mg/m2/day x 3. An antitumor effect was observed in certain patients with renal, prostate and colon cancer, and non-Hodgkin's lymphoma. The concentrations of flavopiridol (200 to 400 nM) required for CDK inhibition in preclinical models were achieved safely [307449].

Phase IIEligible patients had previously untreated metastatic colon cancer and were treated with a 72-h continuous infusion of flavopiridol at a dose of 50 mg/m2/day and a concentration of 0.1 to 0.5 mg/ml every other week. Dose escalation to 75 mg/m2/day was permitted with ADP (loperamide and cholestyramine) for patients tolerating the lower dose. To date, 14 patients have been entered, out of which 10 patients have been evaluable for response. One patient had prolonged stable disease lasting > 24 weeks. No complete responses or partial responses were observed [411769]. Flavopiridol (50 mg/m2/day), administered by continuous infusion for 72 h every 2 weeks, was ineffective in 35 minimally pretreated patients with metastatic renal cancer [411684]. Flavopiridol, administered as a single agent at dose of 50 mg/m2/day for 72 h every 14 days, was inactive in the treatment of 16 patients with gastric cancer [407096]. Overall, flavopiridol was concluded to be ineffective in all reported phase II trials.

Phase IIINo trial has been planned or is currently underway.

Side Effects and ContraindicationsSide effects of flavopiridol observed in a phase I trial are described supra.

Current OpinionAlthough flavopiridol has demonstrated wide antitumor spectrum against various cancer cells both in vitro and in vivo, its phase II clinical trial results are disappointing. Many factors may affect the clinical outcome. It is still too early to conclude the fate of flavopiridol. Developing new analogs of flavopiridol and continuing studies with the aim of improving its pharmacokinetic characteristics might be future directions that are worth pursuing. As many chemotherapeutic agents such as paclitaxel, cytarabine, topotecan, doxorubicin, and etoposide have shown sequence-dependent synergy with flavopiridol [265644], another rewarding direction may be the development of combination regimens in a clinical setting.

Dr M J Zvelebil, Ludvig Institute of Cancer Research, London, UK

12 December 1997

Synthesis and SARFlavopiridol is a synthetic chloronated flavone which inhibits cyclin-

dependent kinases (CDKs). It is similar to other such inhibitors for instance, butyrolactoneI and olomoucine. The structure of the complex of CDK2 and L-868276 (a des-chloroflavopirdol analog of flavopiridol) was solved by X-ray crystallography to 2.3 angstrom resolution. The inhibitor binds in the ATP binding pocket with the aromatic portion of the inhibitor binding to the adenine-binding pocket of CDK2. While the phenyl group on the inhibitor makes contacts with the enzyme that are not possible in the ATP-enzyme structure. It occupies a region not occupied by any part of the ATP molecule. Most of the hydrophobic ATP-enzyme interaction are conserved in the L-868276 structure, but there are additional contacts between the benzopyran ring which also involve charged residues. Two contact are unique to L-868276 (and analogs). These are contacts with the phenyl ring and His84 and Lys89. These additional contacts explain the specificity of the flavanoid inhibitors to inhibit CDK2 and CD2 while the potency can be explained by the larger number of contacts between L-868276 and the enzyme than in the ATP-complex [250849]. In flavopiridol the chlorophenyl has even more potential to make additional contacts with Leu10, Phe82 and Leu83 which is why the inhibition factor is increased by six over that of L-868276 [250863].

PharmacologyIn vitro studies on human tumor cells have shown that flavopiridol is an effective inhibitor of protein kinase, specifically CDKs [155754], [159704] and is involved in cell cycle arrest at the G1 and G2 phase [25572]4, [161100]. Examination of log phase A549 non-small cell lung cancer cells, HTC8 ileocecal adenocarcinoma, T98G glioblastoma, MCF-7 breast adenocarcinoma and HL-60 leukemia cell showed a 50% reduction in colony uptake at 72 h and between 90% and 50% uptake of trypan blue. In addition RNA synthesis inhibitor 5,6-dichloro-1-beta-D ribofuranosylbenzimidazole or the protein synthesis inhibitor cycloheximide reduced the cytotoxicity of flavopiridol. The above results suggest that flavopiridol is both cytostatic and cytotoxic [250846]. It is active against chemoresistant tumors and synergizes with cisplatin [249995]. Cytotoxicity of flavopiridol with eight other antineoplastic agents was studied in A549 non-small cell lung carcinoma cells in vitro. Seven of the eight agents showed synergy which was dependent on administration schedule. Cisplatin being the only agent that was sequence independent. Paclitaxel, cytarabin, topotecan, doxorubicin and etoposide had to be administered before flavopiridol [265644].

In vivo mouse colon carcinoma showed some anti-tumor effect [155754] While also flavopiridol demonstrated activity against xenografts of two strains of androgen-dependent human prostate cancer in nude mice, the tumors regrew when therapy was halted [250839].

Clinical Development

Phase I A trial of flavopiridol by 72 h continuous intravenous infusion given q2 weeks. Sixty-three patients v aged 29 to 83 years have been entered. The dose-limiting toxicity was intra-infusional secretory diarrhea and the maximal tolerated dose was 50 mg/m2/day. Fourteen stable (3 months) patients (4 renal, 3 colon, 3 prostate, 1 adeno-cystic, 1 mesothelioma, 1 germ cell, 1 non Hodgkins lymphoma) and 3 minor response, ie <50% shrinkage, (2 renal and 1 NHL) were observed [203645]. This study led to recommendation of phase II trials.

Phase II An NCI phase II study (NCI-T96-00) of flavopiridol in patients with metastatic renal cell carcinoma has been approved but is not yet active. The trial will include patients of 18 and over with metastatic or locally recurrent renal cell carcinoma and will aim to determine the objective response rate of patients treated with flavopiridol and the toxic effects of flavopiridol in this population (http://www.findcure.com/newclntr.html) [272937].

Side-effects and ContraindicationsIntravenous infusion in patients showed transaminitis (particularly in patients with liver metastases), diarrhea, fever, fatigue, nausea, anorexia, local tumor pain and pericardial pleural effusions, all grade 2. No bone marrow toxicity was seen [203645].

Current OpinionPhase I trials have shown enough positive data for the initiation of phase II trials. The main advantage of flavopiridol is its specificity and that it is active in chemoresistant tumors. This should be enough evidence to continue trials. Further trials will reveal the efficacy of this drug.

Scientific Data		
Chemistry		
Study Type	Result	Reference
SAR	X-ray structure giving information on binding.	250849
SAR.	Original natural product (rohitukine) as design model for flavopiridol.	411768
Development of formulations.	Intravenous formulations, containing up to 10 mg/ml of flavopiridol and producing negligible precipitation on dilution, were developed.	411725
Synthesis/SAR.	Thio- and oxoflavopiridol analogs, containing a sulfur (16) or oxygen (18) atom linker between a chromone ring and the hydrophobic side chain, were selective CDK1 inhibitors with IC50 values of 110 and 130 nM, respectively.	388424
Synthesis/SAR.	Explored the SAR around the D-ring of flavopiridol to determine the key structural requirements for CDK inhibitory activity.	411733

Biology				
Study Type	Effect Studied	Experimental Model	Result	Reference
In vitro	Protein kinase inhibition.	cdk1 Protein kinase inhibition assay in breast, colon and lung carcinoma cells.	cdk1 Activation inhibited; G1/S phase block induced.	155754
In vivo	Antitumor activity.	Mouse colon carcinoma cells.	Regrowth of tumors when therapy was halted.	250839
In vitro	Growth inhibition.	Bladder cancer cell lines.	Flavopiridol was found to inhibit the growth of bladder cancer cell lines with tumor suppressor gene alterations and/or multidrug resistance.	388854
In vitro	Effect of flavopiridol on hematopoietic cell lines.	Hematopoietic cell lines, including SUDHL4, SUDHL6 (B-cell lines), Jurkat, and	Tested cell lines displayed notable sensitivity to flavopiridol-induced apoptosis.	286600

		MOLT4 (T-cell lines), and HL60 (myeloid).		
In vitro	Antitumor properties of flavopiridol.	Human chronic lymphocytic leukemia cells.	Flavopiridol had significant in vitro activity against human chronic lymphocytic leukemia cells through activation of caspase-3, which appears to occur independently of Bcl-2 modulation, the presence of IL-4, or p53 status.	286615
In vitro	Antitumor properties of flavopiridol.	Head and neck squamous cell carcinoma cells.	Flavopiridol diminished cdc2 and cdk2 activity and potently inhibited cell proliferation (IC50 = 43 to 83 nM).	388857
In vitro	Interactions of flavopiridol with members of the ATP-binding cassette (ABC) transporter family.	Human breast cancer cells.	ATP-binding cassette half-transporter, ABCG2 (MXR/BCRP/ABCP1), plays a role in resistance to flavopiridol.	411724
In vitro	Investigation of mechanisms underlying the diarrheal side effects of flavopiridol.	Human colonic epithelial cell line (T84).	The diarrheal side effects induced by flavopiridol are likely to be multifactorial in origin and may involve interactions with endogenous secretagogues such as acetylcholine and bile acids.	411722
In vitro	Interaction between flavopiridol and phorbol 12-myristate 13-acetate (PMA) in relation to differentiation and apoptosis.	Human myeloid leukemia cells.	Flavopiridol modulated the expression/activity of multiple signaling and cell cycle regulatory proteins in PMA-treated leukemia cells. Such alterations were associated with mitochondrial damage and apoptosis rather than maturation.	411700
In vitro	Effect of P-glycoprotein (Pgp) on flavopiridol sensitivity.	Chinese hamster ovary cell lines differing with respect to level of Pgp expression.	Results suggest that flavopiridol is a weak substrate for Pgp.	411698
In vitro	Sequential administration of flavopiridol and paclitaxel.	Human gastric and breast cancer cells.	In these cell lines flavopiridol enhanced paclitaxel-induced apoptosis only when administered after paclitaxel treatment.	411682
In vitro	Growth inhibition.	MDA-MB-435 breast cancer cells (parental) and	435.eB cells were established by transfecting c-erbB-2 cDNA into MDA-MB-435.	411681

		435.eB (stable transfectant) cells.	Induction of apoptosis was observed in these cell lines.	
In vitro	Cell-cycle arrest and apoptosis.	Non-small cell lung cancers (NSCLC).	At doses of up to 500 nM, maximal cytotoxicity required 72 h of exposure. Flavopiridol-mediated apoptosis was p53-independent.	411680
In vitro	Growth inhibition.	Esophageal adenocarcinoma (SKGT-2, SKGT-4, and SKGT-5) and epidermoid carcinoma (HCE-4) cells.	Flavopiridol inhibited the growth of these cell lines containing variable retinoblastoma, cyclin D1, p16, and p53 expression patterns.	388855
In vitro	Effect of flavopiridol on human umbilical vein endothelial cells (HUVECs).	HUVECs.	Flavopiridol induced apoptosis in these cells.	307451
In vitro	Flavopiridol/mitomycin C combination treatment.	Gastric and breast cancer cells.	Mitomycin C followed by flavopiridol or simultaneous treatment enhanced the cytotoxic effect of mitomycin C by promoting drug-induced apoptosis.	279010
In vitro	Growth inhibition.	Various cancer cell lines.	The GI50 values at 48 h for flavopiridol were: myeloid cell line HL-60 < 100 nM, TF-1 = 1 microM, 32Dc13 = 100 nMand myeloma cell line RPMI-8226 = 100 nM.	411730
In vitro	Effect of flavopiridol on ATPase activity of multiple resistance protein 1 (MRP1).	Plasma membrane vesicles prepared from the MRP1-overexpressing cell line GLC4/ADR.	Flavopiridol stimulates the ATPase activity of MRP1 in a dose-dependent way at low micromolar concentrations.	411683
In vitro	Cytotoxicity of flavopiridol.	Various cancer cell lines.	Flavopiridol is cytotoxic to A549 non-small cell lung cancer, HCT8 ileocecal adenocarcinoma, T98G glioblastoma, MCF-7 breast adenocarcinoma, and HL-60 leukemia cells.	250846
In vitro	Growth inhibition.	Epstein-Barr virus (EBV)-transformed B-prolymphocytic cell line (JVM-2), EBV-transformed B-CLL cell line (I83CLL), and non-	Flavopiridol downregulated bcl-2 mRNA and Bcl-2 protein expression within 24 h.	286602

		EBV transformed B-CLL cell line (WSU-CLL).		
In vitro	Effect of flavopiridol on VEGF gene expression.	Transient transfection studies.	Flavopiridol might have anti-angiogenic as well as direct antiproliferative effects.	360600
In vivo	Antitumor properties of flavopiridol.	Panel of human tumor xenografts.	Flavopiridol affected prostate cancer xenograft regression in PRXF1337 and tumor stasis lasting for 4 weeks in PRXF1369. Treatment (5 mg/kg per day ip) by flavopiridol for 5 days led to the appearance of apoptotic cells in the head and neck squamous cell carcinoma tumor xenografts and caused a 60 to 70% reduction in tumor size.	250839
In vitro	Identification of cellular targets.	Enzyme derived from non-small cell lung carcinomas.	Cytosolic ALDH-1 was identified as a cellular target of flavopiridol.	411732
In vivo	Effect of flavopiridol on normal and malignant cells.	Normal lymphoid cells and human leukemia and lymphoma xenografts.	Flavopiridol induced apoptosis of normal lymphoid cells, caused immunosuppression, and had potent antitumor activity in vivo against human leukemia and lymphoma xenografts.	286595
In vitro	Combination treatment of flavopiridol with various antineoplastic agents.	A549 human non-small cell lung carcinoma cells.	Cisplatin was the only agent that resulted in schedule-independent synergy when combined with flavopiridol. For paclitaxel, cytarabine, topotecan, doxorubicin, and etoposide, synergy was more pronounced when the agents were administered before flavopiridol.	265644
In vitro	Cell-cycle arrest.	MDA-468 breast carcinoma cells.	Flavopiridol prevented progression through G2 by inhibiting the G2-related increase in histone H1 kinase activity mediated by cyclin-dependent kinase I.	161100

Metabolism				
Study Type	Effect Studied	Experimental Model	Result	Reference

In vitro	Hepatic metabolism.	Isolated perfused rat liver system.	Glucuronidation is the major mechanism of hepatic flavopiridol biotransformation. Metabolites are mainly excreted into bile but also released into systemic circulation.	307452
In vitro	Hepatic metabolism.	Rat and human liver microsomes.	The enzymatic pathways of flavopiridol were elucidated.	411712

Clinical			
Effect Studied	Experimental Model	Result	Reference
Establishment of effective dose.	Phase I study in patients with refractory malignancies and prior disease progression.	The dose of 50 mg/m2/day x 3 was recommended for phase II.	307449
Efficacy of flavopiridol monotherapy.	Phase II study in patients with metastatic renal cancer.	Flavopiridol was ineffective in this trial.	411684
Efficacy of flavopiridol monotherapy.	Phase II study in patients with gastric cancer.	Flavopiridol was inactive in this trial.	407096
Efficacy of flavopiridol monotherapy.	Phase II study in 14 previously untreated metastatic colon cancer patients.	No complete or partial responses were observed.	411769
Safety, toxicity, pharmacokinetics and antitumor response.	Continuous (72 h) iv infusion every 2 weeks. 63 Patients aged 29 to 83 years. Dose range: 4 to 50 mg/m2/day.	Grade 3 diarrhea at highest dose. Other toxicities: transaminitis (only in parts with liver metastases), diarrhea, fever, fatigue, nausea, anorexia, local tumor pain and pericardial pleural effusions, all grade 2. Pharmacokinetic parameters: clearance 2.5 to 41.8 l/h, volume of distribution-beta = 1.8 to 13.9 l/kg, t1/2 = 2 to 48 h; dose-dependent increase in AUC. Antitumor effect: 14 patients with stable disease (3 months) and 3 with up to 50% of tumor shrinkage.	203645

Exhibit VI

http://www.iddb3.com/iddb3/iddb3_2/reports.display?id=20637&template=Drug&i_query_id=5383468&i_clear_trail=Y

seliciclib	
Company	Cyclacel Ltd
Highest Dev Status	Phase 2 Clinical
Indications	Lymphoid leukemia Non-small-cell lung cancer Glomerulonephritis Mantle cell lymphoma Multiple myeloma Inflammation Breast tumor Cancer
Actions	Anticancer Apoptosis modulator Anti-inflammatory Cyclin-dependent kinase-1 inhibitor Cyclin-dependent kinase-2 inhibitor Cyclin-dependent kinase-5 inhibitor Cell cycle inhibitor
Technologies	Oral formulation
Reason for update on 01-Jun-2005	
1 reference added [605112]	

Summary

Seliciclib ((R)-roscovitine, CYC-202, NSC-701554), the lead compound from the CYC-200 series of orally-available small-molecule CDK inhibitors, is under development by Cyclacel Ltd for the potential treatment of various cancers and inflammatory diseases, including glomerulonephritis [303669]. Phase IIa trials in non-small-cell lung cancer (NSCLC) and breast cancer were initiated in January 2003 [476817]. At that time, phase II trials in glomerulonephritis were expected to be initiated later in the year [476817], [466924]. In March 2004, clinical trials in mantle cell lymphoma, multiple myeloma (MM) and lymphoid leukemia were initiated [563072].

CLINICAL DATACANCERB-cell malignanciesIn March 2004, phase II trials in B-cell malignancies (mantle cell lymphoma, multiple myeloma and B-cell lymphocytic leukemia) were initiated. The open-label European study was designed to recruit a minimum of 12 patients in each disease indication [563072], [530649], [575023].

NSCLCIn January 2003, an open-label European phase IIa trial of seliciclib, in combination with gemcitabine (qv) and cisplatin (qv), was initiated for the treatment of stage IIIb/IV NSCLC and was expected to recruit up to 30 patients [476817]. In May 2005, additional data on seliciclib, in combination with gemcitabine (qv) and cisplatin (qv), were presented at the 41st ASCO meeting in Orlando, FL. In the phase IIa trial, 27 patients with NSCLC (median age = 61 years; age range = 31 to 75 years) were assigned to three dose groups. Group A received oral seliciclib (400 mg bid) on days 1 to 4, 8 to 11 and 15 to 18, gemicitabine (1000 mg/m2; 30 min iv infusion) on days 5 and 12, and cisplatin (75 mg/m2; 2 h iv infusion) on day 5, of a 21-day cycle. Group B received the same regimen except oral seliciclib (800 mg bid) and Group C received the same regimen except oral seliciclib (1200 mg bid). Patients received a maximum of 6 cycles. Treatment-related

INFLAMMATIONBy October 2002, seliciclib was in phase Ib trials for inflammation and was being investigated for use in glomerulonephritis [464120], [466686]. In January 2003, phase II trials in glomerulonephritis were expected to be initiated later in the year [476817], [466924].

PRECLINICAL DATACANCERIn May 2005, preclinical data on seliciclib were presented at the 41st ASCO meeting in Orlando, FL. Seliciclib (IC50 = 15 to 25 microM) induced cytotoxicity in multiple myeloma (MM) cell lines both resistant and sensitive to convential chemotherapy, and to patient MM cells. Seliciclib time- and dose-dependently induced apoptosis in MM cells. It also down-regualted Mcl1 and pSTAT3 in a time- and dose-dependent manner [603576], [601317].

In April 2005, preclinical data on seliciclib were presented at the 96th AACR meeting in Anaheim, CA. Seliciclib (10 microg/ml) inhibited cell proliferation of MDA-MB-231 breast tumor cells in a calcium-independent, irreversible manner, and at the same concentration induced apoptosis [597506]. In B-cell chronic lymphocytic leukemia cells, seliciclib (30 microM) caused dephosphorylation of RNA pol II leading to a decrease in the anti-apoptotic protein MCL-1 and the induction of apoptosis [592253].

In December 2004, preclinical data on seliciclib were presented at the 27th Annual San Antonio Breast Cancer meeting in San Antonio, TX. In in vivo studies in nude mice bearing MCF-7 xenografts, the cytotoxic effects of doxorubicin were enhanced with the co-administration of seliciclib. Tumors treated with doxorubicin alone were reduced by 48% compared to tumors treated with the combination, which were reduced by 70%. The tumor doubling time was 7 days in control mice, 11 days in doxorubicin-treated mice and 23 days in combination-treated mice [577087].

In October 2004, preclinical data on seliciclib were presented at the Third Annual Drug Discovery and Development Studies of Protein Kinases meeting in Munich, Germany. Seliciclib was also investigated in BCL tumors and demonstrated significant G1 arrest and induction of apoptosis at a concentration of 10 microM [570614]. In December 2004, preclinical data on the in vitro activity of seliciclib in MM cells were presented at the 46th ASH meeting in San Diego, CA. Data showed that seliciclib has potent cytotoxic effects against both sensitive (MM1.S, RPMI 8226, U266, H929) and resistant (MM1.R, Dox-40, LR5, MR 20) MM cells to conventional chemotherapy. MM cell line cytotoxicity was noted at 24 h, with IC50 values around 25 to 50 mmol. Treatment was not toxic to normal PBMC. Seliciclib (25 mmol) induced an increase (35 to 50%) in MM cells in sub-G1 phase, suggesting that seliciclib triggers apoptosis. Seliciclib triggered a rapid down-regulation of MCL-1. Treatment of MM cells with seliciclib also resulted in decreased phosphorylation of pRb. Protein expression of CDC2, CDK4, and CDK6, were also down-regulated after treatment. Ongoing studies at this time were delineating the specific signaling cascades affected by seliciclib treatment [574156], [575023].

Seliciclib has demonstrated an antitumor effect in a number of tumor xenograft models [424627], including human lung cancer H460 xenografts in immune-deficient nude mice [515664], nude mice bearing the KM12 tumor [390823], and MF1 nude mice with established HT29 xenografts [446647]. Synergy with docetaxel has also been observed in vivo in immune-deficient nude mice bearing H460 xenografts. No toxicity has been noted in the combination therapy [515664].

Preclinical data on the activity of seliciclib in a number of cell lines have been presented at a number of scientific meetings. The compound showed activity in a panel of 103 human tumor cell lines representing 20 tumor types [497537] and was synergistic with doxorubicin in pRb

negative Leiomyosarcoma cells [485411], [445408], [471287]. In four human mantle cell lymphoma cell lines (REC, Granta-519, JeKo-1 and NCEB-1) exposed to seliciclib, an antiproliferative effect was observed from 24 to 48 h of exposure to the compound [530649]. Seliciclib has been shown to induce apoptosis in HTLV-I-infected transformed T-cells, implicating CDK2 in this process [447130], and in multiple myeloma cells by downregulation of Mcl-1 [530645]. Similar data were presented in October 2004 at the Third Annual Drug Discovery and Development Studies of Protein Kinases meeting in Munich, Germany [570614].

In addition to CDK2 inhibition, seliciclib also inhibits CDK2/A, CDK7/H, ERK-2 and CDK1/B with potencies ranging from 10 to 15 microM [457966]. Seliciclib displayed IC50 values of 2.7, 0.7 and 0.1 micromolar against CDK1/cyclin B, CDK2/cyclin A and CDK2/cyclin E, respectively [482285]. Other data described the sustained concentration- and time-dependent increase in ERK phosphorylation following treatment of colon carcinoma cell lines with seliciclib [446300]. Elsewhere, the compound was described as being a submicromolar inhibitor of CDK7/cyclin H and induces p53 accumulation [446302].

INFLAMMATIONIn November 2004, Cyclacel presented preclinical data showing activity of seliciclib in lupus nephritis and crescentic glomerulonephritis at the American Society for Nephrology meeting in St Louis, MO. In one study, seliciclib significantly improved survival of animals with lupus nephritis and at the same time had a protective effect on kidney function. In the arm of the study where the drug was administered as preventive treatment early in disease progression, seliciclib decreased indicators of renal damage and increased the life span of treated over untreated animals. In a second study in animals with established disease, seliciclib treatment in combination with a low dose of methylprednisolone markedly improved survival over untreated animals, reduced proteinuria and delayed the onset of renal damage compared with either treatment alone. Seliciclib treatment also reduced the levels of serum anti-DNA antibodies in both studies. Seliciclib also attenuated disease a murine model of crescentic glomerulonephritis, preventing cellular proliferation, crescent formation and renal impairment [569870].

In November 2003, at the 36th Annual Meeting of the American Society of Nephrology in San Diego, CA, investigators from New York University's School of Medicine reported that seliciclib attenuated or reversed renal disease in a mouse model of collapsing glomerulopathy by targeting cell cycle progression. In addition, investigators from the University of Aachen, Germany, reported that seliciclib was effective in a model of membranous nephritis and can be administered in renal diseases characterized by podocyte injury. Podocyte desmin expression was markedly upregulated in almost all glomeruli and not significantly different between the three groups. No tubulointerstitial damage was noted in any group. Biological activity of seliciclib was observed at day 30 as a dose-dependent decrease in glomerular mitosis compared to control. Seliciclib activity was further noted as numbers of mitotic cells in the tubulointerstitium decreased significantly after low dose seliciclib at day 9 and high dose at days 9 and 30 [513392], [515372].

MISCELLANEOUSIn October 2004, data on seliciclib against nephrotoxic nephritis in Wistar Kyoto rats were presented at the 37th ASN meeting in St Louis, MO. Seliciclib po at induction of nephritis decreased proteinuria and improved renal function at day 14. In addition, seliciclib reduced glomerular crescents and glomerular cell proliferation. The effect of delayed treatment was also tested in animals with established disease resulting in a significant reduction in proteinuria at day 7 and 14, and a reduction in serum creatinine and glomerular crescent score. A decrease in glomerular macrophage and cell proliferation was also observed [570796].

In December 2004, preclinical data on seliciclib were presented at the Alzheimer's Disease: From Molecular Mechanisms to Drug Discovery meeting in Cancun, Mexico. Seliciclib has < 1 microM potency for CDK1, 2, 5, 7 and 9, and > 1 to 40 microM versus CaMKII, CK1, DYRK, EPHB2, ERK1/2, and FAK [587023].

In October 2004, preclinical data on the mechanism of action of seliciclib were presented at the 34th SFN meeting in San Diego, CA. The compound may act on calcium channels by a CDK-independent mechanism, as it prolonged the deactivation kinetics of N-type calcium currents recorded from chick ciliary ganglion neurons. Seliciclib also increased neurotransmitter release from the adult frog neuromuscular junction, and increased EPP amplitute, quantal content and mEEP frequency [564891].

A study published in 1998 showed that seliciclib inhibits HSV replication. It was believed that late-G1/S-phase-specific cellular functions may be required for HSV replication [299970].

For an expert analysis of the development of this drug, as of October 2004, please see the Drug Evaluation.

Development Status

Detailed status for Cyclacel Ltd

Indication	Country	Status	Reference	Date
Breast tumor	UK	Phase 2 Clinical	476817	20-01-2003
Glomerulonephritis	UK	Phase 1 Clinical	466686	14-10-2002
Inflammation	UK	Phase 1 Clinical	464120	09-09-2002
Lymphoid leukemia	Western Europe	Clinical	563072	31-03-2004
Mantle cell lymphoma	Western Europe	Clinical	563072	31-03-2004
Multiple myeloma	Western Europe	Phase 2 Clinical	575023	07-12-2004
Non-small-cell lung cancer	UK	Phase 2 Clinical	476817	20-01-2003

Chemistry

Structure

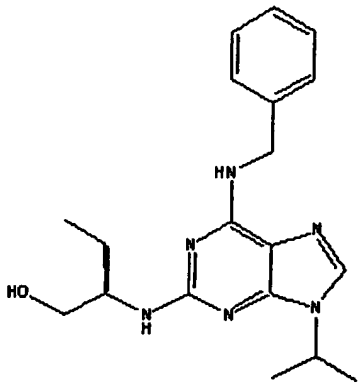

Confidence Level : 1

Compound names associated with this drug

Name	Type

186692-46-6	CAS RN
Roscovitine	
CYC-200	Research Code, Analogue
CYC-201	Research Code, Analogue
CYC-204	Research Code, Analogue
NSC-701554	Research Code
CYC-200 series	Analogue
CDK inhibitors, Cyclacel	
(R)-roscovitine, Cyclacel	
CYC-202	Research Code
(R)-roscovitine	
seliciclib	PINN

Literature Evaluation

Timothy Guzi, Schering-Plough Research Institute, Chemical Research, Infectious Diseases and Tumor Biology, 2015 Galloping Hill Road, Kenilworth, NJ 07033, USA

Submission date: 6 May 2004
Publication date: 13 October 2004

IntroductionNon-small cell lung cancer (NSCLC) afflicts more than one million people per year worldwide, with the current five-year survival rate in the US alone standing at 15% [564088]. Currently available first-line treatments, which typically include combinations of carboplatin with taxol, or cisplatin with gemcitabine, result in an overall response rate of only 20 to 30%. Second-line therapies, including taxotere, typically give an overall response rate of 5 to 10%, with median survival of 5 to 7 months. Clearly, the development of novel therapies for the treatment of NSCLC is warranted [564091].

The cyclin-dependent kinases (CDKs) are a family of serine/threonine kinases that function as regulators of cell-cycle progression. Inhibition of cell-cycle progression in tumor cell lines has been shown to induce an apoptotic response, and inhibitors of CDKs have been actively pursued as potential antitumor agents [334414], [563959]. CDK2 was initially targeted, as inhibition of this CDK was originally believed to be sufficient to induce an antiproliferative response. However, it was later reported that other CDKs might also regulate cancer cell proliferation [550561]. Several CDK inhibitors are currently under clinical evaluation. For example, flavopiridol (alvocidib) is under clinical development by the NCI, and the CDK2/cyclin E inhibitor BMS-387032 is being developed by Bristol-Myers Squibb Co [483107], [510232]. Cyclacel Ltd's CYC-202 (R-roscovitine) arose from an effort to produce more potent and selective CDK inhibitors following the identification of 6-dimethylaminopurine in screening studies.

CYC-202 is the lead compound from the CYC-200 series of CDK inhibitors in development for the potential treatment of cancer, glomerulonephritis, and inflammatory diseases [556873]. It is a selective inhibitor of several members of the CDK family with little cross-reactivity with other kinases [250831]. Consistent with this mechanism of action, CYC-202 has been shown to arrest the cell cycle in the G2/M phase and inhibit retinoblastoma protein (RB) phosphorylation [498797]. Is also exhibits transcriptional activity, which is manifested in the downregulation of cyclin B [250831]. In addition, CYC-202 has been shown to have moderate antiproliferative

activity in a variety of tumor cell lines [498797], [530649], [550556] and in vivo xenograft models [400792], [429318], [446647]. CYC-202 is being developed as an oral CDK inhibitor and has entered phase II clinical trials for NSCLC in combination with gemcitabine and cisplatin, and for advanced breast cancer in combination with capecitabine [520471]. In addition, clinical trials have recently been initiated in patients with mantle cell lymphoma (MCL), multiple myeloma and B-cell lymphocytic leukemia [530649], [563072]. Cyclacel has also announced plans to evaluate the efficacy of CYC-202 for the treatment of glomerulonephritis in phase II trials [476817].

Synthesis and SARCYC-202 is a chemically and chirally pure form of R-roscovitine [563121]. This 2,6,9-trisubstituted purine was discovered through traditional medicinal chemistry techniques utilizing 6-dimethylaminopurine as the lead. The compound is synthesized in two basic steps beginning with the known 6-benzylamino-2-chloropurine [WO-09720842], [556873]. In this pathway, 6-benzylamino-2-chloro-9-isopropylpurine is synthesized from 6-benzylamino-2-chloropurine, from which CYC-202 is then synthesized [WO-09720842].

Potency was improved against the lead compound by the addition of the lipophilic isopropyl group in the 9-position [348340], [556874]. Additional gains in potency were achieved by substitution of the 2-position with the amino alcohol functionality. More recently, the SARs for purine derivatives were explored utilizing parallel and combinatorial synthetic techniques. Alternative amino alcohol substitution in the 2-position as well as modification of substitution in the 6-position led to increases in the in vitro and cellular potency compared with CYC-202 [348340], [556874].

Preclinical DevelopmentCYC-202 is a CDK-selective kinase inhibitor with little or no activity noted against numerous other protein kinases evaluated (protein kinase C isoforms, cAMP-dependent protein kinase, cGMP-dependent protein kinase, myosin light-chain kinase, casein kinase 2, ASK-gamma, insulin-receptor tyrosine kinase, s-src and v-abl). The IC50 values of CYC-202 versus CDK2/cyclin B, CDK2/cyclin A, CDK2/cyclin E, and CDK5/p35 were determined to be 0.65, 0.7, 0.7 and 0.2 microM, respectively. CYC-202 does not inhibit CDK4/cyclin D1 or CDK6/cyclin D2, and weakly inhibits ERK1 and ERK2 with IC50 values of 34 and 14 microM respectively [250831].

The potency of CYC-202 was evaluated in the NCI-60 panel of cell lines where it showed an average IC50 value of 16 microM. In this analysis, no correlation between the sensitivity of the cell lines and the presence of wild-type or mutated p53 was noted [250831]. Antitumor activity was assessed in vitro in a panel of 103 human tumor cell lines, which represented 20 tumor types. CYC-202 showed activity between 0.3 and 100 microM in a dose-dependent manner. CYC-202 at 30 microM inhibited colony formation by 70% in 60% of the cell lines, while 100 microM inhibited colony formation by the same amount in 90% of cell lines. This study also indicated possible tumor selectivity of the compound for NSCLC, sarcoma, pleuramesothelioma, mammary and prostate cancer [497537].

In MDA-MB-231 breast epithelial cells, CYC-202 inhibited cell growth in a dose-dependent fashion and induced apoptosis [550556]. The application of 10 microg/ml CYC-202 completely prevented the exponential growth phase, and reduced the number of viable confluent cells by 50%. Another preclinical study examined the effect of CYC-202 on human breast cancer MCF-7 cells [510456]. The results showed that CYC-202 (1 to 20 microM) induced nucleolar disruption, prior to cell cycle arrest and apoptosis. CYC-202 disrupted argyrophilic nucleolar organizer regions, increasing nucleolar fragmentation in a time-dependent fashion. Cell-cycle progression

was significantly disrupted and there was a 3-fold increase in the accumulation of cells in the G2/M phase. CYC-202 also inhibited DNA synthesis in a dose-dependent manner, with 2.5 microM inducing a 50% inhibition. Decreased cell proliferation was observed as 40 and 90% reductions in the number of cells upon application of 10 or 20 microM of CYC-202, respectively. The direct cytotoxic effect of the compound (20 microM) was evidenced by a 20% reduction in adherent cells after 24 h of treatment [510456]. Induction of apoptosis (50%) was also observed in HT29 cells [521030], and following administration of 5 microg/ml CYC-202 to 26 B-cell chronic lymphocytic leukemia samples Annexin V assay revealed the first signs of apoptosis within 8 h. By 16 h, a dramatic loss of viability and a concomitant increase in the proportion of B-CLL cells in early apoptosis were evident [515909]. In an HTLV-I-infected cell line, CYC-202 induced apoptosis in a dose-dependent manner [447130].

CYC-202 was also shown to inhibit phosphorylation of the RB protein and promote accumulation of cells in the G2/M phase in human colon cell lines [498797]. CYC-202 exhibited synergy with doxorubicin in growth inhibition in RB-deficient SK-UT-1 cells. This synergistic effect was absent in the SK-LMS-1 cell line expressing wild-type RB. These effects are postulated to occur through the inhibition of the activity of the CDK2/cyclin A complex [445408], [471287], [485411]. In human colon cancer cell lines CYC-202 at 3-fold the IC50 concentration was shown to be sufficient in inhibiting RB phosphorylation [498797]. There was a concomitant arrest of cells in all stages of the cell cycle, particularly in the G2/M phase. Concurrent with the inhibition of RB phosphorylation, application of CYC-202 also led a decrease of cyclin D1 protein levels and cyclin D1, A, and B1 mRNA, and an increase in ERK1/2 phosphorylation [550558]. There was also a loss of RNA polymerase II phosphorylation and total RNA polymerase protein. These effects are indicative of an inhibition of transcription, possibly through inhibition of CDK7 and CDK9 complexes [550558]. In the light of recent evidence as to the disposability of CDK2 in cancer cell proliferation, it is likely that the inhibition of proliferation and induction of apoptosis may proceed through both CDK2/cyclin E and cdc2/cyclin B inhibitory events [550559], [550561], [550566]. Confirmation of cdc2 inhibitory activity was shown by inhibition of cdc2-phosphorylated vimentin in the L1210 cell line [250831]. Additionally, in combination with a farnesyltransferase inhibitor (FTI), CYC-202 showed a synergistic effect regarding the induction of apoptosis in human cancer cell lines. The combined treatment enhanced the activation of caspase-3 10-fold compared with treatment with FTI alone. CYC-202 also enhanced FTI-mediated release of cytochrome C from mitochondria and inhibition of RB protein phosphorylation [389091].

An antiproliferative effect was also described in human MCL cell lines. This effect was evident following 24 h exposure to CYC-202 at the specific IC50 calculated for each cell line (25 microM for REC, Granta-519 and JeKo-1 cells; 50 microM for NCEB-1) in Granta-519 and NCEB-1 cells, and after 48 h in REC and JeKo-1 cells. There was also an accumulation of REC, Granta-519 and NCEB-1 cells in the G2/M phase and an induction of apoptosis in the JeKo-1 cell line [530649].

CYC-202 is a less potent CDK inhibitor in cell culture than the CDK inhibitor flavopiridol or the CDK2/cyclin E inhibitor BMS-387032. These CDK inhibitors are also in clinical development for the potential treatment of cancer [483107], [510232]. In the NCI-60 panel of cell lines, flavopiridol was found to have an average IC50 value of 66 nM, compared with 16 microM for CYC-202. Likewise, BMS-387032 was found to exhibit cytotoxicity against A2780 cells with an IC50 value of 90 nM, and against 40 additional tumor cell lines. Similarly to CYC-202, these competitive agents show cross-reactivity with several members of the CDK family of protein kinases [550579], [550584].

distributed in fasted adult patients. The compound showed a Tmax of 2 h and a Vd of 3144.6 l, and clearance occurred at 736.7 l/h with a t1/2 of 3.5 h [446227], [449612], [445078]. In a further phase I study, the oral bioavailability of CYC-202 (100 to 1600 mg po bid for 5 days every 3 weeks; n = 25) varied between patients with the mean Cmax ranging from 627 to 6191 ng/ml and mean AUCs ranging from 2226 to 64682 ng/ml.h [491902], [514387]. Exposure to the recommended dose of 2500 mg/day produced a Cmax of 3596 ng/ml, an AUC of 31607 ng/ml.h, a Vd of 203 l and a t1/2 of 3.65 h [514387]. The pharmacokinetics for CYC-202 were examined in patients with advanced malignancy on the seventh day of treatment (100, 200 or 800 mg po bid; n = 21) [543715]. While the Cmax and AUC increased with dose (Cmax = 163, 311 and 3088 ng/ml at 100, 200 and 800 mg bid, respectively), dose-dependent changes in Tmax, Vd, t1/2 and clearance were non-linear. In the 100-, 200- and 800-mg treatment groups Tmax was 3.2, 1.0 and 1.6 ng/ml, Vd was 501, 896 and 474 l, t1/2 was 4.0, 9.0 and 3.2 h, and clearance was 89, 144 and 85 l/h, respectively. These studies collectively establish a pharmacokinetic profile for CYC-202; however, the effect on these parameters of the co-administration of other compounds with CYC-202 has yet to be reported.

ToxicityCYC-202 appears to be well tolerated at doses as high as 2000 mg/kg given orally to mouse, and 25 mg/kg administered intravenously to rat, with no adverse events reported [390823], [550588]. In dogs at 100 mg/kg CYC-202 causes vomiting [457966].

Clinical DevelopmentPhase IPatients with a variety of advanced malignancies (n = 19) received CYC-202 (100 to 1250 mg po bid) for 5 days every 3 weeks [470724]. At doses of up to 800 mg, no dose limiting toxicity (DLT) was observed, but at 1000 mg administered twice daily, grade 3 nausea and vomiting, as well as asthenia, were noted. The MTD was not established. In an additional phase I study in patients with advanced malignancy (n = 21) [470724], [491898], [543715], CYC-202 (200 to 1600 mg/day po) was administered for 7 consecutive days every 3 weeks. Half of the daily dose was administered in the morning and the remainder in the afternoon to patients who fasted for 2 h before and after each administration. DLTs of skin rash (grade 3) and hypokalemia (grade 4) were observed at 1600 mg/day after an average of two cycles.

A further phase I study was conducted to investigate the tolerability of increasing doses of CYC-202 (200 to 3200 mg/day po bid; n = 25) given for 5 consecutive days every 3 weeks [491902], [514387]. The MTD in this study was determined as 3200 mg/day with vomiting as the DLT. The recommended dose from this schedule was 2500 mg/day. In an extension of the study the tolerability of increased treatment durations was examined in 12 patients who were given a fixed dose of 2000 mg/day for 10 days. The trial included patients expressing a variety of tumor types including nine gastrointestinal, six breast, three NSCLC, three sarcoma, two prostate, two neuroendocrine, one cylindroma, one uterine, one adrenocortical and one adenocarcinoma of unknown primary origin. The patients included in the trial were aged between 30 and 70 years with a mean age of 55 years. Sustained tumor stabilization, for > 5 months, was observed in five patients on the first schedule and a partial response was observed in one patient in the extension schedule. In an analysis of six patients on the increased treatment duration schedule, the DLT was found to be grade 3 hypokalemia (two patients) and grade 3 skin rash (one patient). A third schedule (n = 8) was also explored with 2400 to 3600 mg/day administered bid or tid for 3 days every 2 weeks. No DLT toxicities were observed in either the 2400 or 3200 mg/day arms [491902], [514387].

Studies to identify biomarkers in order to monitor CYC-202 in clinical trials established methods by which the impact of the compound on gene and protein expression, post-translational modifications, and apoptosis could be monitored. Changes in some of these biomarkers were

detected in blood samples taken from patients in phase I trials [497390].

Phase IICYC-202 entered phase II clinical trials in January 2003 for the treatment of NSCLC in combination with gemcitabine and cisplatin and for advanced breast cancer in combination with capecitabine [476817]. These open-label, international trials have enrolled up to 30 patients and are to assess the impact of the drug combinations on tumor progression and predefined biomarkers. No data from these trials are available at present. Recently, on the basis of positive preclinical data, a clinical trial has also been initiated in patients with B-cell malignancies [530649], [563072]. The open-label trial is designed to assess the efficacy of CYC-202 in patients with MCL, multiple myeloma and B-cell lymphocytic leukemia, and it is planned to recruit a minimum of 12 patients for each indication. In addition, CYC-202 is also to be evaluated in phase I/II trials for glomerulonephritis [466924], [476817].

Side Effects and ContraindicationsThe dose-limiting toxicities associated with CYC-202 appear to be dose and schedule related. No toxicities were reported in a trial in patients with solid tumors (n = 5) treated with CYC-202 (50, 100 and 200 mg po) [446227], [449612], or in advanced malignancy patients administered oral CYC-202 up to 800 mg twice daily [543715]. In another phase I, dose-escalating trial of CYC-202 (200 to 1600 mg/day po), toxicities included hypokalemia and skin rash at the highest dose [491898]. Other side effects noted included nausea, vomiting, asthenia, reversible renal impairment and transaminitis [470724], [491898], [491902], [514387]. To date, the side-effect profile of CYC-202 used in combination with other chemotherapeutic agents such as gemcitabine and cisplatin has not been established.

Patent CommentaryIn October 2001, Cyclacel applied for WO-00172745, which claimed the use of 2-substituted 4-heteroaryl-pyrimidines for the treatment of proliferative disorders including cancer, leukemia and psoriasis. It was from this series of small-molecule CDK inhibitors that CYC-202 emerged as the lead compound.

WO-03082337, published in October 2003 and assigned to Cyclacel, claimed the worldwide rights to the use of CYC-202 in combination with doxorubicin for the treatment of proliferative disorders such as cancer. In May 2004, Cyclacel also claimed the use of CYC-202 in combination with mitoxantrone, cisplatin, docetaxel, gemcitabine and doxorubicin for the treatment of proliforative disorders [WO-2004041262], [WO-2004041267], [WO-2004041268], [WO-2004041308], [WO-03082337].

Current OpinionCYC-202 is a purine-derived CDK inhibitor that has been shown to exhibit antiproliferative effects and to induce apoptosis in certain cell lines. It shows selective potency against CDK1, 2, 5, 7 and 9, but not against CDK4 or 6. It also lacks activity against a variety of other kinases screened. In cell culture, CYC-202 exhibits relatively low potency with an IC50 of 16 microM against the NCI-60 panel of cell lines. It was also shown to induce cell-cycle arrest and inhibit RB phosphorylation. This is consistent with a CDK inhibitory mechanism of action. Additionally, CYC-202 decreases transcriptional activity, possibly through the inhibition of CDK7 and CDK9. The activity of CYC-202 is weak compared with other CDK inhibitors in clinical development, including flavopiridol and BMS-387032, which are up to 1000-fold more potent in cell culture.

In vivo, CYC-202 has shown antitumor activity in several human tumor xenograft models. To induce this activity, multiple high doses of CYC-202 are required, given either orally or by intraperitoneal injection. This activity can be categorized as modest when compared to that of the CDK inhibitors BMS-387032 and flavopiridol. However, CYC-202 has a significant clinical

advantage over these compounds, in that it has in vivo activity upon either intraperitoneal or oral dosing, whereas BMS-387032 and flavopiridol are both in development as intravenous formulations only.

The serum concentrations of CYC-202 achieved upon oral dosing are within the range of what is presumed efficacious, although quantitative data on this has yet to be published. The high micromolar concentrations postulated to be necessary for efficacy might explain the lesser activity observed with CYC-202 relative to the more potent CDK inhibitors BMS-387032 and flavopiridol. Additional pharmacokinetic analysis of serum concentrations in mouse relative to efficacy might be helpful in defining the appropriate exposure necessary for optimal treatment.

In general, while a MTD for several dosing schedules has been determined, CYC-202 is well tolerated even at very high doses. The DLTs associated with CYC-202 are not generally associated with the proliferative compartment as one might expect based upon the mechanism of action. The bioavailability at the highest doses is good, but the weak activity of the compound makes it unclear as to whether or not substantial efficacy is achievable on utilizing CYC-202 as a single agent. CYC-202 has entered phase II trials for NSCLC in combination with gemcitabine and cisplatin, and for advanced breast cancer in combination with capecitabine. The increase in activity upon combination with other antitumor agents may improve the clinical efficacy of CYC-202, although the effect on DLTs remains unknown. As CYC-202 works through a cell-cycle arrest mechanism, rigorous evaluation of the dosing schedule will be an important aspect of further clinical evaluation.

Biology

Study Type	Effect Studied	Experimental Model	Result	Reference
In vitro	Kinase inhibitory activity.	[32P]-incorporation assay.	CYC-202 inhibited cdc2/cyclin B, CDK2/cyclin A, CDK2/cyclin E, and CDK5/p35 with IC50 values of 0.65, 0.7, 0.7, and 0.2 microM respectively.	250831
In vitro	Antiproliferative activity.	Sulforhodamine B protein assay in human tumor cell lines.	CYC-202 showed a median activity of 16 microM against the NCI-60 cell line panel.	497537
In vitro	Apoptosis.	MDA-MB-231 human breast carcinoma cells.	CYC-202 (10 microg/ml) inhibited cell growth and induced apoptosis in a dose-dependent fashion.	550556
In vitro	Intracellular effects of CYC-202 on the expression and phosphorylation of target proteins.	Human colon cancer cell lines.	CYC-202 inhibited RB phosphorylation in a dose- and time-dependent manner. It also increased phosphorylation of ERK1/2 and reduced protein expression of cyclin D1 and cyclin D1, A, and B1 mRNA. There was also a loss of RNA polymerase II phosphorylation and total RNA	550558

			polymerase protein.	
In vivo	Antitumor activity.	Mouse model of human HT29 xenograft.	CYC-202 (100 mg/kg tid) administered for 4 days resulted in an 8% reduction in tumor size versus a 34% increase in the control group.	446647
In vivo	Antitumor activity.	Nude mice with implanted human tumor xenografts.	CYC-202 (100 mg/kg ip tid) demonstrated in vivo antitumor activity against LoVo colon xenografts.	400792

Metabolism				
Study Type	Effect Studied	Experimental Model	Result	Reference
In vivo	Pharmacokinetics.	Rats administered a single dose of CYC-202 (25 mg/kg iv).	Single-dose administration resulted in a mean plasma AUC of 168 microg/ml.min, a Vd of 3.45 l/kg, a clearance of 29.5 ml/min and a t1/2 of 26 min. Serum concentrations were below the limit of detection after 3 h.	550588
In vivo	Bioavailability and pharmacokinetics.	Mice were administered a single dose of CYC-202 (50 mg/kg iv).	Single-dose administration gave an AUC and a t1/2 of 21 microM.h and 1.35 h, respectively. CYC-202 was found to be 80% orally bioavailable and displayed non-linear pharmacokinetics upon doses of 50, 500, and 2000 mg/kg.	390823
In vivo	Metabolism.	BALB/c mice given CYC-202 (50 to 200 mg/kg).	The major metabolic pathway of CYC-202 is oxidation of the carbinol to the carboxylic acid, which was detected in plasma in addition to urine. Increasing doses increased the ratio of metabolite to parent from 2.6 at 50 mg/kg to 3.5 at 200 mg/kg.	550601
In vivo	Pharmacokinetics.	CYC (50, 100 and 200 mg po) was given to fasted, adult patients (n = 5).	CYC-202 was well absorbed and distributed. The compound showed a Tmax of 2 h, a Vd of 3144.6 l, and clearance occurred at 736.7 l/h with a t1/2 of 3.5 h.	446227

Clinical			
Effect Studied	Experimental Model	Result	Reference
Safety and tolerability.	Patients with a variety of advanced malignancies (n = 19) received CYC-202	At doses of up to 800 mg, no DLT was observed, but at 1000 mg administered twice daily, grade 3 nausea and vomiting,	470724

	(100 to 1600 mg po bid) for 5 days every 3 weeks.	as well as asthenia, were noted.	
Safety, tolerability and efficacy.	Phase I trial in advanced cancer patients (n = 25). CYC-202 (200 to 3200 mg/day) was administered for 5 days every 3 weeks.	The MTD in this study was determined as 3200 mg/day, with vomiting identified as the DLT. Sustained tumor stabilization for > 5 months, was observed in five patients. Following an increased duration of exposure, the DLTs were found to be hypokalemia and skin rash.	491902

Exhibit VII

http://www.iddb3.com/iddb3/iddb3_2/reports.display?id=44337&template=Drug&i_query_id=5383479&i_clear_trail=Y

SNS-032	
Company	Bristol-Myers Squibb Co
Highest Dev Status	Discovery
Indications	Cancer
Actions	Anticancer Apoptosis stimulator Cyclin-dependent kinase-7 inhibitor Cell cycle related kinase inhibitor Cyclin-dependent kinase-2 inhibitor
Technologies	Oral formulation Intravenous formulation
Reason for update on 29-Apr-2005	
indexing updated , one or more development status entries have been updated , 1 reference added [598246]	

Summary

Sunesis, under license from Bristol-Myers Squibb (BMS), is investigating SNS-032 (structure shown), a cdk-2, -7 and -9 inhibitor for the potential iv or oral treatment of solid and hematological cancers. In April 2005, the company was planning to start a phase I trial in solid tumors and lymphoid malignancies during that year [598246].

BMS was developing the compound as BMS-387032, which was the lead in a series of aminothiazole CDK2 inhibitors (qv) [404071]. By March 2003, phase I studies had been initiated [483107]; however, by November 2004, BMS did not have any cdk/cyclin inhibitors in clinical development [572056] and in April 2005, it outlicensed rights to Sunesis [598246].

CLINICAL DATAIn April 2005, Sunesis was planning a phase I trials of SNS-032 administered iv as a single agent and in combination with leading cancer therapies [598246].

In June 2003, two phase I studies were presented on BMS-387032 at the 39th annual ASCO meeting in Chicago, IL. Both studies were open label dose escalation trials in which BMS-387032 was delivered as either a 1-h or 24-h infusion every 3 weeks to patients with metastatic solid tumors refractory to other chemotherapeutic treatments. In the 1h infusion study, BMS-387032 was escalated from 9.6 to 85 mg/m2. The Cmax and exposure of BMS-387032 increased in a dose proportional manner; at 9.6 mg/m2, Cmax and AUC were 278 +/- 73 ng ml and 531 +/- 321 ng.h/ml, respectively while at 85 mg/m2, Cmax and AUC were 1563 +/- 406 ng/ml and 3362 +/- 48 ng/h/ml, respectively. The drug was well tolerated with transient neutropenia of unknown etiology noted as the primary toxicity. Transient liver aminase elevations (grade 1 to 3) affected seven patients receiving doses between 17.5 to 59 mg/m2. Gastrointestinal toxicity was mild to moderate (grade 1 to 2); nausea, vomiting, diarrhea and anorexia occurred in 33, 16, 23 and 19% of patients, respectively. Grade 1 to 2 fatigue, alopecia, myalgia and sensory neuropathy occurred in 44, 9, 9 and 7% of patients, respectively. Prolonged stable disease (> 6 months) was achieved in patients with renal cell carcinomas, NCSCL, head and neck cancers and leiomyosarcoma [492075]. In the 24-h infusion study, a total of 28 patients received doses ranging from 4.8 to 30.3 mg/m2. Pharmacokinetic data available from 17 patients treated at doses of 4.8 (n = 1), 7.2 (n = 3), 9.6 (n = 6) 12.8 (n = 2), 17.3 (n = 3), and 22.7 (n = 2) mg/m2 revealed t1/2 values of 6.6, 15.8, 14.7, 12.5, 13.2 and 14, AUC values of 145, 361, 308, 589, 793 and 917 ml/min, Vss values

nM) for 24 h followed by cisplatin (62.5 to 2000 nM) for 24 h resulted in a 1.5 to 5.0 fold increase in cell death ($p < 0.01$) when compared to simultaneous treatment with both drugs for 24 h. Cytotoxic synergy was also observed for this sequential treatment when a fixed ratio of 1:3 (BMS-387032:cisplatin) was used. When SV-1 cells were allowed to recover for 48 h between drug treatments, sequential treatment with BMS-387032 first resulted in additive toxicity; if cisplatin was administered first antagonistic toxicity resulted. In cell lines that contain plasmids allowing the stable expression of cyclin D1 (SWS101), results similar to those seen in the SV-1 were observed. However, if SWS101 cells were allowed to recover for 48 h between drug sequences, and cisplatin was administered first, low doses of drug produced antagonistic toxicity while high doses of drug resulted in synergistic toxicity [484205].

Further preclinical data on BMS-387032 were presented in July 2003 at the 94th AACR meeting, Washington, DC. BMS-387032 showed significant selectivity against a panel of protein kinases representative of Ser/Thr as well as Tyr kinases. When tested in a panel of diverse human tumor cell lines, BMS-387032 showed significant cytotoxicity. It induced cell cycle arrest and apoptosis, with concomitant inhibition of phosphorylation of cdk2 substrates. Further, it was demonstrated in vitro in cultured cells that the compound can be used in combination with chemotherapeutic agents to achieve additive or synergistic activity [497571].

In March 2003, preclinical data were presented on BMS-387032 at the 225th ACS meeting in New Orleans, LA. The compound was tested in mice, rats and dogs and its half life values were 4.8, 5.3 and 7 h, respectively. It had an IC50 value of 48 nM and had a higher selectivity for this complex over the cdk1/cyclinB and cdk4/cyclinD complexes (481 and 925 nM respectively). BMS-387032 also showed an IC50 value of 90 nM in a cytotoxicity assay (A2780 cells) AUC total values were 4.8, 6.3 and 2.1 microM per hour, respectively, while the bioavailabilities were 100, 31 and 28%, respectively. Oxidative metabolism of the compound was low, it did not inhibit cytochrome P450, and the aqueous solubility was 0.28 mg/ml. The plasma protein binding in humans was 63%. In a nude mouse model, 9 out of 16 human ovarian xenografts were completely cured and no tumor cells were evident, when treated at 48 mg/kg [482028], [483107], [484811], [485395]. Similar data were presented in November 2003 at the 15th AACR-NCI-EORTC meeting in Boston, MA. Treatment with BMS-387032 regulated 300 genes in A2780 tumor cells and human peripheral blood mononucleocytes. Among these genes, one was found to be consistently induced by 5- to 20-fold in treated cells [515670].

ADDITIONAL INFORMATIONIn April 2005, Sunesis acquired exclusive worldwide development and commercialization rights to BMS-387032 and changed its name to SNS-032 [598246].

Development Status

Detailed status for Bristol-Myers Squibb Co

Indication	Country	Status	Reference	Date
Cancer	US	Discontinued	598246	28-04-2005

Detailed status for Sunesis Pharmaceuticals Inc

Indication	Country	Status	Reference	Date
Cancer	US	Discovery	598246	28-04-2005

Licensing

Summary	Reference
Sunesis Pharmaceuticals Inc	
In April 2005, Sunesis obtained worldwide development and commercialization rights to Bristol-Myers Squib's BMS-387032. BMS would receive an upfront equity stake of $8 million in Sunesis, while Sunesis would make milestone payments of up to $29 million. Additional development and commercialization milestones could total up to $49 million. Sunesis would also pay royalties to BMS in return for an exclusive, worldwide license to CDK inhibitors derived from the BMS-387032 intellectual property [598246].	598246

Chemistry
Structure
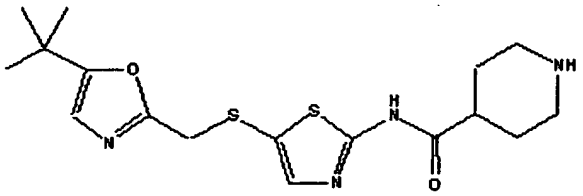 Confidence Level : 1

Compound names associated with this drug	
Name	Type
345627-80-7	CAS RN
BMS-387032	Research Code
SNS-032	Research Code